


217
21

THE CHARACTERIZATION OF THE FLOWFIELD
OF A DUMP COMBUSTOR

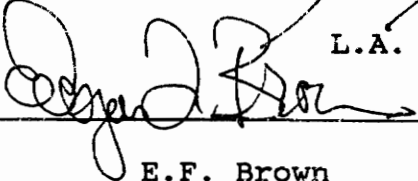
BY
ROBERT S. GABRUK

Thesis submitted to the Faculty of the
Virginia Polytechnic Institute and State University
in partial fulfillment of the requirements for the degree of
Master of Science
in
Mechanical Engineering

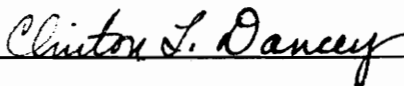
APPROVED:



L.A. Roe, Chairman



E.F. Brown



C.L. Dancey

September 1990
Blacksburg, Virginia

LD

5655

V855

1990

6339

C.2

CHARACTERIZATION OF THE FLOWFIELD
OF A DUMP COMBUSTOR

BY

ROBERT S. GABRUK

Committee Chairman: L.A. Roe

Mechanical Engineering

(ABSTRACT)

To provide quality benchmark data (that can be used in numerical simulation comparisons) and to examine the effects of combustion on a typical ramjet engine flowfield, a water-cooled, stainless steel dump combustor model was developed. A two-component Laser Doppler Anemometer (LDA) was used to measure the mean and turbulent velocities in the axial and tangential directions and provide a comparison between combusting and isothermal flows. However, before any LDA measurements could be taken, the combustor had to be configured to run in a suitably stable mode.

Stability was identified by the pressure spectra obtained under various running conditions using piezoelectric pressure transducers wired to a spectrum analyzer. Operational parameters such as fuel composition, fuel injection location, acoustic configuration, and equivalence ratio were varied until instabilities were minimized. The optimal configuration ran with upstream fuel injection (premixed mode) at the duct centerline and an orifice plate installed immediately upstream

of the fuel injectors, with propane as the fuel.

Once stability was achieved, LDA data was taken. The results showed some significant differences between the reacting and nonreacting flows. The most significant effect was the difference between the inherent recirculation regions for each case. Combustion decreased the length of the region by approximately 50 percent, while increasing the maximum negative velocities. This made for a more compact, but stronger, recirculation region. Since the recirculation region acts as the main flame holder and is a major source of turbulence, the changes in this region significantly altered the dump combustor flowfield.

ACKNOWLEDGEMENT

The research effort presented here was sponsored by the Air Force Systems Command and the Air Force Office of Scientific Research. Universal Energy Systems also deserves recognition for providing all of the information necessary for a comfortable and productive research session. This project would not have been possible without the support of Abdollah Nejad and Saad Ahmed. They provided the tools needed to carry out the research effort, as well as providing needed encouragement.

TABLE OF CONTENTS

	page
ABSTRACT	ii
ACKNOWLEDGEMENT.	iv
LIST OF FIGURES AND TABLES	vii
CHAPTERS	
I. INTRODUCTION.	1
II. LITERATURE REVIEW	6
Nonreacting flows	6
Reacting flows.	10
III. RESEARCH PROGRAM.	17
Program goals	17
Dump combustor model.	18
LDA system.	22
Conventional transducer measurements.	27
IV. COMBUSTION INSTABILITY.	29
Literature review	29
Instability in present system	33
V. VELOCITY RESULTS.	43
Inlet velocity profiles	44
Centerline measurements	46
Mean velocity and turbulence profiles	53
VI. CONCLUSIONS	64
REFERENCES	66

APPENDICES

A.	VELOCITY PROBABILITY DENSITY FUNCTIONS. .	70
B.	VELOCITY PROFILES	97
VITA		148

LIST OF FIGURES AND TABLES

FIGURE	TITLE	
1	SCHEMATIC OF COMBUSTOR FLOWFIELD	3
2	OVERALL VIEW OF INLET DUCT AND COMBUSTOR . .	19
3	CROSS-SECTIONAL VIEW OF COMBUSTOR	20
4	SCHEMATIC OF THE LDA OPTICAL SYSTEM.	24
5	POWER SPECTRUM FOR DOWNSTREAM INJECTION WITH NO ORIFICE.35
6	POWER SPECTRUM FOR DOWNSTREAM INJECTION WITH ORIFICE37
7	COHERENT OUTPUT POWER AS A FUNCTION OF RADIAL POSITION	38
8	COHERENT OUTPUT POWER AS A FUNCTION OF EQUIVALENCE RATIO	40
9	POWER SPECTRUM FOR UPSTREAM INJECTION WITH ORIFICE.	42
10	INLET VELOCITY PROFILES	45
11	CENTERLINE MEAN AXIAL VELOCITY.	47
12	CENTERLINE DISTRIBUTION OF AXIAL TURBULENCE.	48
13	CENTERLINE DISTRIBUTION OF TANGENTIAL TURBULENCE.	49
14	PHOTOGRAPHS OF COMBUSTION PROCESS	52
15	EVOLUTION OF MEAN AXIAL VELOCITY PROFILES . .	54
16	CONTOUR PLOT OF CONSTANT VELOCITY LINES . . .	57
17	EVOLUTION OF AXIAL TURBULENCE PROFILES. . . .	61

18 EVOLUTION OF TANGENTIAL TURBULENCE PROFILES . 62

TABLE

I CORNER RECIRCULATION ZONE LENGTH. 59

CHAPTER I

INTRODUCTION

Detailed experimental studies must be carried out before the accuracy of any numerical simulation can be determined. The application of mathematical methods to complex turbulent flowfields continues to be the focus of many current studies, as numerical modeling of turbulent flows provides a cost-efficient and time-saving method of engineering design. Most of the past experimental studies have concentrated on understanding the behavior of turbulent flows and have not been aimed at improving the accuracy of computational modeling. Lower order predictive codes require various assumptions in the solution of the Navier-Stokes equations, and experimental data must be available to determine the validity of these assumptions. The data presented within this report are experimental results for eventual comparison to numerical models currently under development, and for the analysis of the effects of heat release on a turbulent flowfield.

One focus of these experimental and numerical studies has been on sudden expansion (or dump) combustors, typically found in many air-breathing propulsion systems, and in particular, the ramjet engine. Ramjets are used in unison with rocket boosters to provide integral propulsion systems for missiles. The rocket booster is designed to provide the necessary

propulsion in the initial stage of flight, with the ramjet engine taking over as the propulsion system once the rocket reaches the required flight speed. The basic configuration of a ramjet engine is that of a dump combustor. Therefore, much can be learned about the ramjet through studies on a sudden expansion combustor.

The flowfield of a dump combustor is a complex combination of turbulent fuel-air mixing, flow separation, flow recirculation, flow reattachment, and various other flow phenomena, as shown in Fig. 1. Flow recirculation may be the most important part of the dump combustor flowfield. A high adverse pressure gradient in the recirculation region (immediately downstream of the dump plane) promotes flow instability by producing large eddies that are concentrated sources of turbulence. Subsequent convection, diffusion, and decay of these eddies have a significant effect on the flowfield of the combustor. The high adverse pressure gradient also causes flow reversal. These factors help to increase combustion efficiency by providing a way of reintroducing hot well-mixed reactants back into the combustion process. In other words, previously unburned reactants that have already passed through the combustion region can be returned to this region by recirculation. The recirculation region acts as the main flame holder (without physical interjection) by providing a region with low velocity

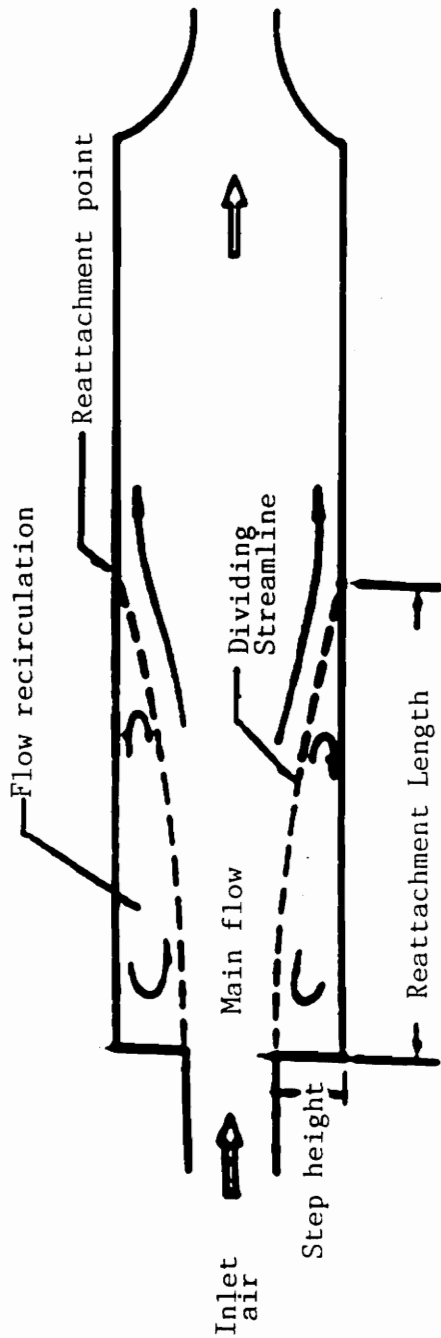


Fig. 1 Schematic illustration of a dump combustor flowfield.

reactants. Hence, the recirculation zone improves the blow-off limits and reduces particulates and gaseous pollutants by increasing the completeness of reaction.

Flow separation and reattachment are other very important aspects of the combustor flowfield, as they are directly associated with recirculation. A shear layer grows between the recirculation region and the extremely turbulent high speed core. This shear layer is formed from the flow separation that occurs at the dump plane. The location where the dividing streamline (an imaginary line between the core flow and the recirculation region) attaches itself to the combustor wall is called the reattachment point.

Past studies have concentrated mainly on isothermal (cold) flows through dump combustors because of the difficulties involved with taking velocity measurements in highly turbulent reacting flowfields. Therefore, a significant amount of detailed flowfield data for cold flows is readily available. In addition, most of the prior studies on actual dump combustors have been limited to measurements of quantities such as combustion efficiency, and velocity measurements were not available. Those studies that do contain velocity data fail to provide the inlet conditions and, therefore, the initial conditions needed in a numerical simulation.

Many experimentalists believe that simulated dump combustors (those using cold flows) can be used to predict

the effect of various flow and geometric parameters on the combustor flowfield. However, detailed comparisons with reactive flows are necessary in order to test the usefulness of this assumption.

A comparison of this type was made by Drewry (1). He found that simulated flowfield results could be used to predict overall combustor performance trends for dump combustors. However, these results were far from conclusive and fail to address some significant concerns of reacting flows. For example, cold flow studies fail to describe anything about the chemical reactions or heat release. Furthermore, Drewry's studies failed to present detailed velocity data and, therefore, could not provide a quality set of benchmark data that could be used in numerical simulation.

This thesis documents a study done on combusting flow through a dump combustor with zero inlet swirl. (In future experiments, the effects of inlet swirl on the flowfield will be studied). Velocity measurements (both mean and turbulent) are provided by a Laser Doppler Anemometer (LDA) and are the major point of information. The data will be used to make some general conclusions as to the effects of heat release on the flowfield of a dump combustor by directly comparing combusting and isothermal flows. This data is also to be used as a benchmark set of data for future comparisons with numerical models.

CHAPTER II

LITERATURE REVIEW

A literature review is presented here to give an overview of the nature of this research and to provide an overall base of knowledge on similar research. There exists a fair amount of background material on isothermal flows through sudden expansion chambers of the same basic geometry as in this research. However, there is a limited amount of documentation concerning reacting flows through sudden expansion combustors. The logical progression of presentation is to first discuss previous research on nonreacting flows and then consider reacting flow experiments.

The nonreacting flow references all involve combustors that were geometrically similar to the research combustor used in the present experiment. However, only two reacting flow references have the same basic geometric configuration. Of these two, neither provides detailed information on the inlet velocity profiles. Other references are summarized to provide a general background on separated flows.

NONREACTING FLOWS

Research on ramjet-type combustors has been going on since the early to mid 1970's. Drewry (1) was one of the first to take an in-depth look at the isothermal flowfield of a dump combustor and try to make comparisons to that of an actual ramjet. His studies (on a representative duct) included flow

visualization and gas sampling and no velocity measurements were taken.

Flow visualization tests, using a surface oil flow technique, clearly demonstrated the complex nature of the flow recirculation region downstream of the dump. In addition, based on the results from his effort and the data of Pennucci (2), Phaneuf (3), and Boaz (4), Drewry determined that the recirculation zone length was on the order of 8 step heights.

Gas sampling results showed that the simulated fuel concentration in the primary flow recirculation region was essentially uniform and quite high as compared to the duct centerline. Furthermore, the flow approached a fully mixed condition in downstream locations of the combustor. A direct comparison between cold flow mixing and ramburner combustion efficiency was made as a function of combustor length to diameter ratio. Drewry found that cold flow mixing data could be useful in predicting combustion efficiency.

B.T. Yang and M.H. Yu (5) obtained LDA velocity data in cold flow studies performed in a plexiglass sudden-expansion model. The reattachment length, in this study, was determined to be 4.5 step heights downstream of the dump plane. This was much shorter than that predicted by Drewry (1). Yang and Yu believed that a higher back pressure caused the shorter reattachment length.

Turbulent energy contours showed that the shear layer, a

region with a high velocity gradient, was a location of high energy levels. The maximum turbulent level was located on the dividing streamline. Yang and Yu believed that high turbulent energy was transported in and out of the recirculation region by diffusion and convection.

Samimy et al. (6) took measurements of mean and turbulent velocities (both with and without inlet swirl) in a nonreacting axisymmetric dump combustor flowfield. Their mean velocity results showed a reattachment length of approximately 8 step heights, which is consistent with the results reported by Drewry (1). The results of the research were typical of the sudden expansion combustor flowfields documented by Lilley (7) and Smyth (8).

The turbulence results showed local peak values of turbulence intensities in the shear layer generated between the core flow and the corner recirculation flow. There was a very slow development of turbulent intensities in the streamwise direction. These turbulent results also showed good agreement with Lilley (7) and Smyth (8).

Nejad et al. (9) used a two-component LDA in a cold flow dump combustor model to obtain detailed mean and turbulence data for both swirling and non-swirling inlet flows. Their main goal was to compare experimental data with numerical results. This was an extension of the experiments done by Samimy et al. (6). The experimental results of Nejad et al.

agreed very closely with those of Samimy and other investigators. In addition, they concluded that the k-e turbulence model was inadequate in representing complex turbulent flows.

Favaloro et al. (10) performed experiments on cold flows through an axisymmetric dump combustor. These experiments were actually another extension to those performed by Nejad et al. (9) and Samimy et al. (6).

Mean flow profiles were very similar to those of past experiments. From the axial velocity profiles, the recirculation length was determined to be 8 step heights. Radial profiles resembled those of confined jets. The radial velocity in the core flow was towards the wall, but near the dump, changed direction. This correctly depicted the flow pattern in the corner recirculation zone. Tangential mean velocities were zero, as would be expected in the absence of inlet swirl.

Turbulent velocity profiles showed that the axial rms turbulence velocities had local peak values in the shear layer generated between the core flow and the recirculation zone. This was consistent with the results of other studies previously mentioned (5,6,9). The radial and tangential turbulence profiles were similar to those of the axial.

REACTING FLOWS

Baker et al. (11) and F.K. Owen (12) investigated the region of flow downstream of a coaxial jet. Although the combustor geometries were different than that of the present research, helpful background material concerning separated reacting flows was obtained.

Baker and Owen observed that although the general trends for the cold and hot flows were similar, quantitative differences were apparent. Regions of recirculation were generally longer with combustion. Furthermore, increased axial velocities and stresses, along with a negative pressure gradient, accompanied combustion. Turbulent kinetic energy contours were very similar to the contours of axial normal stresses. Only a small degree of turbulence isotropicity was demonstrated. Of further interest in Owen's experiment was his conclusion that turbulence models based on local equilibrium principles would not accurately describe the physics of the combusting flowfield studied.

Smith and Giel (13) experiments were performed in a ducted, subsonic, axisymmetric combustor that was very similar to a coaxial configuration. Experiments were carried out for both nonreacting and reacting cases. Chemical reactions significantly altered the size and location of the recirculation region. The reattachment length increased with reaction. This could be seen in comparisons of the locus of

zero mean velocity locations (and the wall static pressure distribution) for the reacting and nonreacting flows.

For both the nonreacting and reacting cases, the maximum turbulence (normalized with the jet exit mean velocity) was approximately the same magnitude. However, the location of this maximum shifted farther downstream of the primary jet exit for the reacting flow. The reason, Smith and Giel concluded, was that for both cases, the maximum turbulence location occurred near the center of the mixing zone, which extends farther downstream with chemical reaction. The magnitude of the radial turbulence was greater than the mean radial velocity for almost every location.

The flowfield in a two-dimensional combustor with a rearward facing step was studied by Ganji and Sawyer (14), Banhawy et al. (15), and Pitz and Daily (16). These experiments were conducted in a two-dimensional regime, but once again, valuable insight on separated flows was obtained.

Ganji and Sawyer (14) found that both nonreacting and reacting flows were dominated by large-scale, coherent vortex structures. The flame region was controlled by the fluid dynamics of these vortices. The size of the vortices also dictated the thickness of the shear layer. The eddies of the reacting flow had a lower growth rate, were more closely distributed in space, and had a smaller rate of coalescence than those of the nonreacting flow. Fresh reactants from the

core flow, as well as reacted products entrained in the shear layer, were enveloped before their disappearance into eddies. One similarity between hot and cold flows is that for both, the number of vortices decayed exponentially downstream.

Among the observations of Banhawy et al. (15) was that, in contrast to the general deceleration of the isothermal flow, the combusting flow accelerated significantly with axial location. In addition, Banhawy found that the size of the step influenced flow in the near-step region. The reattachment length decreased from 3.5 step heights to 3 step heights when the step height was doubled. This was probably due to differences in the shape of the velocity profiles in the plane of the steps. This points out the need for documentation on the inlet velocity profiles.

Although many of the results reported by Pitz and Daily (16) were similar to previous studies (14 and 15), they were able to make some interesting observations. The reacting shear layer (defined by the mean velocity) was shifted towards the recirculation zone for the reacting case. This was caused by heat expansion from the reacting eddies that propagated into the premixed reactants. The velocity at the top of the shear layer increased and lowered the upper boundary of the shear layer. Hence, the velocity difference in the lower edge of the shear layer increased and caused the recirculation region to shrink.

Local turbulence levels were also affected by combustion. Heat release shifted the peak turbulence levels towards the recirculation region. In the mixing layer, the reacting maximum turbulence levels were much higher. Turbulence levels decreased quickly (in both cold and hot flows) between 1 and 2 step heights before shear layer reattachment.

Stevenson et al. (17) compared nonreacting and reacting flows through an axisymmetric sudden expansion combustor. The combustor configuration was very similar to the one used in this research effort, however, the step height and combustor length were somewhat different. This study failed to report detailed LDA inlet velocity profiles. The main objective of the study was to determine the effects of combustion on the flowfield.

There were significant differences found in the mean centerline velocities between the isothermal and reacting cases. The axial centerline mean velocity decreased with axial position for cold and hot flows. However, due to a density change in the reacting case, the decrease occurred with a much smaller gradient.

Furthermore, combustion had a significant effect on the corner recirculation zone. Maximum negative velocities in this region were greater with combustion. The recirculation region was, therefore, somewhat stronger in the hot flow case. In addition, the region was smaller for the reacting flow; a

reattachment length of 7.4 step heights compared to 8.6 step heights for the isothermal case. The cold flow reattachment length was somewhat longer than the 8 step heights reported by others (1,6,9,10).

As with the mean velocities, there were some differences in streamwise turbulence intensities between hot and cold flow cases. Fairly low levels of turbulence were found in the central core of the inlet core flow, whereas large turbulent levels were present in the shear layer at the edge of the inlet pipe. Although the normalized turbulence intensities were found to be of the same magnitude for the cold and hot flows, the local turbulence intensities were not. The hot flow local turbulence levels were much lower because dilation of the heat release competed with or dominated turbulence energy production by shear, notably in the vicinity of the corner recirculation zone. The turbulence measurements also indicated a significant difference in shear layer position and rate of turbulence decay for the hot case.

As the final piece of literature that was reviewed, the preliminary findings of Nejad et al. (18) are presented. The reacting results were obtained using the same combustor rig and instrumentation as in the present thesis, however, these results were obtained only as a preliminary investigation to the present study.

The LDA velocity measurements, although taken in a sparse

spatial matrix, gave some insight as to the trends of the flowfield. An extrapolation of the velocity data showed a decrease in the corner recirculation zone with combustion. The reattachment length decreased from 8.2 (consistent with the results of other experiments (1,6,9,10)) step heights downstream of the dump plane to 3.7 step heights for the combusting case. The reacting flow reattachment length was significantly shorter than that of Stevenson et al. (17). Furthermore, the hot flow was characterized by a much faster flow recovery, meaning flat mean velocity and turbulence profiles were found closer to the dump plane.

Similar turbulence levels were found in the near field and in the core flow for both reacting and nonreacting case. However, the maximum turbulence level moved closer to the wall for the reacting flow.

The potential core was clearly identified by the velocity and turbulence profiles. For the hot and cold flows, the core extended to about 8-10 step heights downstream of the dump plane.

In the far field, turbulent velocities were lower for the reacting case. The heat release increased the mean axial velocities and, in turn, decreased the local turbulence levels. This suggests that there was significant reduction in turbulent transport and mixing.

Although the previously mentioned papers for both

isothermal and combustng flows indicate some general trends one might expect to find in the flowfield of a dump combustor, more detailed experiments are needed. In particular, further research on combustng flows would help to alleviate some of the discrepancies found in previous results such as the effects of combustion on the centerline axial velocities and axial turbulence intensities. Furthermore, past papers have neglected to provide the detailed inlet conditions needed for comparing separate experiments and numerical simulations.

CHAPTER III

RESEARCH PROGRAM

The main goal of this research effort was to provide a benchmark set of LDA flowfield data that could be used in comparisons with numerical simulation. Much time and effort in the past (and present) has been dedicated to numerically modeling complex turbulent flows. Numerical modeling can be an extremely valuable research tool because, if a particular flowfield can be mapped on a computer rather than in a test lab, both time and money can be saved. However, in order to test these models, quality experimental data is needed for comparison. Past studies have failed to provide quantities (such as inlet velocity profiles) that are needed for numerical simulation.

The second goal of this research effort was to study the effects of heat release, mixing processes, and chemical reactions on the flowfield of a ramjet engine. A significant amount of data is available on nonreacting flows in the same basic geometric design as the dump combustor. However, as stated earlier, there is a lack of data for reacting flows. Understanding the effects of combustion, such as the degree of isotropicity, on a particular flowfield should provide valuable insight that can be used in future experimental and numerical design projects.

DUMP COMBUSTOR MODEL

All experiments were conducted in a stainless steel model of a ramjet dump combustor as shown schematically in Figs. 2 and 3. The combustor wall contained a high-quality quartz window for optical access to the flow. Since the dump plane (or piston, as shown in Fig. 3) was mounted on precision rails, it could be positioned at any axial location relative to the window. This provided a good way to take LDA measurements at any axial location downstream of the dump plane. The inlet duct also contained a high-quality quartz window in order to obtain inlet flow conditions. The combustor walls were surrounded by a water-cooled jacket. The jacket outlet temperature was constantly monitored to ensure that the water temperature was well below boiling.

The rig was of the same basic design as the plexiglass model used in the nonreacting studies of Favaloro et al. (10). A 4-inch diameter inlet duct supplied air to a 6-inch diameter combustor. This corresponds to a 2.25 area ratio. The combustor, which had a 6-inch long exit nozzle with 60% area reduction, had a maximum length of 63 3/4 inches when the piston was at full stroke. The inlet air was supplied by high pressure compressors to achieve a 60 ft/sec average velocity, corresponding to a 1.18×10^5 Reynolds number. Inlet pressures and temperatures were ambient (80 F, 14.7 psia). A screen (flame arrester) was located 18 1/4 inches upstream of

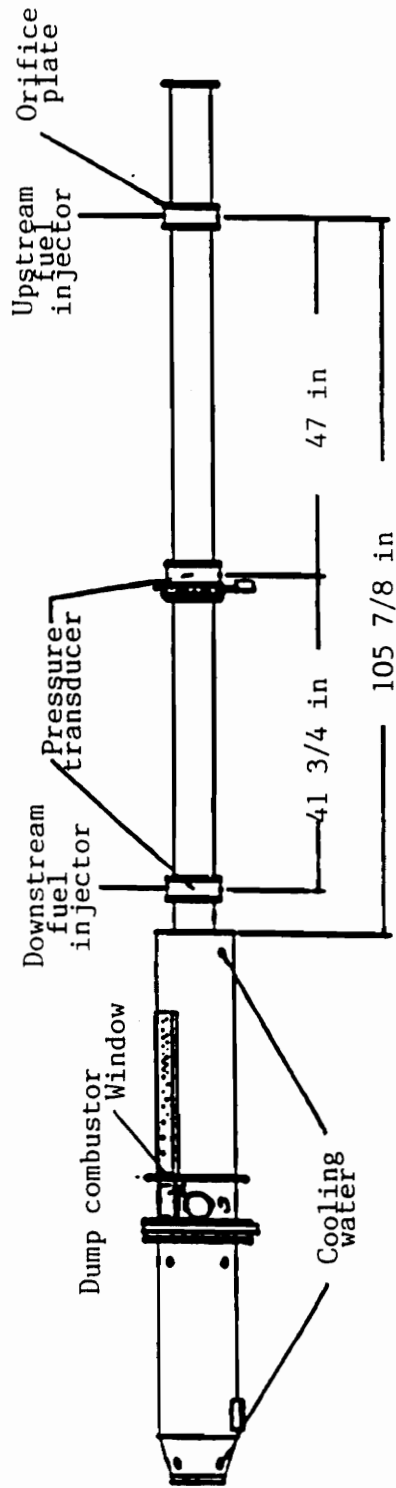


Fig. 2 Overall view of inlet duct and dump combustor.

the dump plane to guard against flashback.

The combustor was built with various in-house designed features, including the fuel injection system, the ignition system, and the LDA particle seeding system. The fuel, which was propane, was injected 11 feet upstream of the dump plane through four 0.125-inch diameter injector tubes. Each tube had a 0.065-inch diameter fuel orifice located in the side, intruded radially into the flow, and could be adjusted to inject at various radial positions. (Nitrogen was used in the nonreacting flow study to simulate fuel injection.) Ignition was accomplished via in-house built spark plugs located at the dump plane and positioned at 90 and -90 degrees from the horizontal.

The seeding material, TiO_2 , was produced from the chemical reaction between $TiCl_4$ and the moisture in the ambient air. The seed size was on the order of one micron in diameter. Seed injection occurred just upstream of a flow settling chamber (located 122 7/8 inches from the expansion plane) from a seeder built in-house. Since the seed was injected far upstream of the combustor in a low velocity settling chamber and then accelerated through a long section of inlet duct, the seed distribution was assumed to be uniform at the inlet to the combustor.

Furthermore, an orifice plate was mounted in the inlet duct downstream of the settling chamber and just upstream of

the fuel injectors. This orifice reduced airflow-coupled instabilities and isolated the reaction region from the large acoustic resonant contribution of the settling chamber.

LDA AND DATA ACQUISITION SYSTEMS

The LDA system was made up of mostly TSI components, however, the laser was a 4 W Spectra Physics model 164. The laser operated in the multiline mode at a total output power level of 1.5 W. The blue (488 nm) and green (514.5 nm) components were used to measure flow velocities. Each of these beams (blue and green) was split into two beams, with one beam of each color receiving a frequency shift for directional sensitivity.

The optical system, which operated in the backscatter mode, consisted of a standard TSI beam splitter, a frequency shifter (TSI model 9180-3A) operating at 40 MHz for each channel, and a 3.75 X beam expander with a 35 mm entrance beam separation and a focal length of 450 mm. The entire optical system was mounted on a three-axis traversing table with a resolution of 0.02 mm. Fringe inclinations were aligned at 45.7 and 135.2 degrees from the combustor centerline. These angles were determined by projecting the laser beams through the combustor on to a wall and measuring the angles from the horizontal. The velocity components were resolved by data analysis. This provided better accuracy by using both beams to derive component velocities. Only axial and tangential

velocities were measured since the laser probe volume could only be positioned in a horizontal (axial-radial) plane.

Some in-house modifications were made to the TSI system and the alignment procedure. These included micrometer adjustment screws for the field stop lens system and both receiving optic modules, which allowed for adjustment to provide the highest possible data rates and best Doppler signal. A 20 μm aperture (which was smaller than the probe volume) was used in the alignment procedure to ensure all four beams crossed at the same point. A schematic of the optical system is shown in Fig. 4.

Signal processing was accomplished with two TSI counter-type systems that processed the Doppler signal from the photomultiplier. The high filter limit was set to 100 MHz and the low to 20 MHz. The actual data frequency was approximately 38 MHz, well within the filter range.

Individual channels used the 16 fringes per validation setting and a 1 percent comparison level, while a 20 μsec coincidence window was used between channels. The 16 fringes per validation setting and 1 percent comparison level provided a way for determining whether a signal from the photomultiplier is a true Doppler signal. True Doppler signals have the distinction of having the same frequency whether determined from an 8 fringe count, a 16 fringe count, or any other number of fringe counts. To test for this

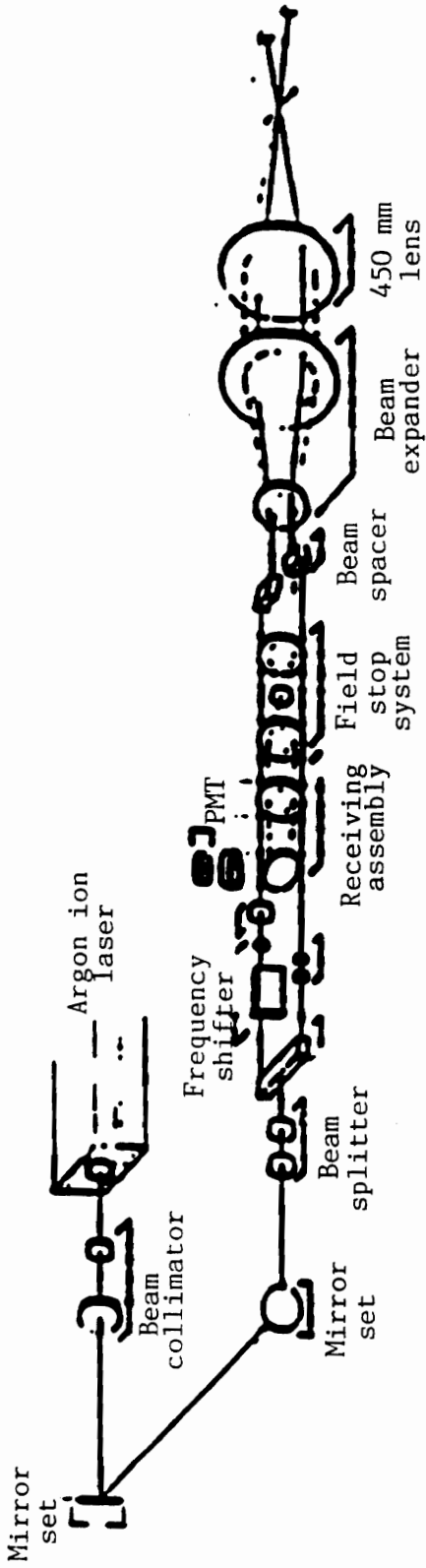


Fig. 4 Schematic of the LDA optical system.

occurrence, the processor separately counted and timed 8 and 16 fringes for each signal. The frequency of the signal was then determined from both the 8 and 16 fringe counts. If the frequencies were within 1 percent, the signal was used in the velocity calculations. Once the signals from the individual channels were determined to be Doppler signals, the 20 usec coincidence window was used to ensure that the separate channels were measuring the same seed particle.

A custom-made interface linked the two LDA processors to the data analysis computer. Double precision calculations of all statistical moments using standard formulae (19) were made at each measurement location. Some processor noise entered into the calculation of velocities. Therefore, post-processing cut-off limits of greater than 3 sigma were made on the calculated velocity histograms.

In any interpretation of LDA velocity data, the method of acquisition and analysis must be considered. Edwards (20), in a report of the special panel (at the Second International Laser Anemometry Symposium) on statistical particle biasing problems in LDA systems, gives recommendations on how LDA measurements should be treated and reported. Although this report tries to follow these guidelines as closely as possible, some of the information (that Edwards suggests to include in any report of LDA data) was impossible to obtain. The indeterminate information included the Taylor time

microscale, the particle arrival rate, and the trigger rate.

Stored data rates (coincident pairs of realizations from each signal processor) ranged from 15 to 500 per second for hot flows and 100-1000 per second for cold flows. Possible reasons for the lower data rates during combustion are: 1) TiO_2 might have lost some of its scattering efficiency at high temperatures and became invisible to the receiving optics, and 2) a rapid accumulation of seeding particles on the quartz window might have partially blocked the path between the probe volume and the receiving optics. At each flow field location, 1024 to 4096 measurements were taken. Although the Taylor time microscale (which is a measure of the time that the flow needs to change one standard deviation and is normally calculated from the Eulerian flow parameters) could not be determined, the storage rates probably ranged in the low category. The Witze (21) and Stevenson (12) experiments were also performed with data rates ranging in the low category.

Both the particle arrival rate and the trigger rate were unavailable quantities. The particle arrival rate is the rate that measurable particles pass through the measurement volume. It was indeterminate due to the separated nature of the flow - only small amounts of seed entered the recirculation region.

Biasing was minimized by both hardware constraints and acquisition techniques. Angle bias was eliminated by the 40 Mhz Bragg cell since this frequency is much greater than that

of the flow. Filter settings of 20 MHz and 100 MHz eliminated the problem of filter bias. In an effort to correct velocity measurements, particle interarrival time weighting was implemented. (Constant time sampling could have also been used, however, this method throws out too many points.) The particle interarrival time method uses the time between each realization as the weighting factor. The method is verified and described in depth by Nejad and Davis (19). The velocity probability density functions that are obtained from the data acquisition system are shown in Appendix A.

CONVENTIONAL TRANSDUCER MEASUREMENTS

A Neff 470 data acquisition system with 1 kHz sampling was used to calculate, display, and monitor all pertinent flow parameters such as mass flow rates, temperatures, and pressures. A program was written within the Neff software to calculate quantities such as equivalence ratio from transducer measurements. Conventional transducer outputs were connected to the analog/digital board of the Neff system. Thermocouples were of the K and R type. K type was used for low to moderately high temperature measurements (such as that of the inlet air) and R type was used for high temperature measurements (such as those taken in the combustor chamber). The thermocouples had a full scale accuracy of ± 1.0 percent. The thin film pressure transducers (CEC-5500) that were used to monitor pressures were accurate to ± 0.4 percent of full

scale. Inlet air flow rates were measured with a Yokogawa vortex flowmeter (YF100), while the fuel flow rates were taken with a Flow Technology turbine type flowmeter (model FT-08aer1-gea-1). The accuracies on the flowmeters were ± 1.5 percent of full scale.

CHAPTER IV

COMBUSTION INSTABILITY

As originally constructed, the combustor operated with significant instabilities (high amplitude vibrations), with a predominance of low frequency vibrations. Under these conditions, quality LDA measurements (those that are representative of an actual ramjet) could not be obtained. So, the first priority was to have the dump combustor running in an acceptable mode of stability.

The main concern of this experimental effort was not necessarily to identify the exact cause of the combustor instability, but to eliminate or reduce the instability to a level where the combustor was operating acceptably. Before explaining the procedure used to "stabilize" the combustor, a brief literature review is presented.

LITERATURE REVIEW OF COMBUSTION INSTABILITY

Many dump combustors exhibit low frequency longitudinal combustion instability between 80 - 300 Hz (Choudhury et al. (22)). Although the exact causes are unknown, it is generally accepted that the interaction of the shock-induced pressure pulsation (in supersonic flows) and the coherent vortex shedding at the dump plane promotes combustion instability.

Both analytical and experimental evidence suggest that instability is caused by a number of mechanisms. Shock wave oscillation in the inlet (supersonic flows), interaction of

various vortex systems in the combustor, combustor acoustics, spray characteristics, and fuel stratification may be responsible for the low frequency combustion instability.

There are studies that show evidence for all of these parameters being mechanisms of instability. Most experiments focus on one area at a time in order to obtain an understanding of how each of the separate events influences instability. Some investigators (23 - 29) identified vortex shedding generated at the dump plane as a possible mechanism. Choudhury et al. (22), on the other hand, showed that periodic distortion of the combustion zone by vortices generated at the inlet may be the culprit in combustion instability. Some (30 - 34) found that upstream propagation of entropy waves which reflect from the exhaust nozzle could be possible causes of instability. Yet others (35 and 36) have found that a change in the fuel distribution and injector characteristics eliminated low frequency combustion oscillation.

A number of studies have been carried out in an effort to identify mechanisms of flashback, a serious contributor to combustion instability. One such study was done by Plee and Mellor (37). They identified four possible mechanisms of flashback in turbulent combustors: 1) flashback due to the flame speed exceeding the flow velocity of the unburned mixture either in the boundary layer or along the flow axis, 2) autoignition upstream of the flame, 3) flame propagation

through reverse flowfields that can occur when the characteristic dimension of a disturbance is of the same order as the distance between the disturbance and the flame holder, and 4) preignition of a separated flow region that may take place when the dimension disturbance is much less than the distance between the disturbance and the flame holder. Coates (38) went further to point out that studies at the National Gas Turbine Establishment showed that low-frequency flow oscillations seem to be the cause of flashback.

The purpose of a study done by Keller et al. (39) was to explore the mechanisms of the instabilities associated with flashback under highly turbulent flow conditions. The study was done in a premixed tunnel of rectangular cross section with a rearward-facing step. It was found that when the flow rate of fuel was decreased toward the lean limit, three modes of instability (which they called humming, buzzing, and chucking) were observed.

Each of these modes had its own distinct features. Humming showed a large increase in the amplitude of the vortex pattern in the turbulent mixing zone. Buzzing was characterized by large scale oscillations of the flame across the chamber that resulted in the destruction of the vortex pattern of the mixing zone. Chucking, on the other hand, was a cyclic phenomenon of reformation of the flame. The growth and convection of recirculating vortices was believed to be

the cause of this mode of instability.

Keller et al. (39) made a number of other observations based on their experimental work. First of all, due to the low flame speed of the mixture (as compared with the inlet flow velocity), the flame front was located along the surface between the products and reactants. Secondly, they observed that when the equivalence ratio was increased by a step change in the fuel flowrate, combustion instabilities appeared. Finally, they found that an unstable combustor can be altered to run more stably by an acoustic field imposed by an outside source or induced as a harmonic component of a standing wave.

Davis (40) investigated combustion instabilities with small changes in an unstable coaxial ramjet dump combustor. The parameters that were varied were fuel/air ratio, inlet length, combustor length, nozzle area, inlet air temperature, inlet velocity profile, and fuel injector location.

The results showed that either low, very low, or high frequency instabilities occurred for almost all test conditions. Very-low-frequency oscillations occurred near the rich operating limit. A longer inlet duct decreased the magnitude of the instability, but did not change the frequency. Shorter combustors increased the frequency only slightly and decreased the amplitude. The most significant effect on instability was the decrease in frequency when the fuel injectors were moved upstream. Typically, the low

frequency (700 to 800 Hz) instabilities occurred only at low fuel/air ratios.

COMBUSTION INSTABILITY IN THE PRESENT SYSTEM

As was stated earlier, the combustor (under the original configuration) ran extremely unstably. Therefore, the first priority was to have the dump combustor running with an acceptable amount of instability. Variable parameters were fuel type, fuel injector location (axially and radially along the inlet duct), equivalence ratio, and acoustic configuration. Piezoelectric pressure transducers mounted in the duct upstream of the dump plane were wired to a Nicolet 660 A dual-channel FFT analyzer. The pressure spectra from the FFT helped identify instabilities. Desirable characteristics included a low operating temperature, low pressure fluctuations, a non-predominance of specific frequencies, and a minimal very-low-frequency component. In the baseline configuration, ignition occurred with a large detonation, and frequent flashback and low-frequency oscillations were produced during operation. The flashback was believed to have occurred in the low velocity regions near the wall of the inlet duct. Therefore, the fuel was changed from ethylene to propane - a fuel with a lower flame speed and longer quenching distance. Although the flashback was eliminated, the combustor operation was still unacceptable.

The coherent output power (COP) spectrum of the baseline

configuration (with propane) is shown in Fig. 5. Coherent output power indicates the acoustic power measured at one transducer that is linearly related to the acoustic power of the other transducer. In other words, the inputs to both channels are analyzed to make sure the same signal is being measured. COP is a good indication of the acoustic power due solely to system response. The total rms pressure level was 0.296 psi in the duct interior. The equivalent value for the nonreacting case was 0.0228 psi.

The next step was to change the axial position of the fuel injectors. With the fuel injectors located just upstream of the dump plane, it was believed that a diffusion flame was being created. Further, this diffusion flame had constantly changing fuel-rich zones which contributed to the instability of the system. Therefore, the fuel injection was moved far upstream, far enough to create a premixing of the air and fuel. The fuel injectors consisted of four 0.125 inch diameter tubes located 11 feet upstream of the dump. Each tube entered the duct radially, had an orifice of 0.065 inch diameter located in the side, and allowed for injection at various radial distances from the duct centerline. Although a decrease in instability was achieved, the combustor was not running in an acceptable mode. Spectral data was not obtained since the combustor would not run under an equivalence ratio of 0.8. This means that the system would only run under

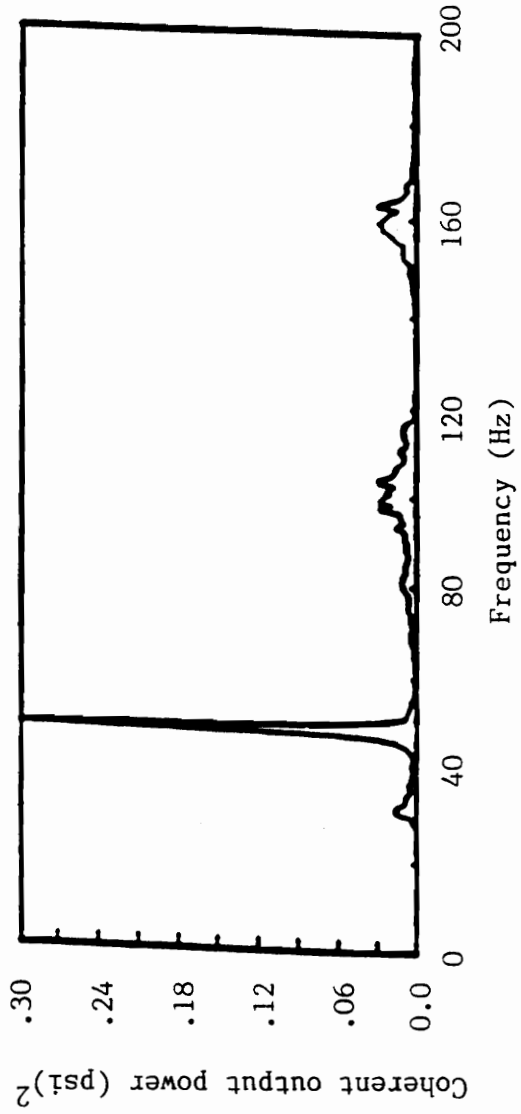


Fig. 5 Power spectrum for downstream injection without orifice.

unacceptably hot conditions.

Further, an orifice plate was implemented just upstream of the new fuel injection location. A 2.00 inch orifice diameter plate was installed in the 4.00 inch diameter inlet duct. It was believed that the plate would reduce airflow-coupled instabilities, isolate the reaction region from the large resonant contribution of the settling chamber, and provide acoustic tuning. The coherent output power of the system with the orifice and downstream fuel injectors is shown in Fig. 6. In comparing Figs. 5 and 6, one can see significant differences. Note the magnitudes on the vertical axes. Although the pressure fluctuations were still dominated by narrow bandwidth signals, the total levels decreased by over an order of magnitude.

Considerable improvement was observed when the fuel injection was moved back to the upstream location while the orifice was in place. Further, even more improvement was discovered as the fuel injection was moved radially inward (at the upstream location). Figure 7 shows the coherent output power versus the radial location of the injection. The fuel injectors were moved radially from the recirculation region (that was caused by the orifice plate), through the high shear regions of the orifice flowfield, and into the high-speed core near the duct centerline. The curve in Fig. 7 demonstrates yet another benefit of adding the orifice

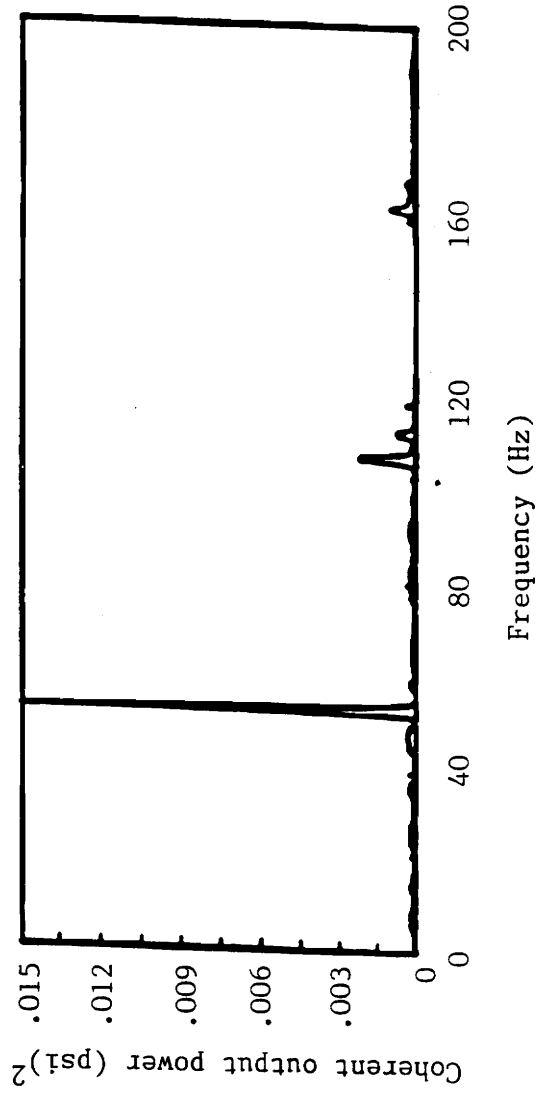


Fig. 6 Power spectrum for downstream injection with orifice.

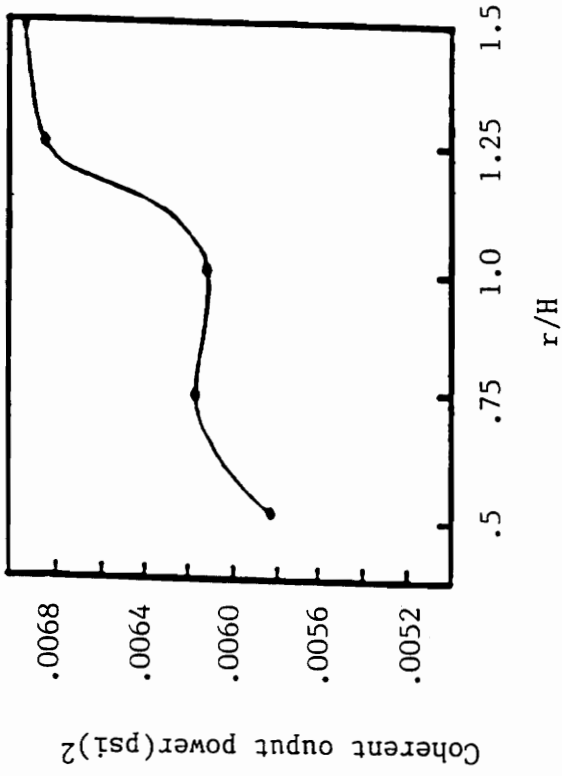


Fig. 7 Coherent output power as a function of radial position for upstream injection with orifice ($\phi = 0.7$).

plate, enhanced mixing. As can be seen from the curve, the coherent output power decreases as the fuel injectors are moved through the orifice recirculation region ($r/H = 1.5$ to 1.25), flattens out near the shear region ($r/H = 1.25$ to 0.75), and drops off further as they are moved through the core region ($r/H = 0.75$ to 0). The lower coherent output power acknowledges the fact that better mixing is occurring in the high-speed core. Note that the coherent output power levels are close to two orders of magnitude lower than that of Fig. 5. The combustor was now running with an acceptable amount of instability.

The next problem was determining what equivalence ratio to operate with. It is important to run at a low equivalence ratio (while maintaining stability) in order to keep combustion temperatures down. Low combustion temperatures are preferable since they decrease hardware fatigue. Equivalence ratios were varied from 0.575 to 0.8 . The results are shown in Fig. 8. At the higher fuel/air ratios, the coherent output power varies directly with fuel flow, as would be expected from efficiency arguments. However, below 0.6 , the power increases as the thermoacoustic energy release decreases. This was accompanied by unstable operation and a shift to low frequency dominant peaks in the power spectrum.

Based on these results, it was decided to continue the research effort under the conditions of premixed combustion

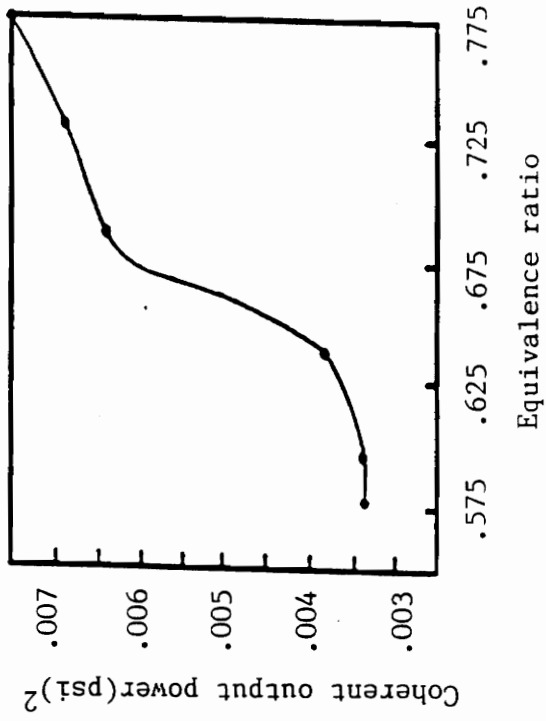


Fig. 8 Coherent output power as a function of equivalence ratio for upstream injection with orifice ($r/H = 0.5$).

with an equivalence ratio of 0.65 and fuel injection near the inlet duct centerline. Figure 9 shows the coherent output power spectrum for this configuration. Compared to the initial configuration (Fig. 5), it can be seen that the spectrum is broadened, shifted to higher frequencies, and the power levels are lowered by two orders of magnitude. The rms average pressure was 0.065 psi, which is 15 percent of that for the original configuration.



Fig. 9 Power spectrum for final dump combustor configuration.

CHAPTER V

VELOCITY RESULTS

Various mean and turbulent velocity data are presented in this section. This information will help accomplish the research goals of providing a set of data that can be used both to compare with numerical simulations and to make general conclusions as to the effects of heat release on the dump combustor flowfield. The data includes the inlet velocity profile, which is a point of information neglected in some other experiments. All velocity results have been normalized with the average inlet duct velocity (U_{ref}). Although obtained in this study, the mean tangential velocity and Reynolds stress data are not presented here. The reason for not presenting this data is that in an absence of inlet swirl, these values should theoretically be equal to zero. It can be seen by inspection of these quantities (which are found in Appendix B) that they are very close to zero.

The main source of error in the mean velocity results was in the ability to set and maintain the inlet flow rate. The maximum error (due to flowrate variance) in the axial and tangential mean velocities was approximately 2.5 percent. The LDA error (which was calculated to be 0.4 percent and 0.35 percent for the axial and tangential mean velocities, respectively) was insignificant compared to errors due to flowrate variance.

The accuracy of turbulence data was not specifically experimentally identified. However, based on previous results and experience (18), the maximum error was predicted to be approximately 5 percent.

Based on comparisons with data from previous research using the same basic combustor and data acquisition systems (18), the reproducibility of the velocity results presented in this section is believed to be within 5 percent. The overall trends in mean and turbulent velocities are very similar. Differences in velocity magnitudes, on the other hand, are apparent. These differences occur mainly in the turbulence intensities and may be due to differences in the inlet inlet conditions, which are not documented in the referenced results.

INLET VELOCITY PROFILE

The inlet velocity profile (at 10 step heights upstream of the dump plane) is shown in Fig. 10. Both the streamwise mean and turbulent velocities (normalized with the average inlet duct velocity) are shown. As can be seen from the figure, the mean velocities are fairly symmetrical about the inlet duct centerline and the turbulent velocities hold approximately constant at 15 percent of the average inlet duct velocity.

As stated earlier, most reacting flow experiments fail to report inlet velocity profiles. Therefore, the direct

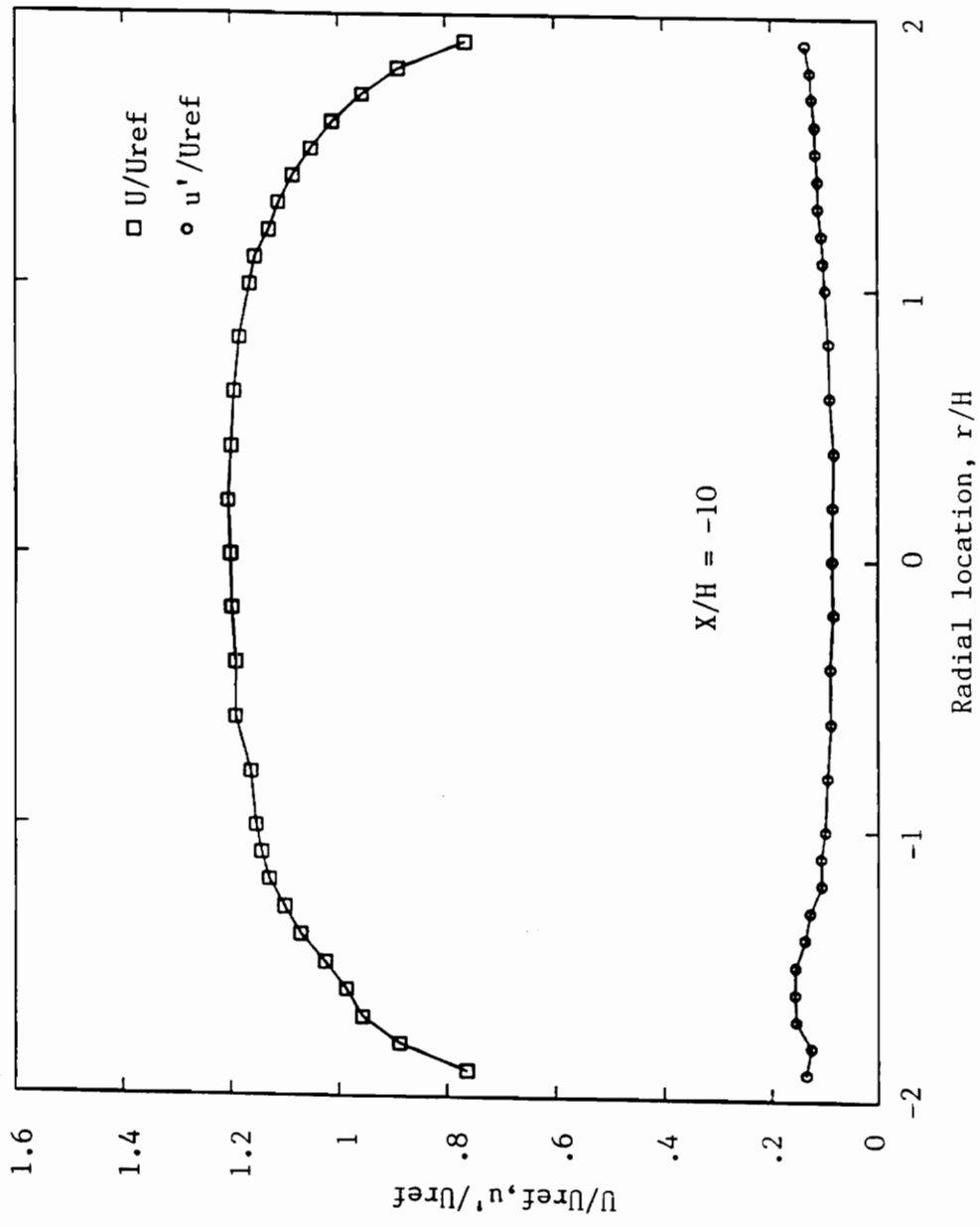


Fig. 10 Inlet velocity profiles

quantitative comparisons that are attempted in this section can be deceiving since a complete comparison should also include inlet velocity profile differences. This holds especially true for the turbulent velocity results and, therefore, quantitative comparisons with the turbulent velocity results of other experimenters is excluded.

CENTERLINE MEASUREMENTS

Centerline mean velocity and turbulence results (for both reacting and nonreacting cases) are shown in Figs. 11-13. These figures were designed to illustrate the effects of heat release on the flowfield of the dump combustor. Figure 11 shows a gradual decay of cold flow centerline axial velocity throughout the length of the combustor. Other experimental data (6-10,17,18) show similar trends. This is consistent with mass continuity principles, i.e., when given constant density, an increase in flow area will cause a decrease in flow velocity.

The cold flow centerline axial and tangential turbulence intensity (Figs. 12 and 13), on the other hand, increased in the downstream direction until approximately 18 step heights. This trend was also typical of the results of other researchers (6-10,17,18). This increase in turbulence intensity was due to the convection and diffusion of high turbulent energy created in the shear layer during flow separation. After 18 step heights, however, the velocities

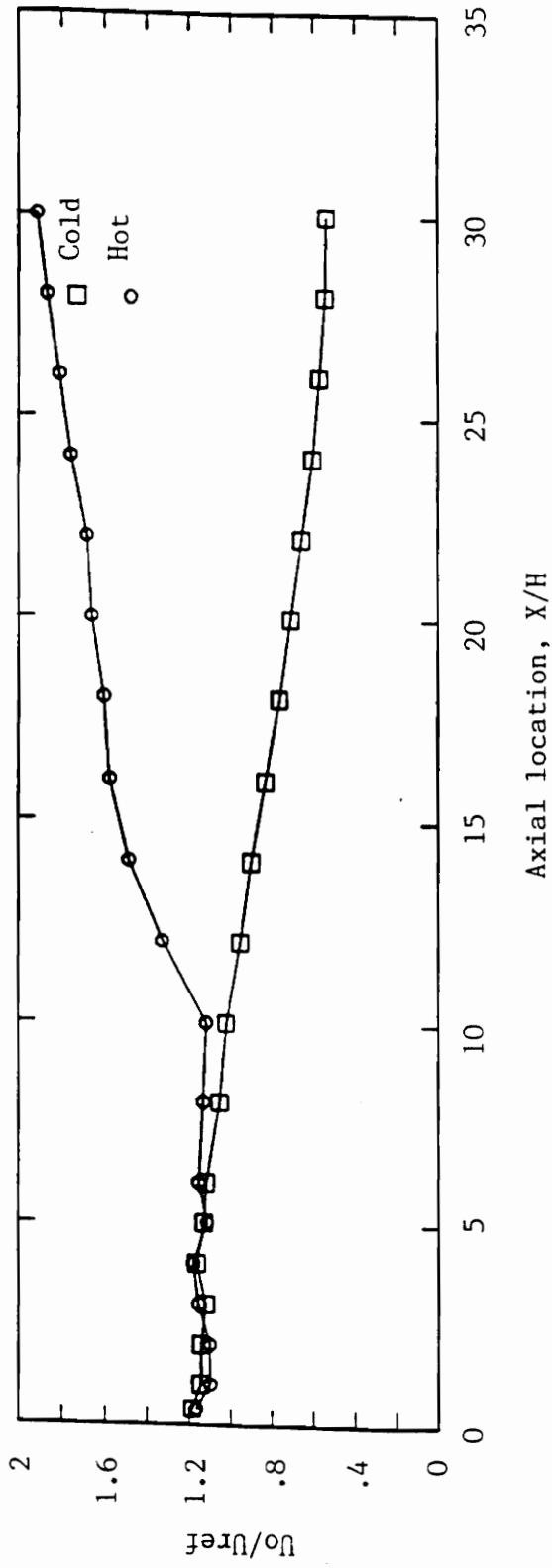


Fig. 11 Centerline mean axial velocity.

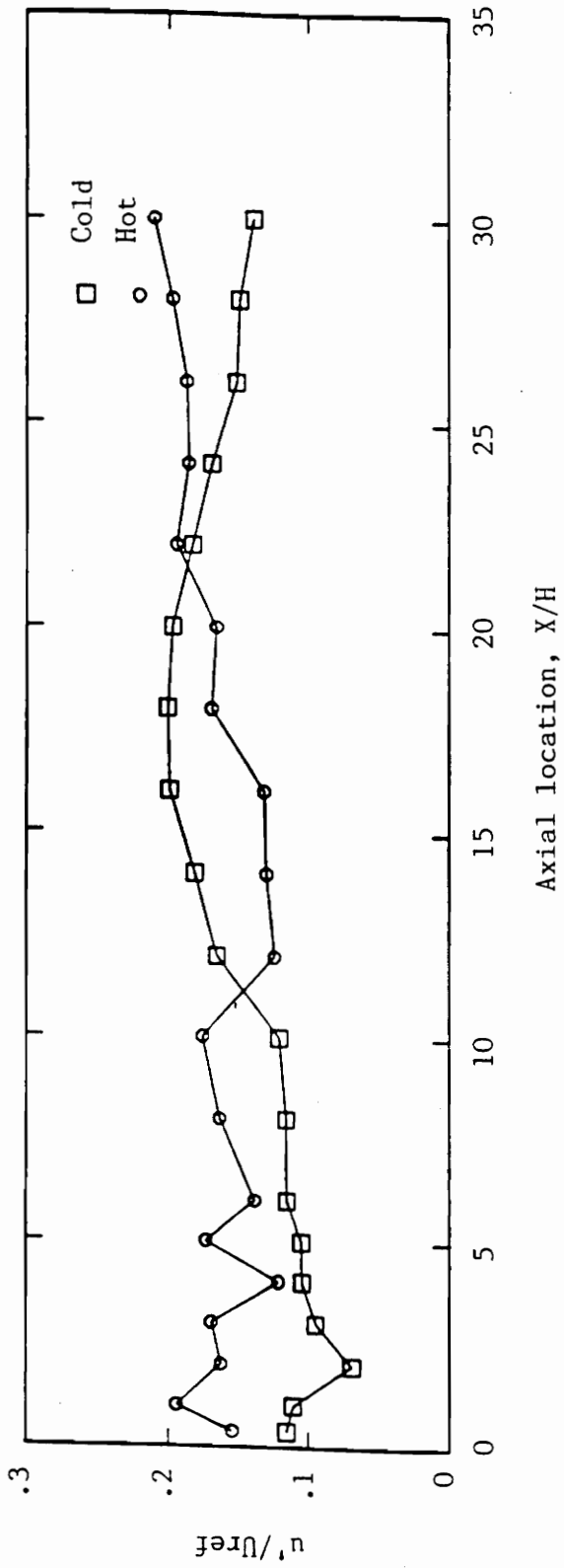


Fig. 12 Centerline distribution of axial turbulence.

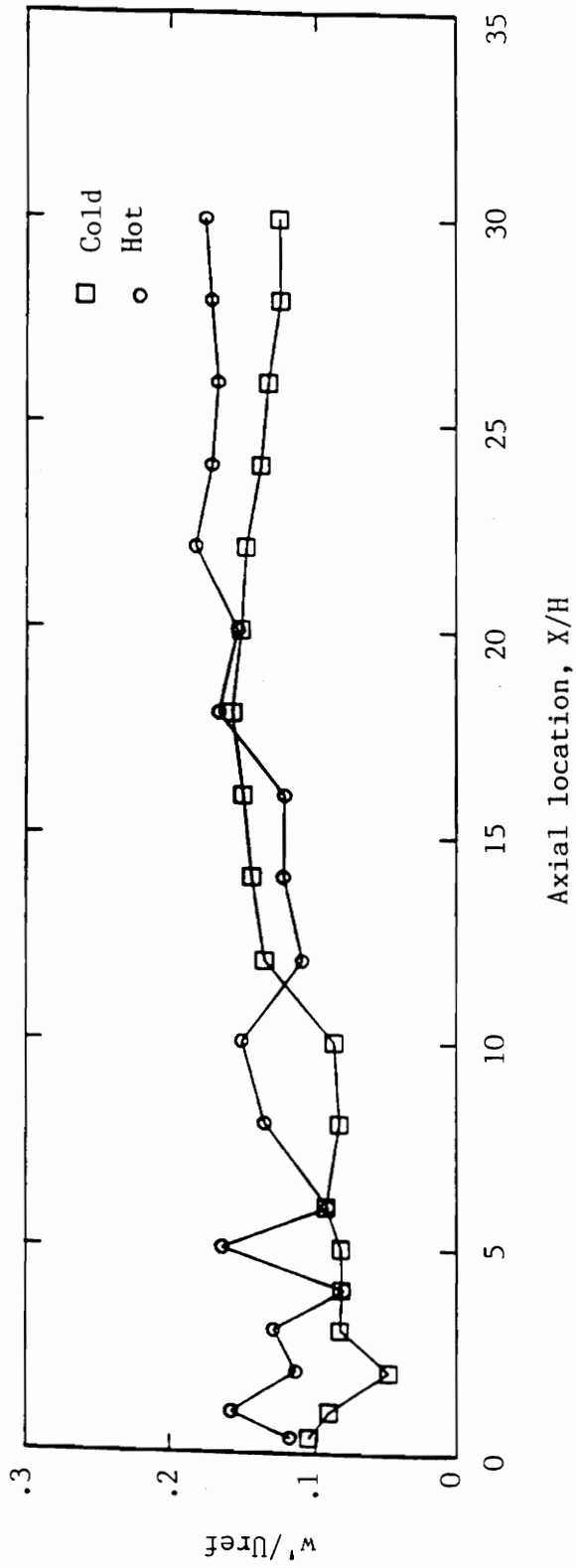


Fig. 13 Centerline distribution of tangential turbulence.

decreased as the flow became more developed. The maximum turbulence level (based on inlet duct average velocity) was about 20 percent at 18 step heights from the dump.

One important observation of the turbulent velocity data is the fact that the axial turbulence levels were always greater than the corresponding tangential levels (Figs. 12 and 13), However, the general trend (of turbulence level with axial location) was almost identical. Similar observations were made by other investigators (11-13,17,18). This is an important observation since this means that the flow demonstrates little turbulence isotropicity. Since many numerical models assume turbulence isotropicity, this puts the validity of the results of these models in question.

At first glance (at Figs. 11-13), one might be inclined to hypothesize that heat release had little effect on the mean centerline velocity in axial locations less than approximately 10 step heights from the dump plane. However, the similarity between the hot and cold flow velocities is due to the lack of combustion that occurred in the high speed potential core in the center of the flowfield. The potential core is a region of the flow where the inlet centerline velocity is maintained. The length of the potential core was on the order of 9 to 10 step heights for the reacting case and 7 to 8 step heights for the nonreacting flow. These potential core lengths are very close to the values reported by both

Stevenson et al. (17) and Nejad et al. (18).

Figure 14, photographs of the combustor cross-section at the exit plane, seems to support the potential core belief. It shows the existence of a cold potential core with rich burning pockets surrounding the core. Temperature measurements in this region could confirm this.

After the end of the non-combusting potential core, heat release had a significant effect in the center of the combustor flowfield. Figures 11-13 illustrate these differences. After $X/H = 10$, the mean axial velocities (for the reacting case) began to increase, a contradiction to the findings of other experimenters (17,18). Conservation of mass principles, however, support the results of this study. At $X/H = 10$, the time mean average flame front penetrated into the potential core and combustion effects began. At the point where heat release effects started, an increase of velocity should occur since the temperature increased (which caused a density decrease).

A deviation from the results of Stevenson et al. (17) is also shown for the axial and tangential turbulence velocities. Although in the Stevenson experiment the reacting flow turbulence intensities in the potential core were somewhat greater than in the nonreacting flow, a much larger difference was found in the present research. The larger difference between hot and cold flow turbulence intensities (in the

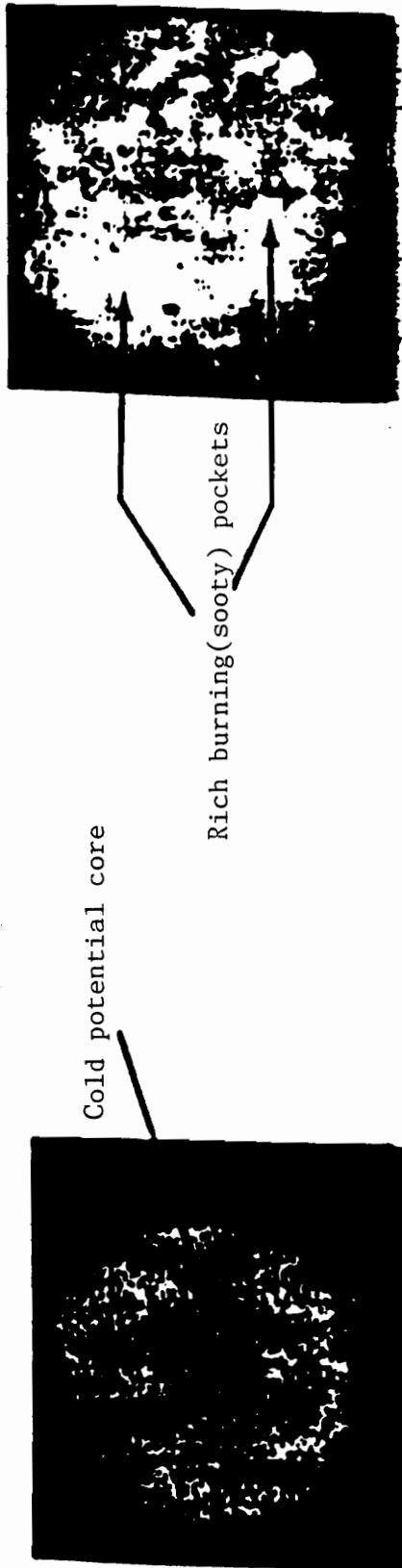


Fig. 14 Photographs of combustion process at the exit plane.

present research) may be partially magnified due to a difference in inlet velocity profiles. However, a comparison of inlet profiles can not be made since Stevenson et al. does not report an inlet turbulent velocity profile.

The difference between the hot and cold flow turbulence intensities can be attributed to the fact that the reacting flow had a more intense corner recirculation region (discussed later in this section). This more intense recirculation region had a higher turbulent energy, so more turbulence was convected into the potential core.

Outside of the potential core, the reacting flow turbulence levels showed a sharp decline just across the flame front and then a gradual rise throughout the remainder of the combustor as the turbulent velocities expanded (increased as the density decreased) with the mean velocities. The flame front is a region of high turbulence, so the sharp decline in turbulence from a location on (or very near) the flame front to a location outside of the flame front is not unexpected.

MEAN AND TURBULENT VELOCITY PROFILES

Profiles of mean velocities at various axial locations are presented in Fig. 15. More detailed profiles are shown in Appendix B. The numbers (0,1,2) shown on the abscissa represent origins for each velocity profile. For example, the first zero marks the origin for the profile taken 0.38 step heights from the dump plane. Any part of the velocity

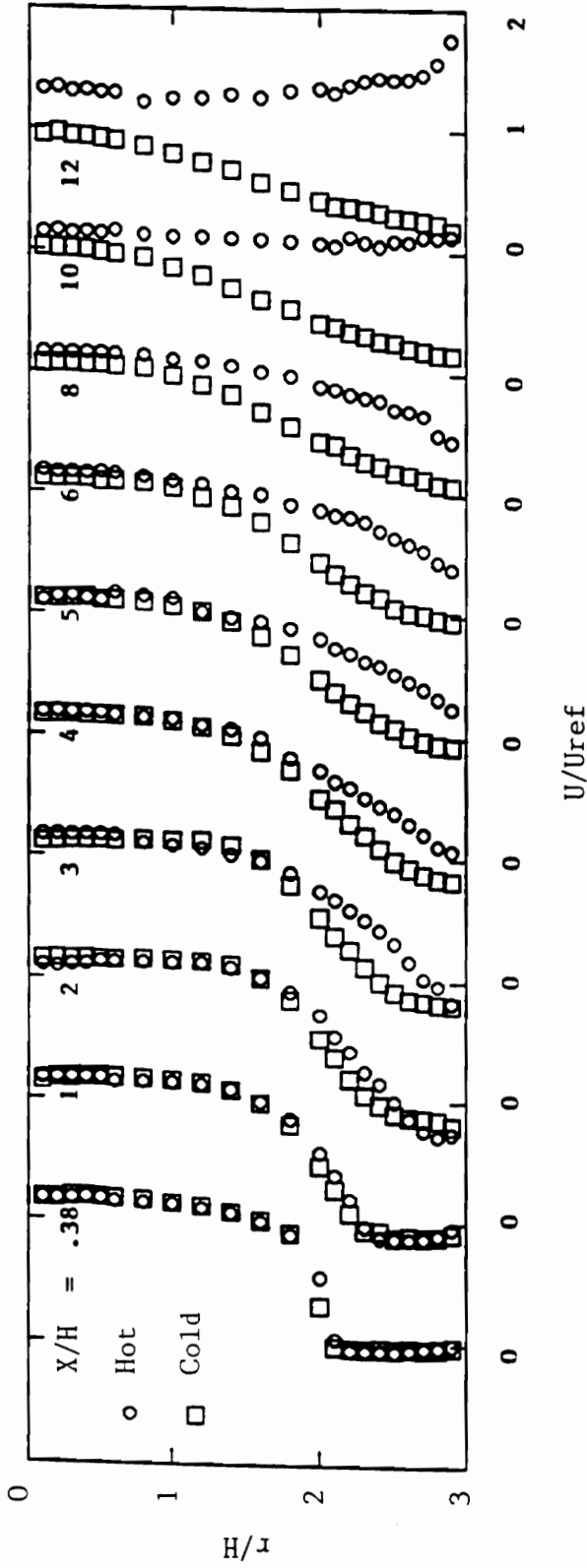


Fig. 15 Evolution of the mean axial velocity profiles.

curves located to the left of the zero tick are negative velocities and those to the right are positive velocities. Velocities were measured from the centerline to one-tenth of an inch from the combustor wall. This figure (15) shows the evolution of mean axial velocity with radial location.

At axial locations of 0.38 to 10 step heights from the dump plane, there is very little difference between the nonreacting and reacting cases in the potential core (r/H is less than 1). This is what would be expected since there was very little combustion occurring in the high speed core near the dump plane.

At axial locations greater than (about) 10 step heights, however, the velocities near the centerline began to deviate from each other. This marked the end of the potential core flow (at $X/H = 9-10$) of the reacting flow, and the effects of heat release began.

There was a significant difference, on the other hand, between the hot and cold flow mean axial velocities outside of the potential core (r/H greater than 2). This became even more apparent as the flow progressed downstream. At axial locations less than 4 step heights from the dump, the high shear region between the potential core and the recirculation region (near the combustor wall) could be clearly identified. The shear region could be identified by the region of flow with the highest velocity gradient. Measurements near the

combustor wall showed rapid velocity decay and a small region of flow reversal in the corner recirculation zone. The corner recirculation region can be clearly identified in Fig. 15 and in a contour plot of constant velocity lines (Fig. 16).

The levels in Fig. 16 identify locations in the flowfield that have the same mean velocity. For example, the lines with the number 7 attached to them represent locations in the flow where the velocity was equal to the inlet centerline mean velocity (hence, UMEA for level 7 is equal to 1.00). Level 2 indicates the zero velocity contour. An extrapolation of the zero velocity line to the combustor wall defines the reattachment point. The distance from the dump plane to the reattachment point is the recirculation length. Note that the zero velocity line is different from the dividing streamline (not represented in the figure) and they only intersect at the separation and reattachment points.

As can be seen from the contour plot, the recirculation length was much shorter for the reacting flow, although the maximum negative velocity was greater. For the hot flow, the recirculation length was approximately 3.5 step heights from the dump plane, opposed to 6.75 for the cold. The trend in these results was consistent with Stevenson et al. (17) and Nejad et al. (18). The difference in recirculation zone length for the cold flow cases of the current study and that of Nejad can be probably attributed to differences in inlet

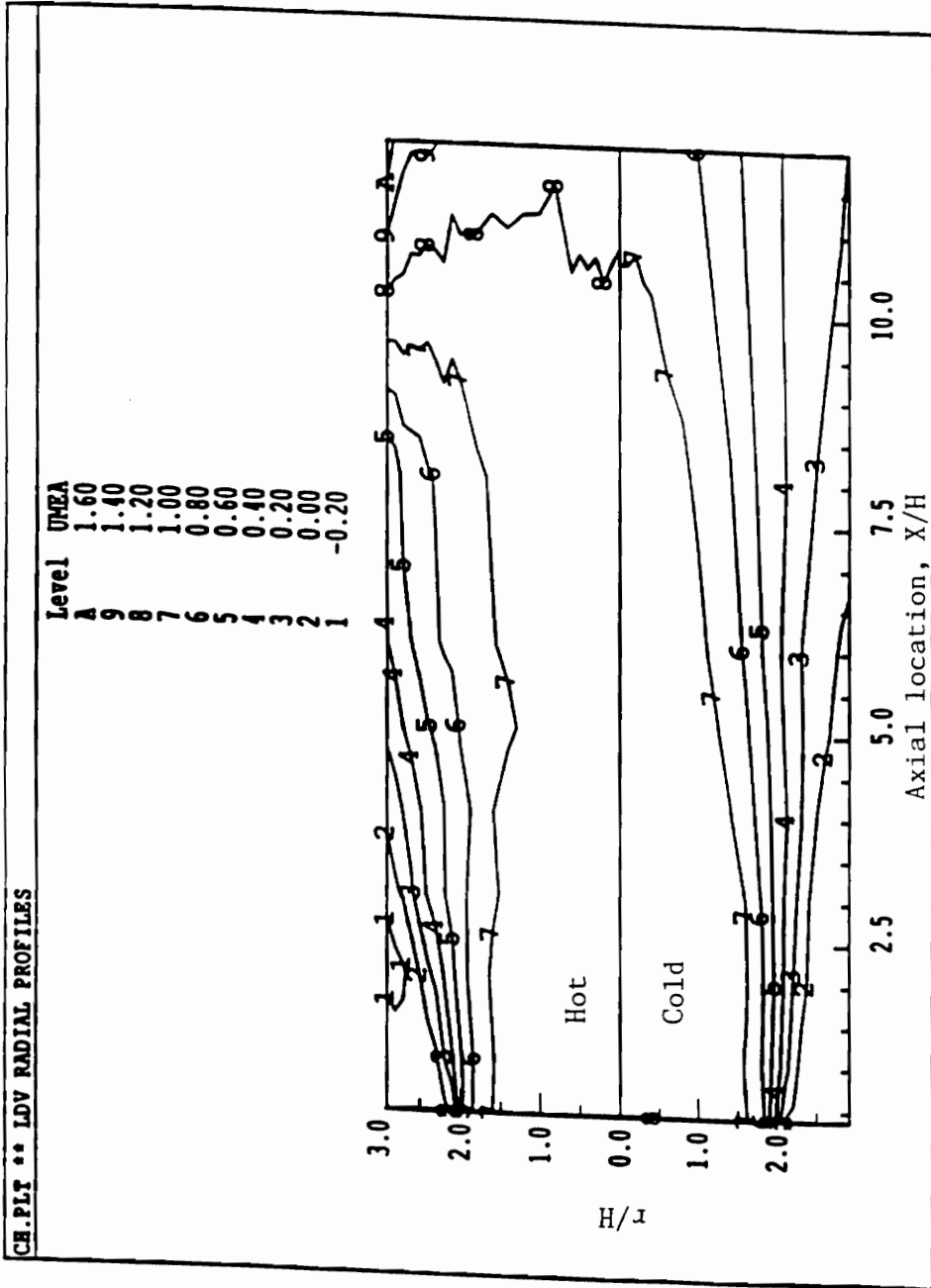


Fig. 16 Contour plot of the constant velocity lines.

profiles and to the fact that the Nejad experiment used a very small matrix (of velocity measurement locations) to extrapolate the zero velocity line to the combustor wall.

Table I gives a comparison of the corner recirculation zone (CRZ) length for a number of studies. Although not shown in the table, Pitz and Daily (16) also reported results showing a similar trend for reattachment with combustion. However, their experiments were performed on reacting turbulent flows after a reattachment-facing step. The variance in the results of Table I can be attributed to fuel type, equivalence ratio, and inlet flow conditions. As mentioned earlier, most previous studies do not include inlet velocity profiles, so it is difficult to conclude how the aforementioned factors affect corner recirculation zone length.

A decrease in corner recirculation zone length with combustion was not reported by all researchers. Smith and Giel (13) found the corner recirculation zone length to increase with combustion, however, their experiments were not performed in a true dump combustor. Their combustor had a high velocity annulus air jet that expanded into a central low velocity fuel stream. Schulz (41) found no significant change in length while studying a sudden-expansion combustor with a diameter ratio of 10, which is very large for aerospace applications.

TABLE I**CORNER RECIRCULATION ZONE LENGTH**

Reference	CRZ Length(X/H)	Diameter Ratio	Phi	Fuel
current study	6.7	1.5	0.00	
current study	3.5	1.5	0.65	propane
Nejad et al.(18)	8.2	1.5	0.00	
Nejad et al.(18)	3.7	1.5	0.65	propane
Stevenson et al.(17)	8.6	2.0	0.00	
Stevenson et al.(17)	7.4	2.0	0.28	propane
Smith and Giel(13)	4.0	2.0	0.00	
Smith and Giel(13)	8.0	2.0	0.12	hydrogen
Schulz(41)	1.0	10.0	0.00	

The turbulent velocity profiles are shown in Figs. 17 and 18. Although a direct comparison between Figs. 17 and 18 is somewhat difficult, one should try to recognize that the axial turbulent velocities were generally greater than the corresponding tangential turbulent velocities, although the maximum turbulence levels occurred at the same radial position. Furthermore, in the beginning region of the core flow (where X/H is less than 5), heat release had only a small effect on both the axial and tangential turbulent intensities, with the exceptions of intensities at $X/H = 1$ and 2. At these locations, the mean axial velocities (Fig. 15) were at their peak negative values. Therefore, these locations ($X/H = 1$ and 2) mark the most intense region of the recirculation zone. Hence, more turbulent energy is convected into the core at these axial locations. A direct comparison with the results of Stevenson et al. (17) and Nejad et al. (18) could not be made since both experiments only reported velocity results in a sparse matrix.

In the vicinity of the high shear region there is a significant difference between reacting and nonreacting turbulence levels. As the flow progressed downstream from the dump plane, the location of the maximum turbulence level (which usually corresponds with the high shear region) shifted towards the wall much sooner for the reacting flow. Since the shear region roughly coincides with the dividing streamline,

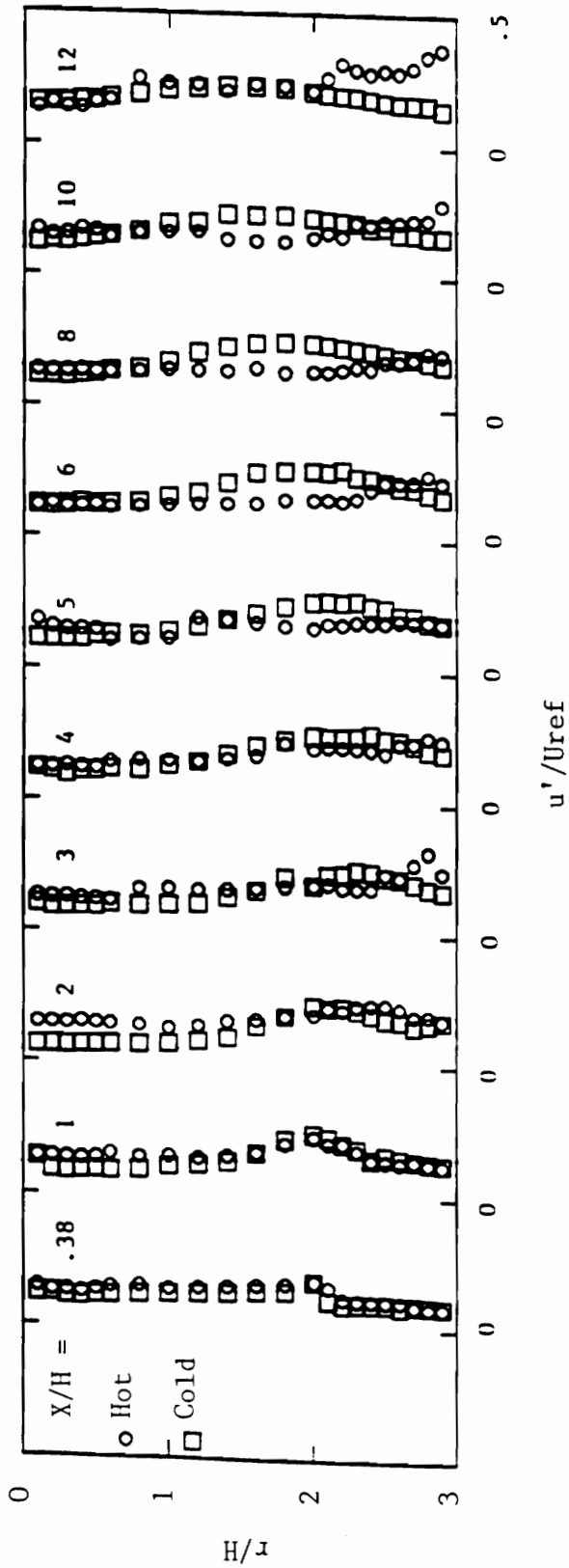


Fig. 17 Evolution of the axial turbulence profiles.

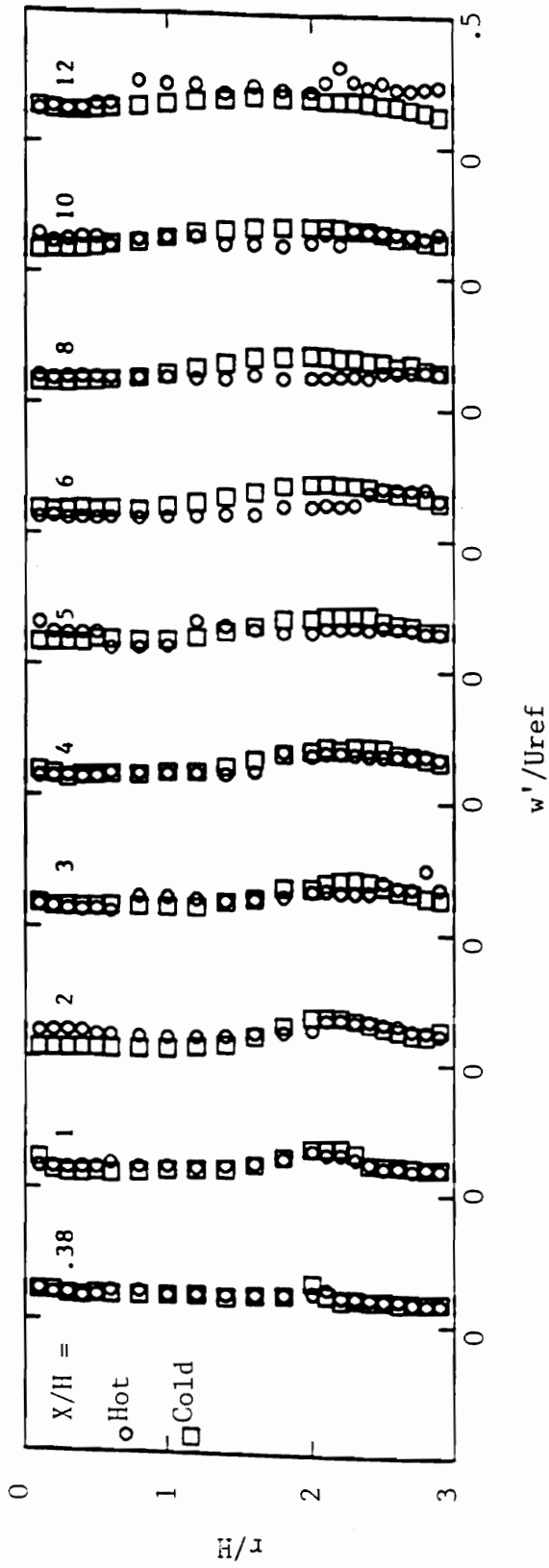


Fig. 18 Evolution of the tangential turbulence profiles.

this suggests a smaller recirculation region. Similar trends were found by Stevenson et al. (17) and Nejad et al. (18).

Further downstream, where X/H is greater than 4, combustion decreased the turbulent levels. This is not a surprise since the recirculation zone length for the reacting case was only 3.5 step heights, while recirculation continued until nearly 7 step heights for the nonreacting case. After the flame front penetrated the potential core, at locations after 10 step heights from the dump, the axial and tangential turbulent velocities expanded (increased as the density decreased) along with the mean velocities.

The turbulent levels near the combustor wall also seem to be affected by combustion, with an apparent increase at some downstream locations (where X/H is greater than 6). Stevenson et al. (17) also encountered this same trend. One possible explanation for this is that the turbulent boundary layer created along the combustor wall after the reattachment point was much more intense for the reacting flow. Not only were the mean velocities greater (at these locations) for the reacting case, but so was the distance from the reattachment point. This means that the boundary layer had more "time" to grow and become more intense. Some of the turbulent energy was being convected radially inward from the very thin boundary layer and appeared as an increase in turbulence in the near wall region.

CHAPTER VI

CONCLUSIONS

The main concern of this study was to document the effects of heat release on the combustor flowfield. Subsonic, recirculating flow experiments were conducted in an axisymmetric dump combustor with a combustor to inlet diameter ratio of 1.5. The fuel/air mixture was supplied at an inlet velocity of 60 ft./sec. with an equivalence ratio of 0.65. From the LDA velocity measurements, it is possible to make various observations and conclusions.

1) Heat release has a significant effect on the corner recirculation region. Therefore, since the recirculation region acts as the main flame holder in the dump combustor, heat release has a significant effect on combustor blow-out limits, stability, and efficiency. The reattachment length was about 6.75 step heights for the isothermal flow and 3.5 for the combusting flow, a 52 percent reduction. Furthermore, maximum negative velocities were greater for the reacting case. Hence, the combusting flow had a shorter, but more intense, recirculation region.

2) The mean and turbulent velocity measurements clearly identified the potential core for both the nonreacting and reacting flows. The potential core is a region in the flowfield where the inlet centerline velocity is maintained and, for the reacting case, very little combustion occurs.

The potential core existed until about 9 to 10 step heights for the reacting flow and 7 to 8 step heights for the nonreacting flow. The small difference in the potential core lengths is due to the small amount of heat expansion that occurred in this region.

3) In the far field, at axial positions greater than 4 step heights from the dump, the combusting flow had lower turbulence levels (around the high shear region) than the isothermal flow values. This seems to suggest that heat release causes a substantial decrease in turbulent mixing and transport.

4) The turbulence levels (based on average inlet velocity) close to the dump plane and in the potential core for the reacting flow were greater. This can be attributed to the fact that the hot flow had a more intense and turbulent recirculation region that convected more turbulent energy into the potential core.

5) Detailed temperature measurements that are coincident with LDA velocity measurements should be taken. A dump combustor flowfield temperature map would not only help identify regions of flow such as the potential core and recirculation region, but it would also be useful in numerical modeling.

REFERENCES

- 1 Drewry, J.E., "Fluid Dynamic Characterization of Sudden-Expansion Ramjet Combustor Flowfields," AAIA Journal, Vol.16, April 1978, pp.313-319.
- 2 Pennucci, M.A., "Parametric Evaluation of Total Pressure Loss and Recirculation Zone Length in a Sudden-Expansion Combustor," Air Force Institute of Technology, GAE-74S-5, Sept. 1974.
- 3 Phaneuf, J.T. and Netzer, D.W., "Flow Characterization in Solid Fuel Ramjets," Naval Postgraduate School, NPS-57-NT74081, July 1974.
- 4 Boaz, L.D., "An Investigation of the Internal Ballistics of Solid Fuel Ramjets," Naval Postgraduate School, NPS-57-NT73031A, March 1973.
- 5 Yang, B.T. and Yu, M.H., "The Flowfield in a Suddenly Enlarged Combustion Chamber," AIAA Journal, Vol.21, Jan. 1983, pp.92-97.
- 6 Samimy, M., Nejad, A.S., Langenfeld, C.A., and Favaloro, S.C., "Oscillatory Behavior of Swirling Flows in a Dump Combustor," AIAA 88-0189, 1988.
- 7 Lilley, D.G., "Swirling Flows in Typical Combustor Geometries," AIAA 85-0184, Jan. 1985.
- 8 Smyth, R., "Turbulent Flow Over a Plane Symmetric Sudden Expansion," Journal of Fluids Engineering, Vol.101, Sept. 1979, pp.348-353.
- 9 Nejad, A.S., Favaloro, S.C., Vanka, S.P., Samimy, M., and Langenfeld, C., "Application of Laser Velocimetry for Characterization of Confined Swirling Flow," ASME 88-GT-159, Amsterdam, 1988.
- 10 Favaloro, S.C., Nejad, A.S., and Vanka, S.P., "An Experimental and Computational Investigation of Isothermal Swirling Flow in an Axisymmetric Dump Combustor," AIAA 89-0620, 1989.
- 11 Baker, R.J., Hutchinson, P., Khalil, E.E., and Whitelaw, J.H., "Measurements of Three Velocity Components in a Model Furnace with and without Combustion," Fifteenth Symposium on combustion, The Combustion Institute, pp.583-588, 1973.
- 12 Owen, F.K., "Laser Velocimeter Measurements of a Confined Diffusion Flame Burner," AIAA 76-33, 1976.

- 13 Smith, G.D. and Giel, T.V., "An Experimental Investigation of Reactive, Turbulent, Recirculating Jet Mixing," AEDC-TR-79-79, May 1980.
- 14 Ganji, A.R. and Sawyer, R.F., "Experimental Study of the Flowfield of a Two-Dimensional Premixed Turbulent Flame," AIAA 79-0017, 1979.
- 15 El Banhawy, Y., Sivasegaram, S., and Whitelaw, J.H., "Premixed Turbulent Combustion of a Sudden Expansion Flow," Combustion and Flame, Vol. 50, 1983, pp.153-165.
- 16 Pitz, R.W. and Daily, J.W., "Combustion in a Turbulent Mixing Layer Formed at a Rearward-Facing Step," AIAA Journal, Vol. 21, Nov. 1983, pp.1565-1570.
- 17 Stevenson, W.H., Gould, R.D., and Thompson, H.D., "Laser Velocity Measurements and Analysis in Turbulent Flows with Combustion," Part II, AFWAL-TR-82-2076, 1983.
- 18 Nejad, A.S., Ahmed, S.A., Roe, L.A., and Gabruk, R.S., "Experimental Studies of Reactive and Non-Reactive Flows in Dump Combustors," ASME Journal, 90-GT-82, 1990.
- 19 Nejad, A.S. and Davis D.L., "Velocity Bias in Two-Component Individual Realization Laser Doppler Velocimetry," Proc. of the 5th International Congress on Application of Lasers and Electro Optics, Arlington, VA, Nov. 1986.
- 20 Edwards, R.V., ed., "Report of the Special Panel on Statistical Particle Bias Problems in Laser Anemometry," ASME Journal of Fluids Engineering, Vol. 109, No. 2, June 1987, pp.89-93.
- 21 Witze, P.O., "Application of LDV to Spark-Ignition Engines," Flow Lines, TSI Incorporated, 1989.
- 22 Choudhury, P.R., Gerstein, M., and Mojaradi, R., "Transient Combustion Dynamics," Final Report AFOSR Grant 82-0222, Oct. 1985.
- 23 Flandro, G.A. and Jacobs, H.R., "Vortex Generated Sound in Cavities in Aeroacoustic: Jet and Combustion Noise: Duct Acoustic," Nagamatse, H., (Ed.), Vol. 37 of the Progress in Astronautics and Aeronautics Series, AIAA, 1975.
- 24 Dunlap, R., "Internal Flowfield Investigation," AFRPL-TR-85-079, United Technologies, Chemical System Division, San Jose, CA, 1985.

- 25 Schadow, K., "Large Scale Structure Research in Ramjet Type Flows," 21st JANNAF Combustion Meeting, JHU/APL, Laurel, MD, Oct. 1-4, 1984.
- 26 Byrne, R.W., "A Note on Longitudinal Pressure Oscillations in Ramjet Combustors", 18th JANNAF Combustion Meeting, JPL, Pasadena, Oct. 19-23, 1981.
- 27 Oppenheim, A.K. and Ghoniem, A.F., "Aerodynamic Features of Turbulent Flames," AIAA 83-0470, 1983.
- 28 Ganji, A.T. and Sawyer, R.F., "Turbulence, Combustion, Pollutant and Stability Characterization of a Premixed Step Combustor," NASA Contractors Report 3230, January 1980.
- 29 Smith, D., Marble, F., and Zukoski, E., "Vortex Driven Combustion Instabilities in Dump Combustors," ONR/NAVAIR Compact Ramjet Combustion Instabilities Conference, Naval Postgraduate School, Monterey, CA, October 24-25, 1984.
- 30 Waugh, R.C. and Brown, R.S., "Entropy Wave Instability-Comparison of Data and Analysis," 21st JANNAF Combustion Meeting, Oct. 1984.
- 31 Sajben, M., et al, "Forced Oscillation Experiments in Supercritical Diffuser Flows with Application to Ramjet Instabilities," AIAA 81-1487, July 1981.
- 32 Sajben, M., "Terminal Shock Response in Ramjet Inlets to Abrupt Perturbations," ONR/NAVAIR Compact Ramjet Combustion Instabilities Conference, Naval Postgraduate School, Monterey, CA, Oct. 24-25, 1984.
- 33 Bolgar, T.J. and Sajben, M., "The role of Convective Perturbations in Supercritical Inlet Oscillations," 21st JANNAF Combustion Meeting, JHU/APL, Laurel, MD, Oct. 1-4, 1984.
- 34 Culick, F.E.C. and Rogers, T., "The Response of Normal Shocks in Inlet Diffusers," AIAA 81-1431, July 1981.
- 35 Waugh, R.C., Brown, R.S., Hood, T.S., Flandro, G.A., Oates, G.C., and Reardon, F.H., "Ramjet Combustion Instability Investigation, Literature Survey and Preliminary Design Study," UTC CSD Report UTC/CSD-2700-IR-1, Jan. 1982.
- 36 Choudhury, P.R., "Characteristics of a Side Dump Gas Generator Ramjet," AIAA 82-1258, June 1982.

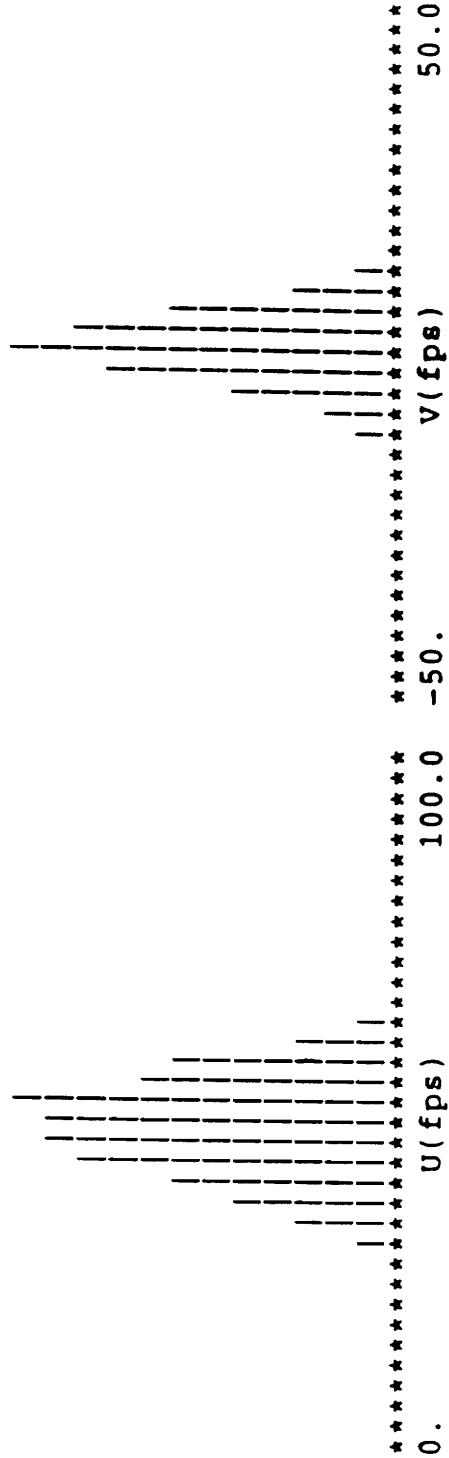
- 37 Plee, S.L. and Mellor, A.M., "Review of Flashback Reported in Prevaporized/Premixing Combustors," Combustion and Flame, Vol. 32, 1978, pp.193-203.
- 38 Coates, C.M., "Comment on Review of Flashback Reported in Prevaporized/Premixing Combustors," Combustion and Flame, Vol. 37, No. 3, 1980, pp.331-333 (Authors Reply, pp.335-336).
- 39 Keller, J.O., Vaneveld, L., Korschelt, D., Hubbard, G.L., Ghoniem, A.F., Daily, J.W., and Oppenheim, A.K., "Mechanism of Instabilities in Turbulent Combustion Leading to Flashback," AIAA 81-0107R, 1981.
- 40 Davis, D.L., "Coaxial Ramjet Combustion Instabilities Investigation," Report of AFWAL/PORT, Sept. 1984.
- 41 Schulz, R.J., "An Investigation of Ducted, Two-stream, Variable Density, Turbulent Jet Mixing with Recirculation," AEDC-TR-76-152, AFOSR-TR-76-187, ADA 034537, 1977.

APPENDIX A
VELOCITY PROBABILITY DENSITY FUNCTIONS

FILE=memory TIME=01-JUN-1990/152 13:18:04 VERSION=L1
TITLE=

BIAS CORRECTION: INTEGRATED LIMITS: ON CH-A: ON CH-B: ON
NPTS= 4096 NSAVE= 4039 RANGE= 1/ 4096 TLAST= 5.887
P=***** DP=***** T=***** X= 0.000 Y= 0.000 Z= 0.000 VREF= 0.0
FS/FV/ANG: CH-A=40.0/ 6.03/ 46. CH-B=40.0/ 5.66/ 138.
UV= -2.91 U2V= 121.1 UV2= -101.6

----- U-component ----- V-component -----
MEAN= 46.0 RMS= 46.7 MEAN= 0.7 RMS= 5.8
SIG= 8.15 TURB= 0.18 SIG= 5.76 TURB= 8.22
SKEW= -0.328 KURT= 3.30 SKEW= 0.387 KURT= 4.71

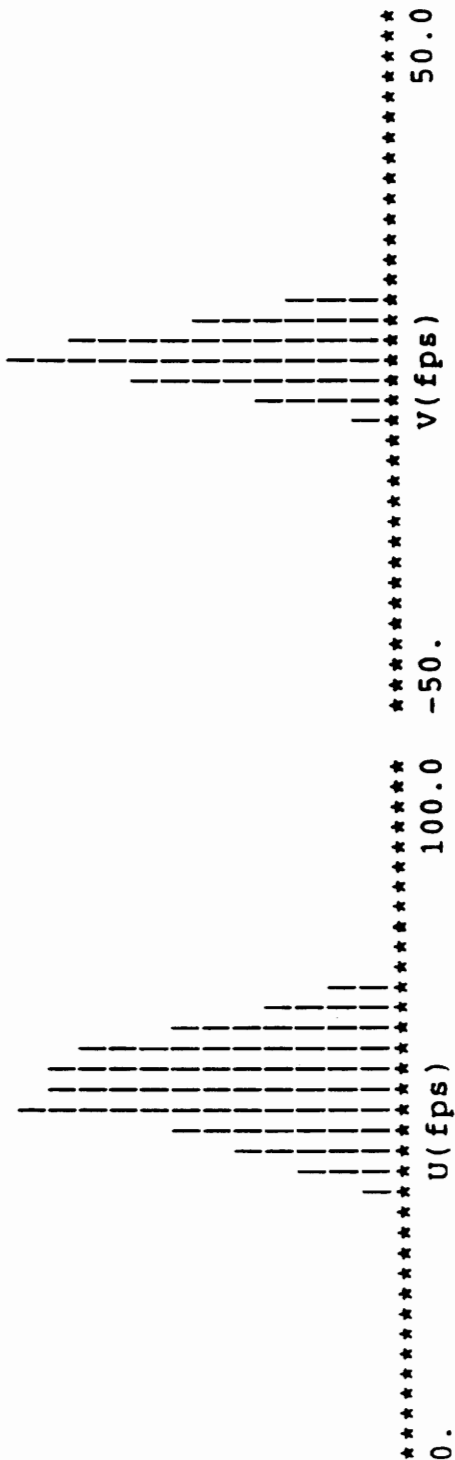


FILE=memory TIME=01-JUN-1990/152 13:18:43 VERSION=L1

TITLE=

BIAS CORRECTION: INTEGRATED LIMITS: ON CH-A: ON CH-B: ON
 NPTS= 4096 NSAVE= 4047 RANGE= 1/ 4096 TLAST= 4.081
 P=***** DP=***** T=***** X= 0.000 Y= 0.000 Z= 0.000 VREF= 0.0
 FS/FV/ANG: CH-A=40.0/ 6.03/ 46. CH-B=40.0/ 5.66/ 138.
 UV= -5.55 U2V= 97.7 UV2= -143.0

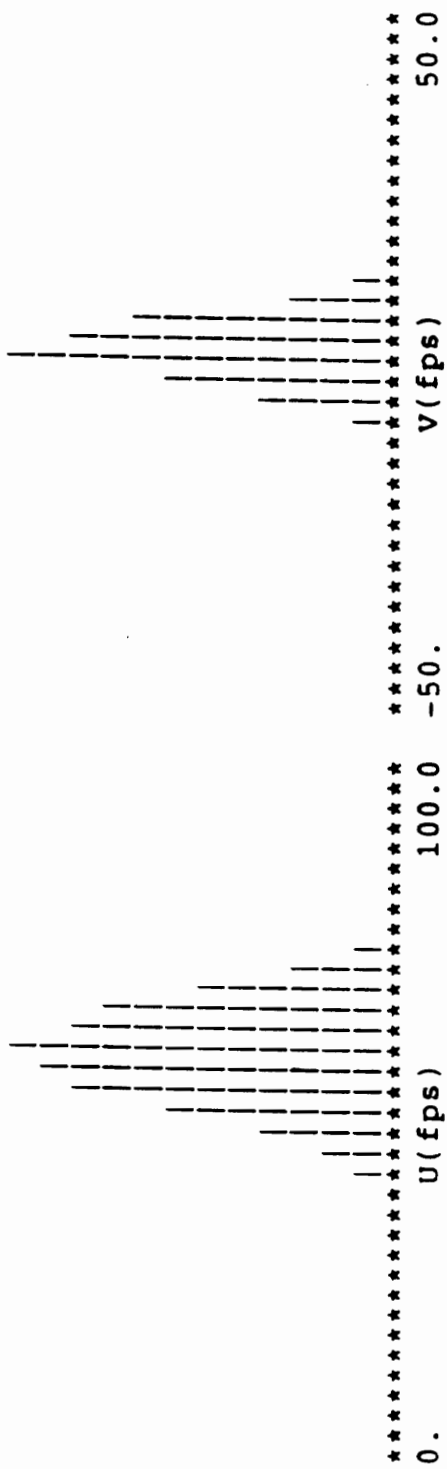
----- U-component ----- V-component -----
 MEAN= 53.5 RMS= 54.0 MEAN= 0.9 RMS= 5.4
 SIG= 7.63 TURB= 0.14 SIG= 5.35 TURB= 5.96
 SKEW= -0.429 KURT= 3.72 SKEW= 0.869 KURT= 7.62



FILE=memory TIME=01-JUN-1990/152 13:19:26 VERSION=L1
TITLE=

BIAS CORRECTION:INTEGRATED LIMITS:ON CH-A:ON CH-B:ON
NPTS= 4096 NSAVE= 4043 RANGE= 1/ 4096 TLAST= 3.806
P=***** DP=***** T=***** X= 0.000 Y= 0.000 Z= 0.000 VREF= 0.0
FS/FV/ANG:CH-A=40.0/ 6.03/ 46. CH-B=40.0/ 5.66/ 138.
UV= -2.42 U2V= 41.7 UV2= -51.2

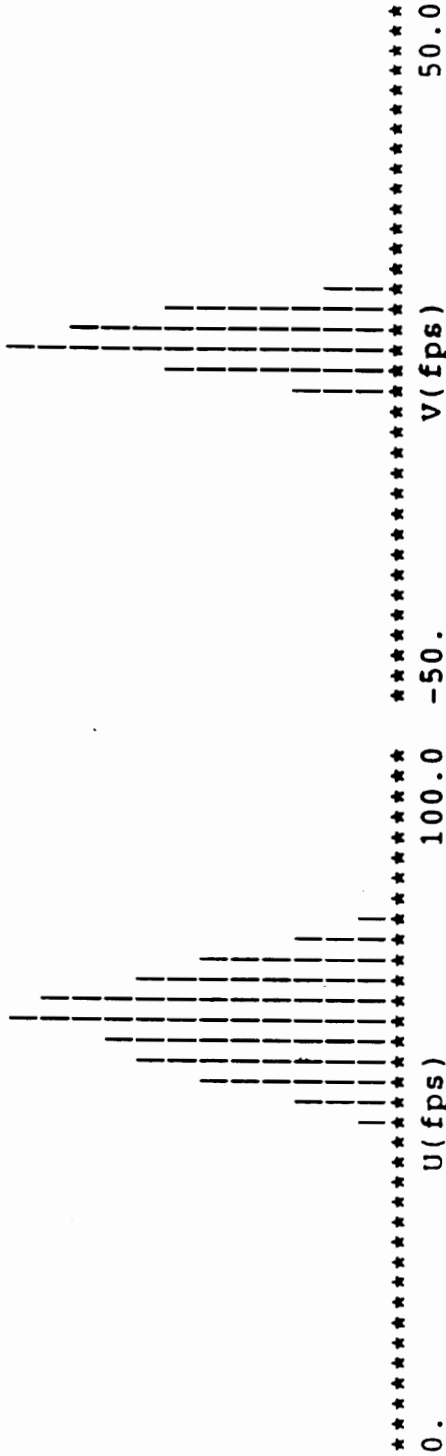
----- U-component ----- V-component -----
MEAN= 58.0 RMS= 58.5 MEAN= 1.4 RMS= 5.2
SIG= 7.48 TURB= 0.13 SIG= 5.05 TURB= 3.63
SKEW= -0.210 KURT= 3.10 SKEW= 0.224 KURT= 5.10



FILE=memory TIME=01-JUN-1990/152 13:20:13 VERSION=L1
TITLE=

BIAS CORRECTION:INTEGRATED LIMITS:ON CH-A:ON CH-B:ON
NPTS= 4096 NSAVE= 4024 RANGE= 1/ 4096 TLAST= 4.600
P=***** DP=***** T=***** X= 0.000 Y= 0.000 Z= 0.000 VREF= 0.0
FS/FV/ANG:CH-A=40.0/ 6.03/ 46. CH-B=40.0/ 5.66/ 138.
UV= -2.39 U2V= 15.1 UV2= -58.8

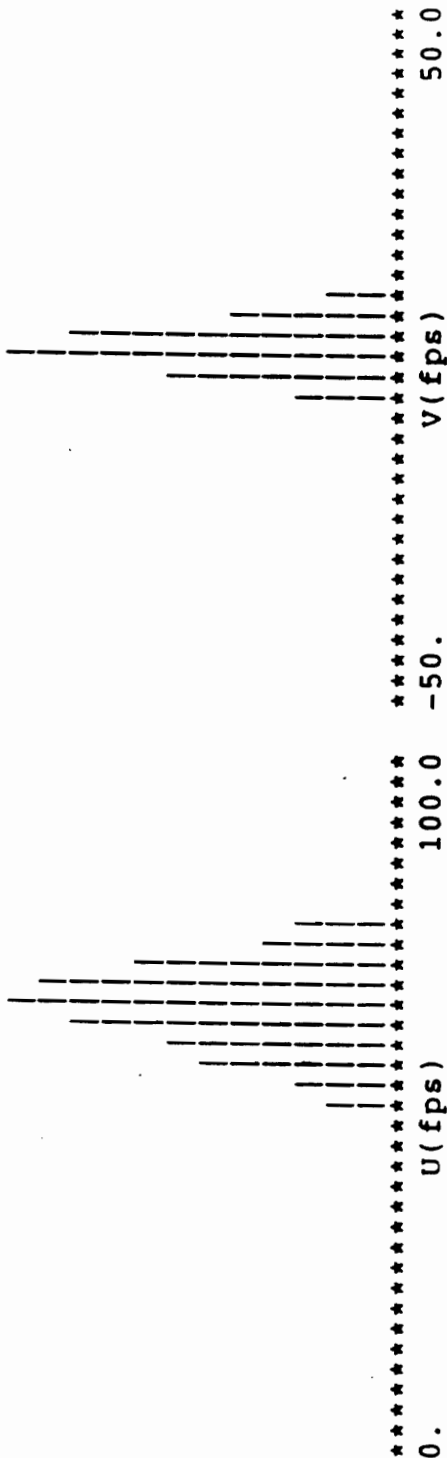
----- U-component ----- V-component -----
MEAN= 61.2 RMS= 61.6 MEAN= 1.1 RMS= 4.8
SIG= 7.08 TURB= 0.12 SIG= 4.68 TURB= 4.29
SKEW= -0.215 KURT= 3.04 SKEW= 0.012 KURT= 6.02



FILE-memory TIME-01-JUN-1990/152 13:20:40 VERSION-L1
TITLE-

BIAS CORRECTION: INTEGRATED LIMITS: ON CH-A: ON CH-B: ON
NPTS= 4096 NSAVE= 4032 RANGE= 1/ 4096 TLAST= 4.949
P=***** DP=***** T=***** X= 0.000 Y= 0.000 Z= 0.000 VREF= 0.0
FS/FV/ANG: CH-A=40.0/ 6.03/ 46. CH-B=40.0/ 5.66/ 138.
UV= -3.02 U2V= 52.6 UV2= -75.0

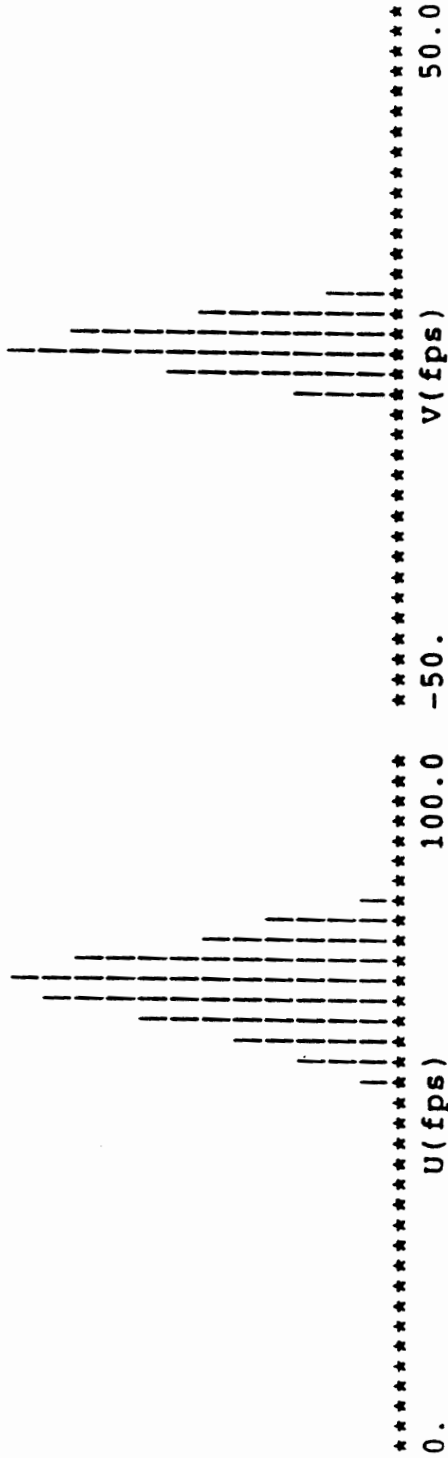
----- U-component ----- V-component -----
MEAN= 63.7 RMS= 64.1 MEAN= 0.9 RMS= 4.4
SIG= 7.07 TURB= 0.11 SIG= 4.35 TURB= 4.76
SKEW= -0.370 KURT= 3.40 SKEW= 0.684 KURT= 8.11



FILE=memory TIME=01-JUN-1990/152 13:21:16 VERSION=L1
 TITLE=

BIAS CORRECTION: INTEGRATED LIMITS: ON CH-A: ON CH-B: ON
 NPTS= 4096 NSAVE= 4035 RANGE= 1/ 4096 TLAST= 3.682
 P=***** DP=***** T=***** X= 0.000 Y= 0.000 Z= 0.000 VREF= 0.0
 FS/FV/ANG: CH-A=40.0/ 6.03/ 46. CH-B=40.0/ 5.66/ 138.
 UV= -2.71 U2V= 18.3 UV2= -47.1

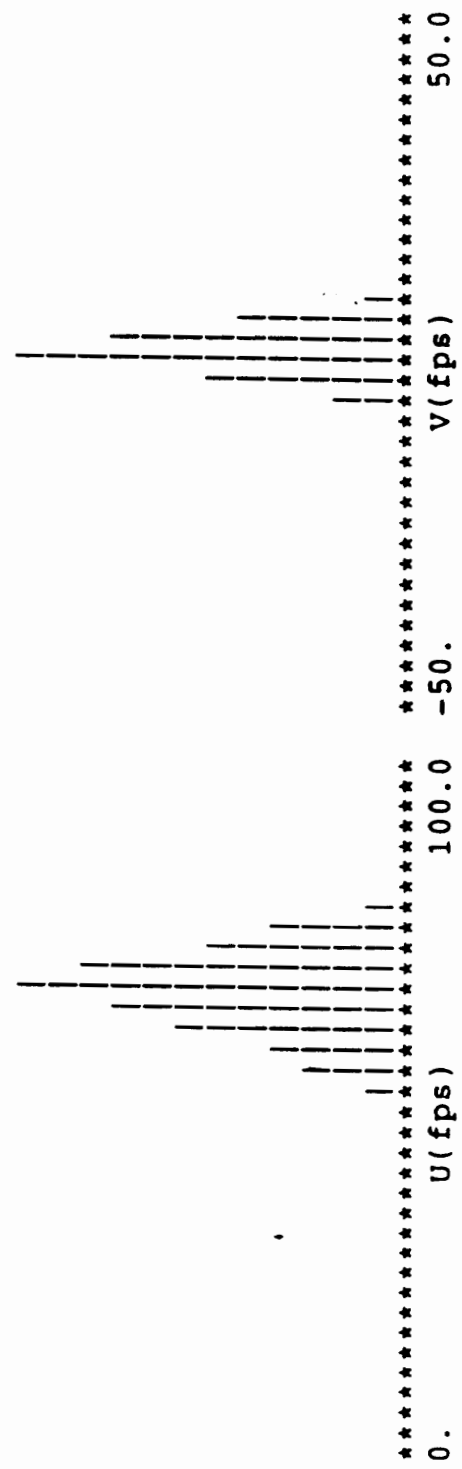
----- U-component -----	----- V-component -----
MEAN= 66.0 RMS= 66.3	MEAN= 1.2 RMS= 4.5
SIG= 6.80 TURB= 0.10	SIG= 4.33 TURB= 3.67
SKEW= -0.476 KURT= 3.68	SKEW= 0.277 KURT= 5.14



FILE=memory TIME=01-JUN-1990/152 13:21:41 VERSION=L1
 TITLE=

BIAS CORRECTION: INTEGRATED LIMITS: ON CH-A: ON CH-B: ON
 NPTS= 4096 NSAVE= 4034 RANGE= 1/ 4096 TLAST= 5.395
 P=***** DP=***** T=***** X= 0.000 Y= 0.000 Z= 0.000 VREF= 0.0
 FS/FV/ANG: CH-A=40.0/ 6.03/ 46. CH-B=40.0/ 5.66/ 138.
 UV= -5.56 U2V= 80.5 UV2= -119.7

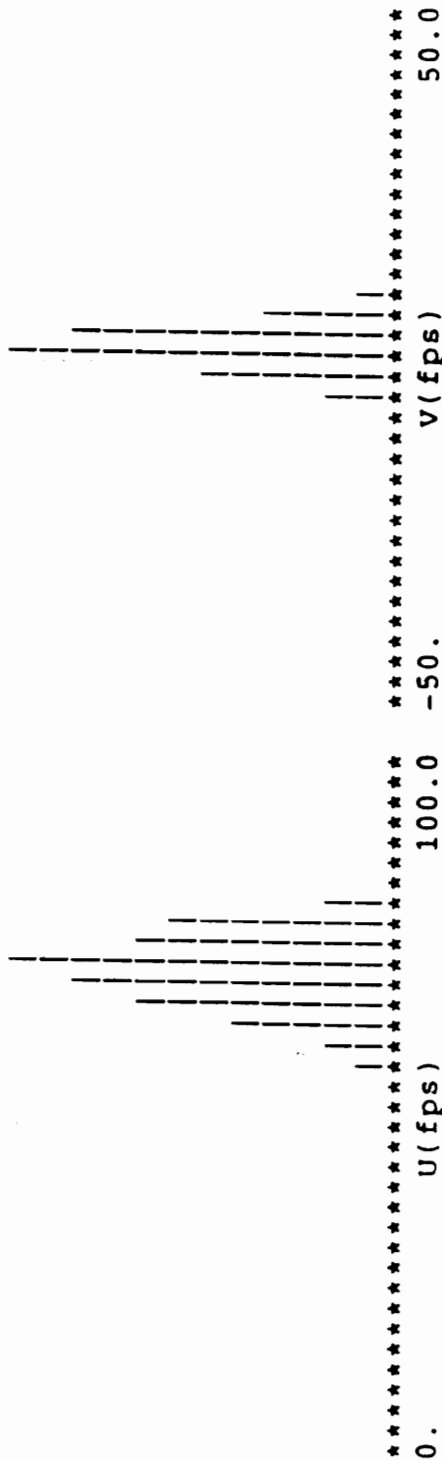
----- U-component -----	----- V-component -----
MEAN= 66.4 RMS= 66.7	MEAN= 1.1 RMS= 4.5
SIG= 6.65 TURB= 0.10	SIG= 4.38 TURB= 4.16
SKEW= -0.584 KURT= 3.83	SKEW= 0.985 KURT= 10.94



FILE=memory TIME=01-JUN-1990/152 13:22:06 VERSION=L1
TITLE=

BIAS CORRECTION:INTEGRATED LIMITS:ON CH-A:ON CH-B:ON
NPTS= 4096 NSAVE= 4023 RANGE= 1/ 4096 TLAST= 5.470
P=***** DP=***** T=***** X= 0.000 Y= 0.000 Z= 0.000 VREF= 0.0
FS/FV/ANG:CH-A=40.0/ 6.03/ 46. CH-B=40.0/ 5.66/ 138.
UV= -5.66 U2V= 85.3 UV2= -127.7

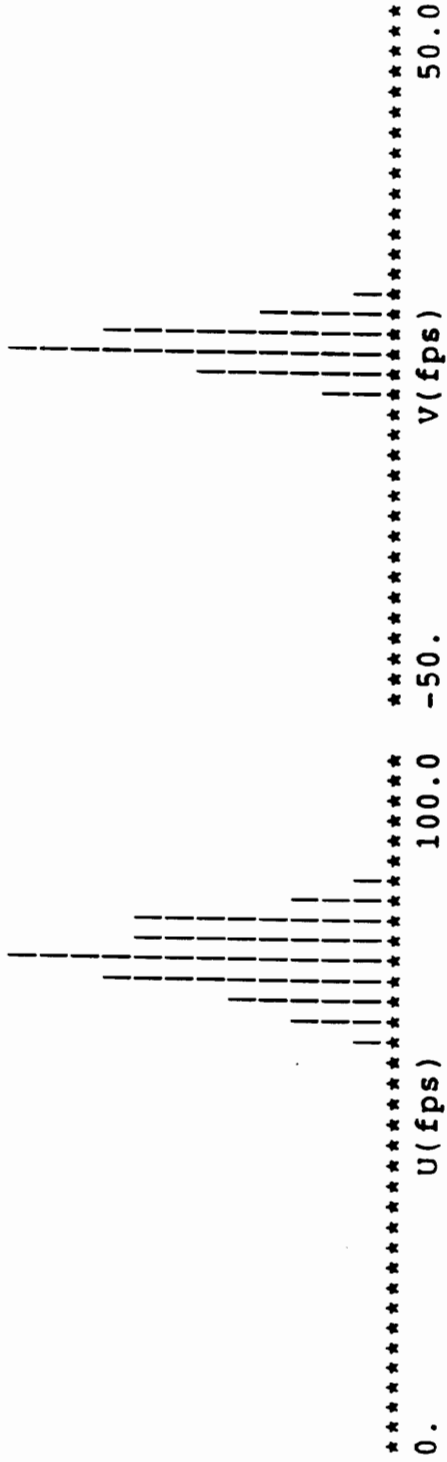
----- U-component ----- V-component -----
MEAN= 68.6 RMS= 68.9 MEAN= 1.1 RMS= 4.5
SIG= 6.45 TURB= 0.09 SIG= 4.35 TURB= 4.12
SKEW= -0.779 KURT= 5.64 SKEW= 1.160 KURT= 10.92



FILE=memory TIME=01-JUN-1990/152 13:23:04 VERSION=L1
 TITLE=

BIAS CORRECTION:INTEGRATED LIMITS:ON CH-A:ON CH-B:ON
 NPTS= 4096 NSAVE= 4011 RANGE= 1/ 4096 TLAST= 5.310
 P=***** DP=***** T=***** X= 0.000 Y= 0.000 Z= 0.000 VREF= 0.0
 FS/FV/ANG:CH-A=40.0/ 6.03/ 46. CH-B=40.0/ 5.66/ 138.
 UV= -3.96 U2V= 39.9 UV2= -78.1

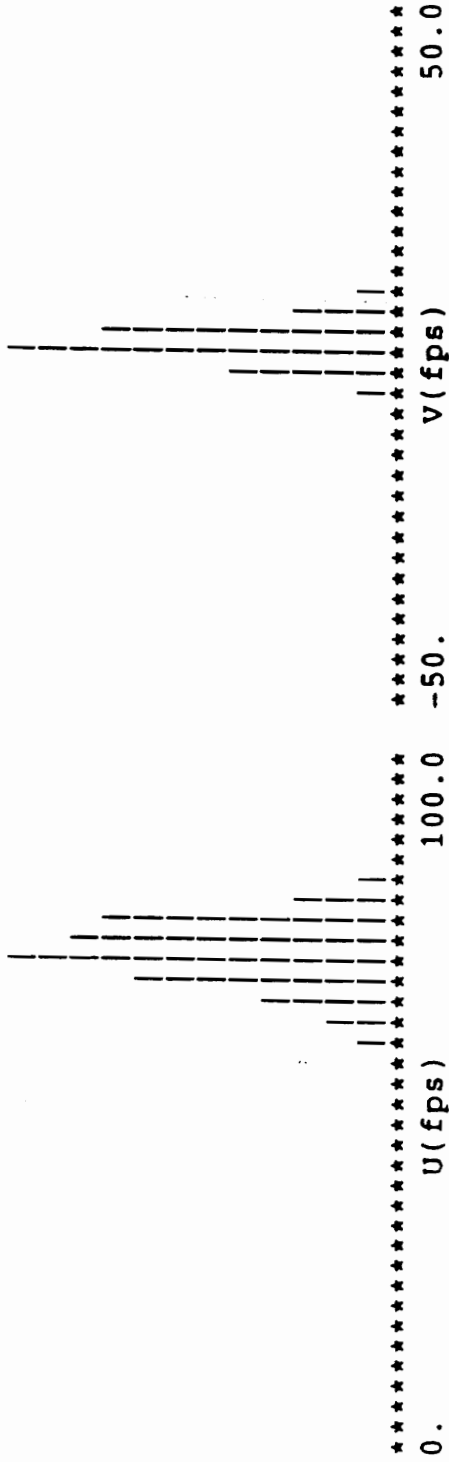
----- U-component -----	----- V-component -----
MEAN= 70.0 RMS= 70.2	MEAN= 1.1 RMS= 4.0
SIG= 5.95 TURB= 0.08	SIG= 3.85 TURB= 3.65
SKEW= -0.678 KURT= 4.63	SKEW= 0.471 KURT= 11.86



FILE-memory TIME=01-JUN-1990/152 13:23:39 VERSION=L1
 TITLE=

BIAS CORRECTION: INTEGRATED LIMITS: ON CH-A: ON CH-B: ON
 NPTS= 4096 NSAVE= 4016 RANGE= 1/ 4096 TLAST= 5.868
 P=***** DP=***** T=***** X= 0.000 Y= 0.000 Z= 0.000 VREF= 0.0
 FS/FV/ANG: CH-A=40.0/ 6.03/ 46. CH-B=40.0/ 5.66/ 138.
 UV= -4.21 U2V= 58.1 UV2= -80.0

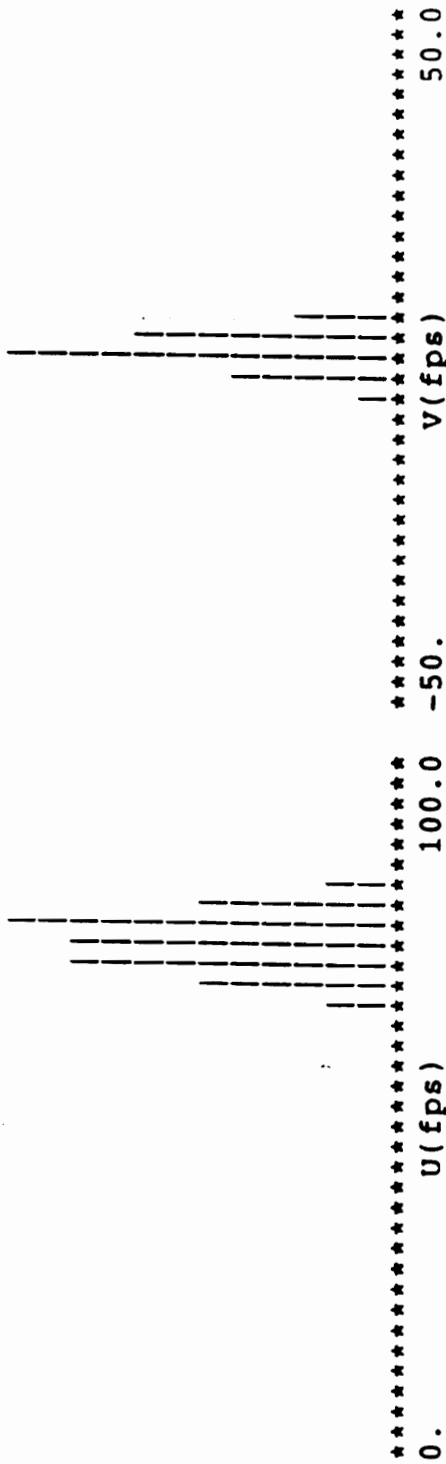
----- U-component -----	----- V-component -----
MEAN= 70.8 RMS= 71.0	MEAN= 1.0 RMS= 3.9
SIG= 5.53 TURB= 0.08	SIG= 3.82 TURB= 3.81
SKEW= -0.684 KURT= 5.26	SKEW= 0.750 KURT= 10.11



FILE-memory TIME=01-JUN-1990/152 13:24:49 VERSION=L1
 TITLE=

BIAS CORRECTION: INTEGRATED LIMITS: ON CH-A: ON CH-B: ON
 NPTS= 4096 NSAVE= 4013 RANGE= 1/ 4096 TLAST= 4.958
 P=***** DP=***** T=***** X= 0.000 Y= 0.000 Z= 0.000 VREF= 0.0
 FS/FV/ANG: CH-A=40.0/ 6.03/ 46. CH-B=40.0/ 5.66/ 138.
 UV= -4.00 U2V= 58.8 UV2= -75.8

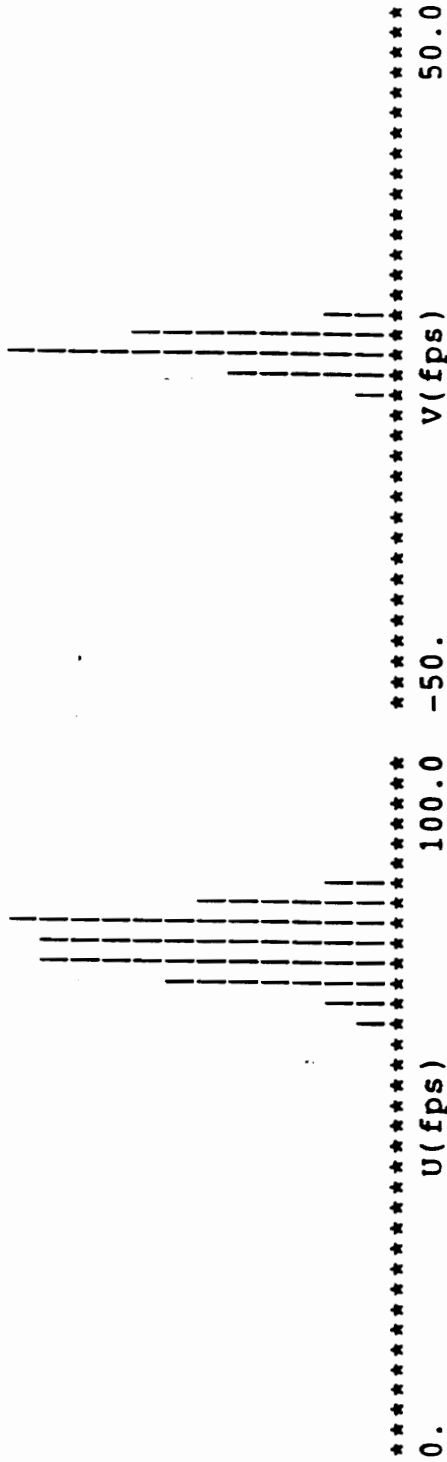
----- U-component -----	----- V-component -----
MEAN= 72.6 RMS= 72.8	MEAN= 0.8 RMS= 3.6
SIG= 5.04 TURB= 0.07	SIG= 3.55 TURB= 4.28
SKEW= -0.567 KURT= 5.01	SKEW= 1.321 KURT= 15.07



FILE=memory TIME=01-JUN-1990/152 13:25:16 VERSION=L1
TITLE=

BIAS CORRECTION:INTEGRATED LIMITS:ON CH-A:ON CH-B:ON
NPTS= 4096 NSAVE= 4024 RANGE= 1/ 4096 TLAST= 5.590
P=***** DP=***** T=***** X= 0.000 Y= 0.000 Z= 0.000 VREF= 0.0
FS/FV/ANG:CH-A=40.0/ 6.03/ 46. CH-B=40.0/ 5.66/ 138.
UV= -5.17 U2V= 76.9 UV2= -86.6

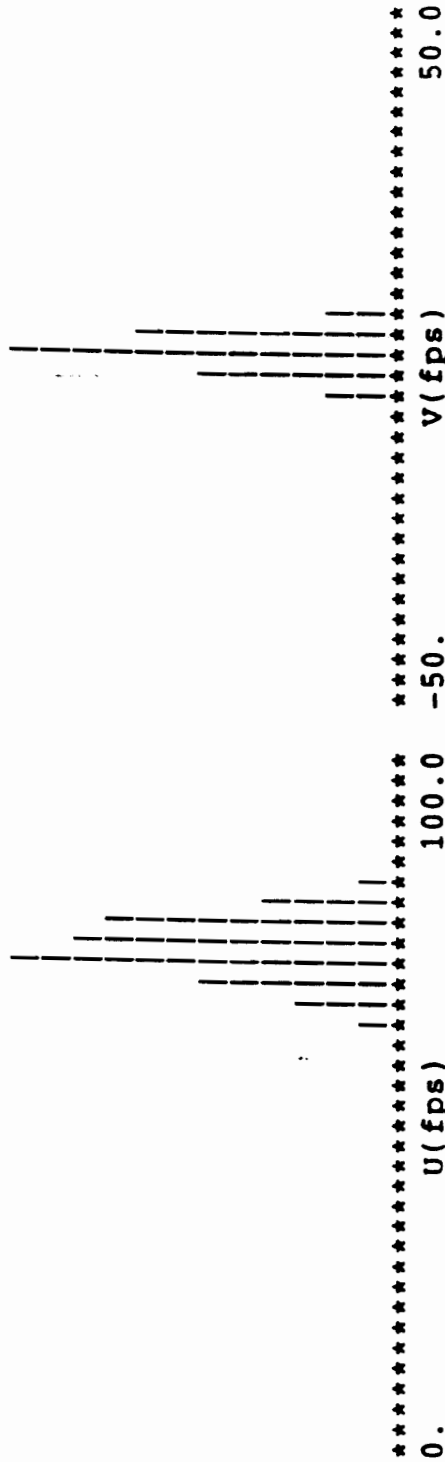
----- U-component ----- V-component -----
MEAN= 72.3 RMS= 72.5 MEAN= 0.7 RMS= 3.7
SIG= 5.13 TURB= 0.07 SIG= 3.67 TURB= 5.40
SKEW= -0.685 KURT= 5.10 SKEW= 1.472 KURT= 11.27



FILE=memory TIME=01-JUN-1990/152 13:26:38 VERSION=L1
 TITLE=

BIAS CORRECTION: INTEGRATED LIMITS: ON CH-A: ON CH-B: ON
 NPTS= 4096 NSAVE= 4000 RANGE= 1/ 4096 TLAST= 6.567
 P=***** DP=***** T=***** X= 0.000 Y= 0.000 Z= 0.000 VREF= 0.0
 FS/FV/ANG: CH-A=40.0/ 6.03/ 46. CH-B=40.0/ 5.66/ 138.
 UV= -1.95 U2V= -10.9 UV2= -89.3

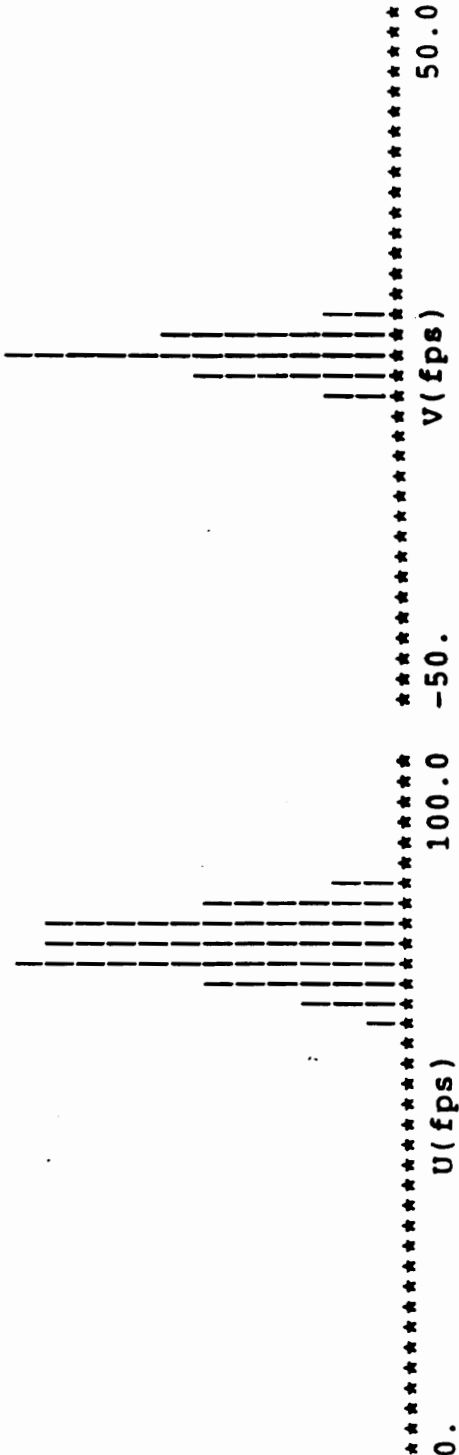
----- U-component -----	----- V-component -----
MEAN= 71.7 RMS= 71.9	MEAN= 0.3 RMS= 3.6
SIG= 5.03 TURB= 0.07	SIG= 3.60 TURB= 12.28
SKEW= -0.965 KURT= 8.81	SKEW= -0.236 KURT= 17.61



FILE-memory TIME-01-JUN-1990/152 13:27:17 VERSION=L1
TITLE-

BIAS CORRECTION: INTEGRATED LIMITS: ON CH-A: ON CH-B: ON
NPTS= 4096 NSAVE= 4029 RANGE= 1/ 4096 TLAST= 10.787
P=***** DP=***** T=***** X= 0.000 Y= 0.000 Z= 0.000 VREF= 0.0
FS/FV/ANG: CH-A=40.0/ 6.03/ 46. CH-B=40.0/ 5.66/ 138.
UV= -4.90 U2V= 69.1 UV2= -166.3

----- U-component ----- V-component -----
MEAN= 72.5 RMS= 72.7 MEAN= 0.5 RMS= 4.2
SIG= 5.47 TURB= 0.08 SIG= 4.19 TURB= 8.98
SKEW= -0.960 KURT= 6.58 SKEW= 0.987 KURT= 16.40

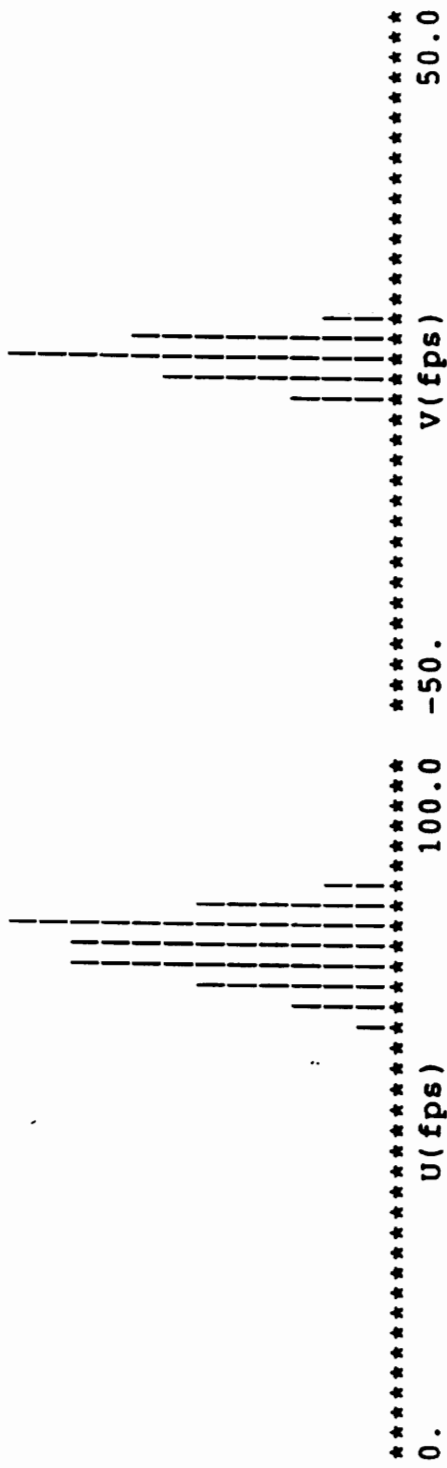


***** U(fps) ***** V(fps) *****
0. 100.0 -50. 50.0

FILE-memory TIME-01-JUN-1990/152 13:27:56 VERSION=L1
 TITLE-

BIAS CORRECTION: INTEGRATED LIMITS: ON CH-A: ON CH-B: ON
 NPTS= 4096 NSAVE= 4013 RANGE= 1/ 4096 TLAST= 8.812
 P=***** DP=***** T=***** X= 0.000 Y= 0.000 Z= 0.000 VREF= 0.0
 FS/FV/ANG: CH-A=40.0/ 6.03/ 46. CH-B=40.0/ 5.66/ 138.
 UV= -4.79 U2V= 92.8 UV2= -118.5

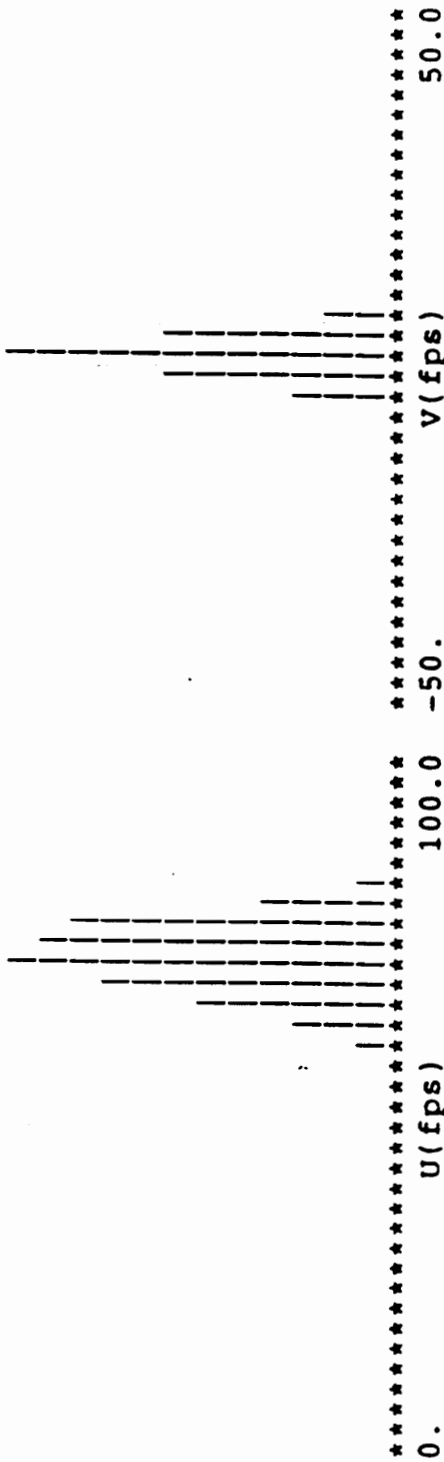
----- U-component -----	----- V-component -----
MEAN= 72.5 RMS= 72.7	MEAN= 0.3 RMS= 4.0
SIG= 5.37 TURB= 0.07	SIG= 4.03 TURB= 12.92
SKEW= -0.796 KURT= 6.07	SKEW= 1.371 KURT= 13.59



FILE-memory TIME=01-JUN-1990/152 13:28:30 VERSION=L1
 TITLE=

BIAS CORRECTION: INTEGRATED LIMITS: ON CH-A: ON CH-B: ON
 NPTS= 4096 NSAVE= 4010 RANGE= 1/ 4096 TLAST= 8.079
 P=***** DP=***** T=***** X= 0.000 Y= 0.000 Z= 0.000 VREF= 0.0
 FS/FV/ANG: CH-A=40.0/ 6.03/ 46. CH-B=40.0/ 5.66/ 138.
 UV= -5.45 U2V= 88.0 UV2= -113.8

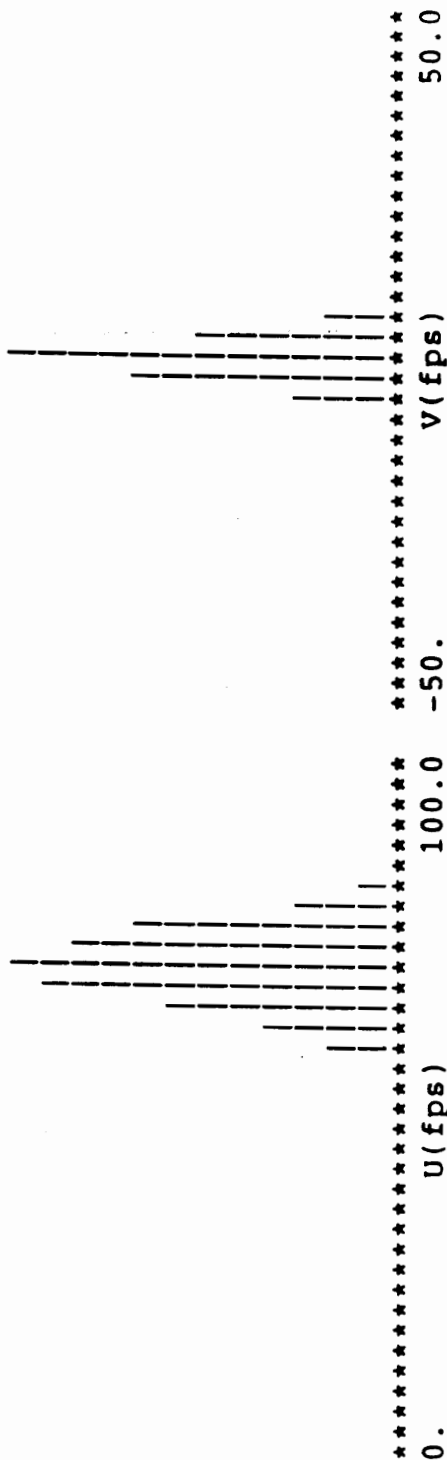
----- U-component -----	----- V-component -----
MEAN= 70.8 RMS= 71.0	MEAN= 0.1 RMS= 4.1
SIG= 5.78 TURB= 0.08	SIG= 4.07 TURB= 55.55
SKEW= -0.746 KURT= 5.04	SKEW= 1.099 KURT= 12.57



FILE=memory TIME=01-JUN-1990/152 13:29:09 VERSION=L1
 TITLE=

BIAS CORRECTION: INTEGRATED LIMITS: ON CH-A: ON CH-B: ON
 NPTS= 4096 NSAVE= 4011 RANGE= 1/ 4096 TLAST= 6.771
 P=***** DP=***** T=***** X= 0.000 Y= 0.000 Z= 0.000 VREF= 0.0
 FS/FV/ANG: CH-A=40.0/ 6.03/ 46. CH-B=40.0/ 5.66/ 138.
 UV= -3.12 U2V= 19.8 UV2= -140.6

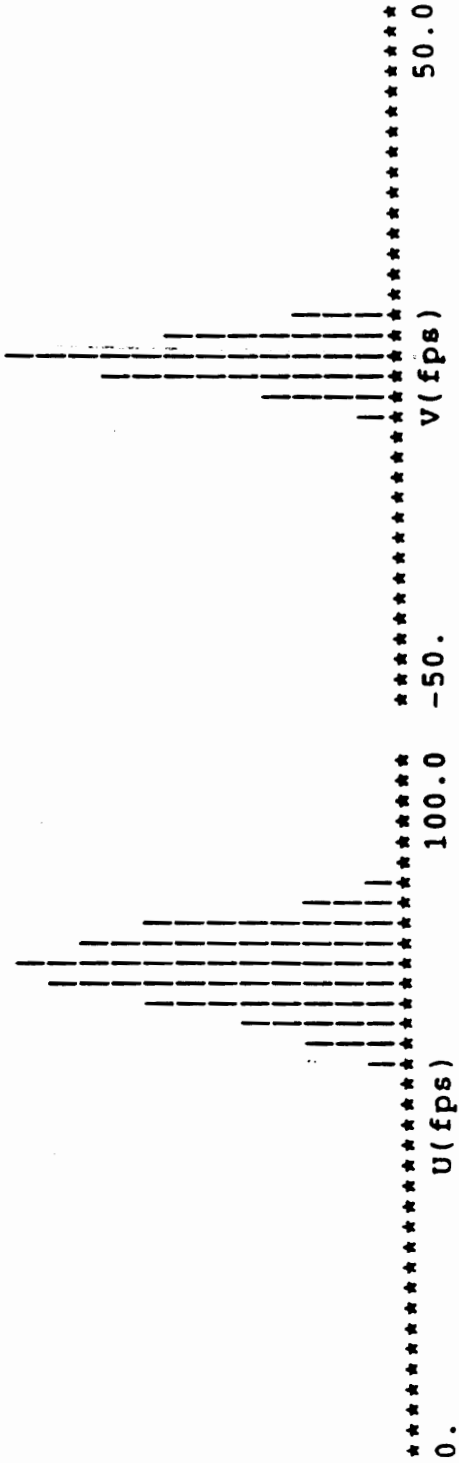
----- U-component -----	----- V-component -----
MEAN= 69.5 RMS= 69.7	MEAN= -0.3 RMS= 4.2
SIG= 6.07 TURB= 0.09	SIG= 4.19 TURB= -15.10
SKEW= -0.662 KURT= 4.50	SKEW= -0.270 KURT= 18.89



FILE-memory TIME-01-JUN-1990/152 13:29:59 VERSION-L1
 TITLE-

BIAS CORRECTION: INTEGRATED LIMITS: ON CH-A: ON CH-B: ON
 NPPTS= 4096 NSAVE= 4023 RANGE= 1/ 4096 TLAST= 10.541
 P=***** DP=***** T=***** X= 0.000 Y= 0.000 Z= 0.000 VREF= 0.0
 FS/FV/ANG: CH-A=40.0/ 6.03/ 46. CH-B=40.0/ 5.66/ 138.
 UV= -8.05 U2V= 123.8 UV2= -154.2

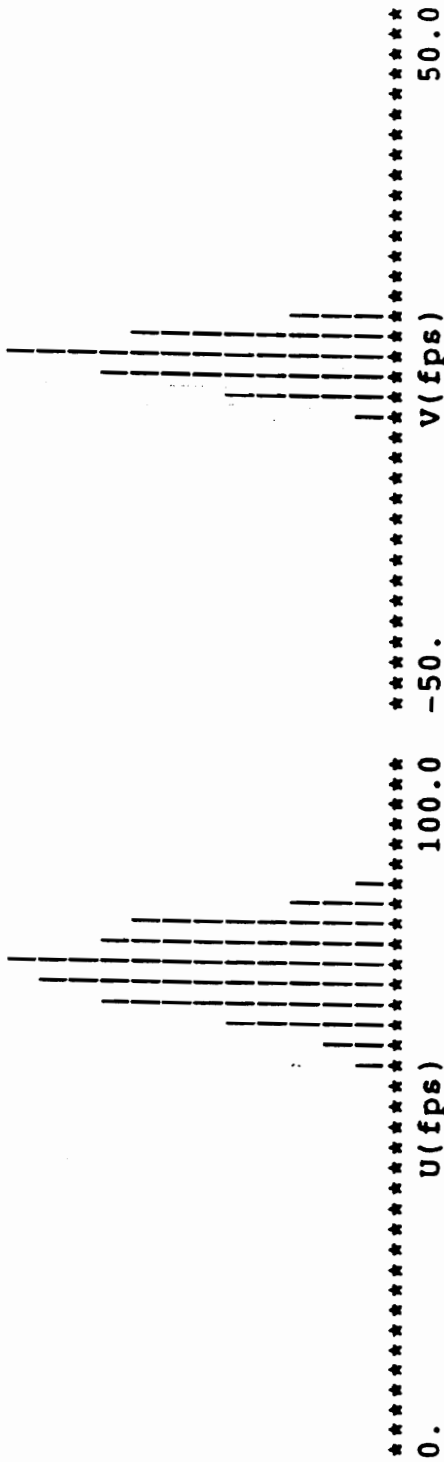
----- U-component -----	----- V-component -----
MEAN= 69.0 RMS= 69.3	MEAN= -0.3 RMS= 4.5
SIG= 6.50 TURB= 0.09	SIG= 4.54 TURB= -16.77
SKEW= -0.745 KURT= 5.49	SKEW= 1.143 KURT= 12.13



FILE-memory TIME-01-JUN-1990/152 13:30:48 VERSION=L1
 TITLE=

BIAS CORRECTION: INTEGRATED LIMITS: ON CH-A: ON CH-B: ON
 NPTS= 4095 NSAVE= 4011 RANGE= 1/ 4095 TLAST= 15.503
 P=***** DP=***** T=***** X= 0.000 Y= 0.000 Z= 0.000 VREF= 0.0
 FS/FV/ANG: CH-A=40.0/ 6.03/ 46. CH-B=40.0/ 5.66/ 138.
 UV= -5.14 U2V= 43.2 UV2= -137.4

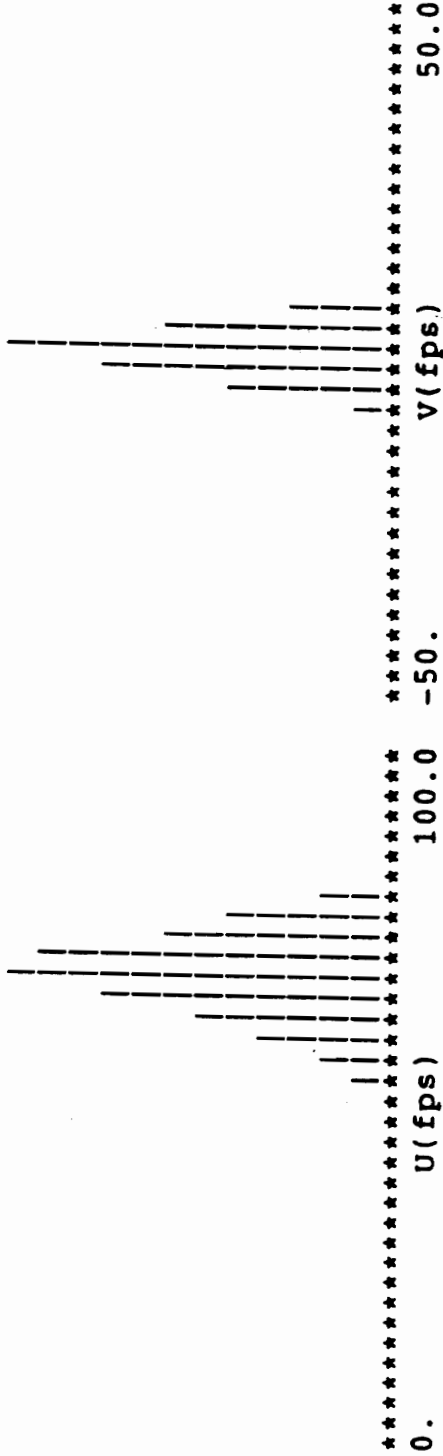
----- U-component -----	----- V-component -----
MEAN= 68.7 RMS= 69.0	MEAN= -0.4 RMS= 4.6
SIG= 6.47 TURB= 0.09	SIG= 4.54 TURB= -12.02
SKEW= -0.837 KURT= 7.20	SKEW= 0.315 KURT= 11.38



FILE=memory TIME=01-JUN-1990/152 13:31:45 VERSION=L1
 TITLE=

BIAS CORRECTION: INTEGRATED LIMITS: ON CH-A: ON CH-B: ON
 NPTS= 4096 NSAVE= 4006 RANGE= 1/ 4096 TLAST= 6.129
 P=***** DP=***** T=***** X= 0.000 Y= 0.000 Z= 0.000 VREF= 0.0
 FS/FV/ANG: CH-A=40.0/ 6.03/ 46. CH-B=40.0/ 5.66/ 138.
 UV= -22.42 U2V= 433.5 UV2= -494.9

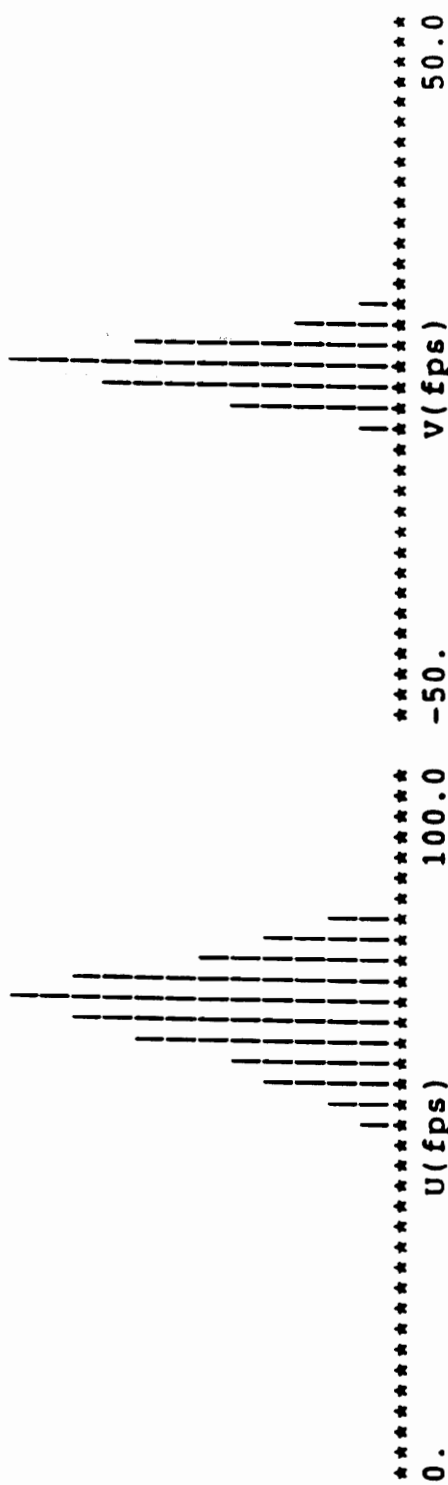
----- U-component -----	----- V-component -----
MEAN= 66.6 RMS= 67.1	MEAN= 0.2 RMS= 6.0
SIG= 7.82 TURB= 0.12	SIG= 6.03 TURB= 31.84
SKEW= -1.287 KURT= 7.19	SKEW= 2.096 KURT= 12.21



FILE-memory TIME-01-JUN-1990/152 13:32:17 VERSION-L1
 TITLE-

BIAS CORRECTION: INTEGRATED LIMITS: ON CH-A: ON CH-B: ON
 NPTS= 4096 NSAVE= 4016 RANGE= 1/ 4096 TLAST= 10.526
 P=***** DP=***** T=***** X= 0.000 Y= 0.000 Z= 0.000 VREF= 0.0
 FS/FV/ANG: CH-A=40.0/ 6.03/ 46. CH-B=40.0/ 5.66/ 138.
 UV= -30.47 U2V= 614.7 UV2= -659.6

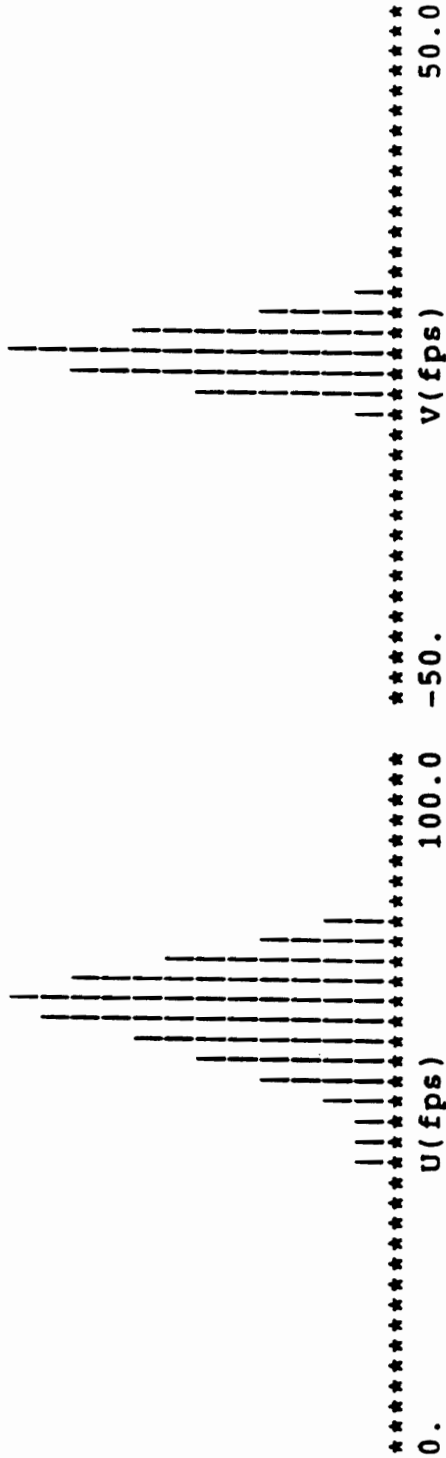
----- U-component -----		----- V-component -----	
MEAN=	65.1	RMS=	6.7
SIG=	8.47	TURB=	10.97
SKEW=	-1.124	KURT=	11.10



FILE=memory TIME=01-JUN-1990/152 13:34:06 VERSION=L1
TITLE=

BIAS CORRECTION:INTEGRATED LIMITS:ON CH-A:ON CH-B:ON
NPTS= 4096 NSAVE= 4003 RANGE= 1/ 4096 TLAST= 23.271
P=***** DP=***** T=***** X= 0.000 Y= 0.000 Z= 0.000 VREF= 0.0
FS/FV/ANG:CH-A=40.0/ 6.03/ 46. CH-B=40.0/ 5.66/ 138.
UV= -47.01 U2V= 1104.5 UV2= -1089.4

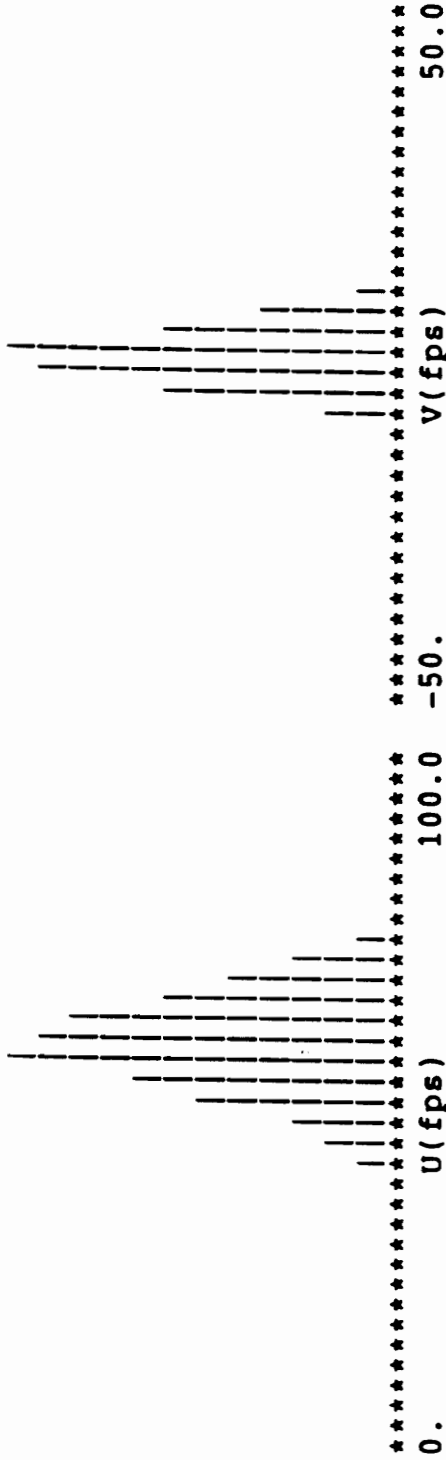
----- U-component ----- V-component -----
MEAN= 61.7 RMS= 62.4 MEAN= 1.4 RMS= 8.0
SIG= 9.63 TURB= 0.16 SIG= 7.87 TURB= 5.71
SKEW= -1.303 KURT= 6.27 SKEW= 2.086 KURT= 9.55



FILE=memory TIME=01-JUN-1990/152 13:37:46 VERSION=L1
TITLE=

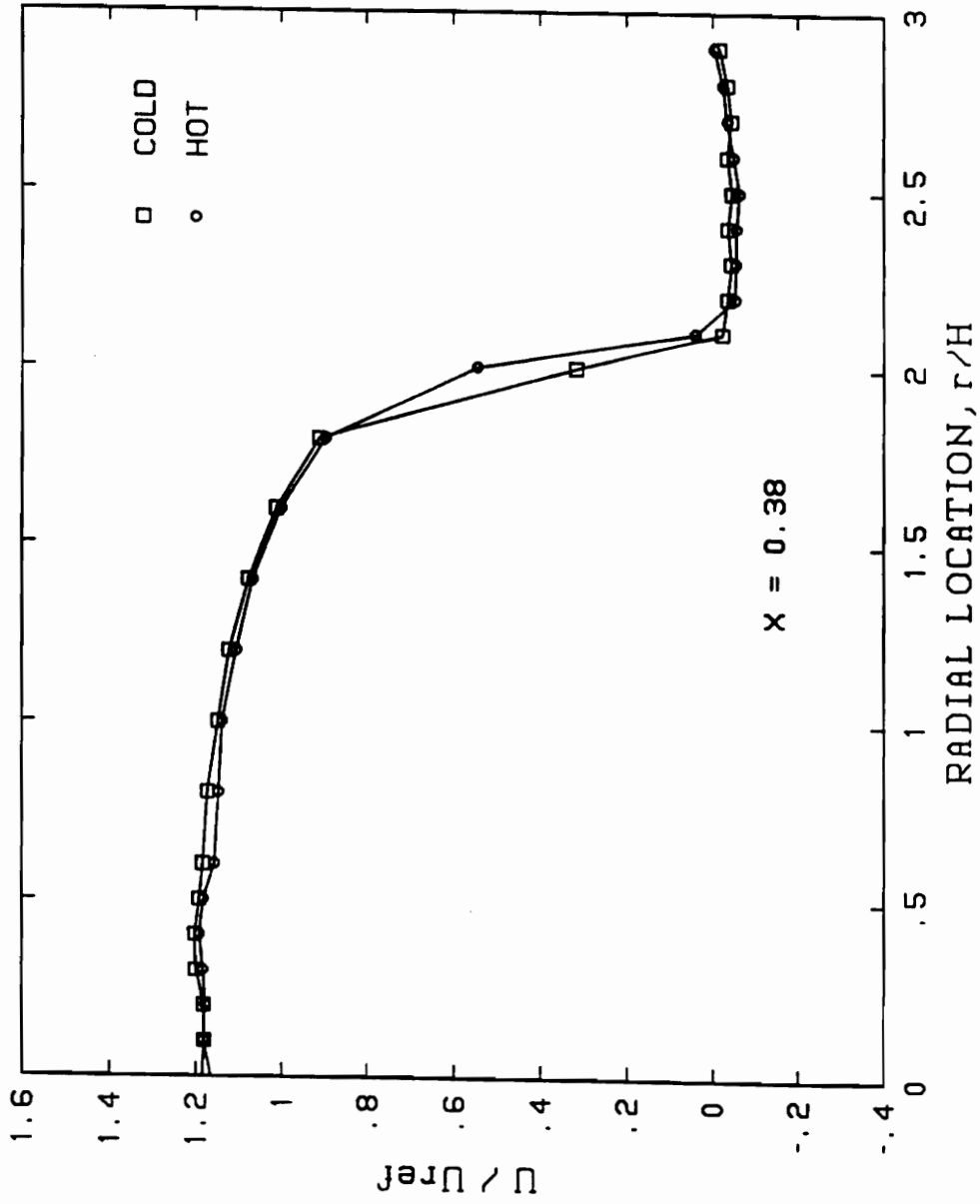
BIAS CORRECTION:INTEGRATED LIMITS:ON CH-A:ON CH-B:ON
NPTS= 1023 NSAVE= 1000 RANGE= 1/ 1023 TLAST= 77.132
P=***** DP=***** T=***** X= 0.000 Y= 0.000 Z= 0.000 VREF= 0.0
FS/FV/ANG:CH-A=40.0/ 6.03/ 46. CH-B=40.0/ 5.66/ 138.
UV= -41.41 U2V= 827.1 UV2= -877.0

----- U-component ----- V-component -----
MEAN= 56.8 RMS= 57.6 MEAN= 0.8 RMS= 7.8
SIG= 9.37 TURB= 0.16 SIG= 7.79 TURB= 9.90
SKEW= -0.947 KURT= 4.76 SKEW= 1.917 KURT= 8.36

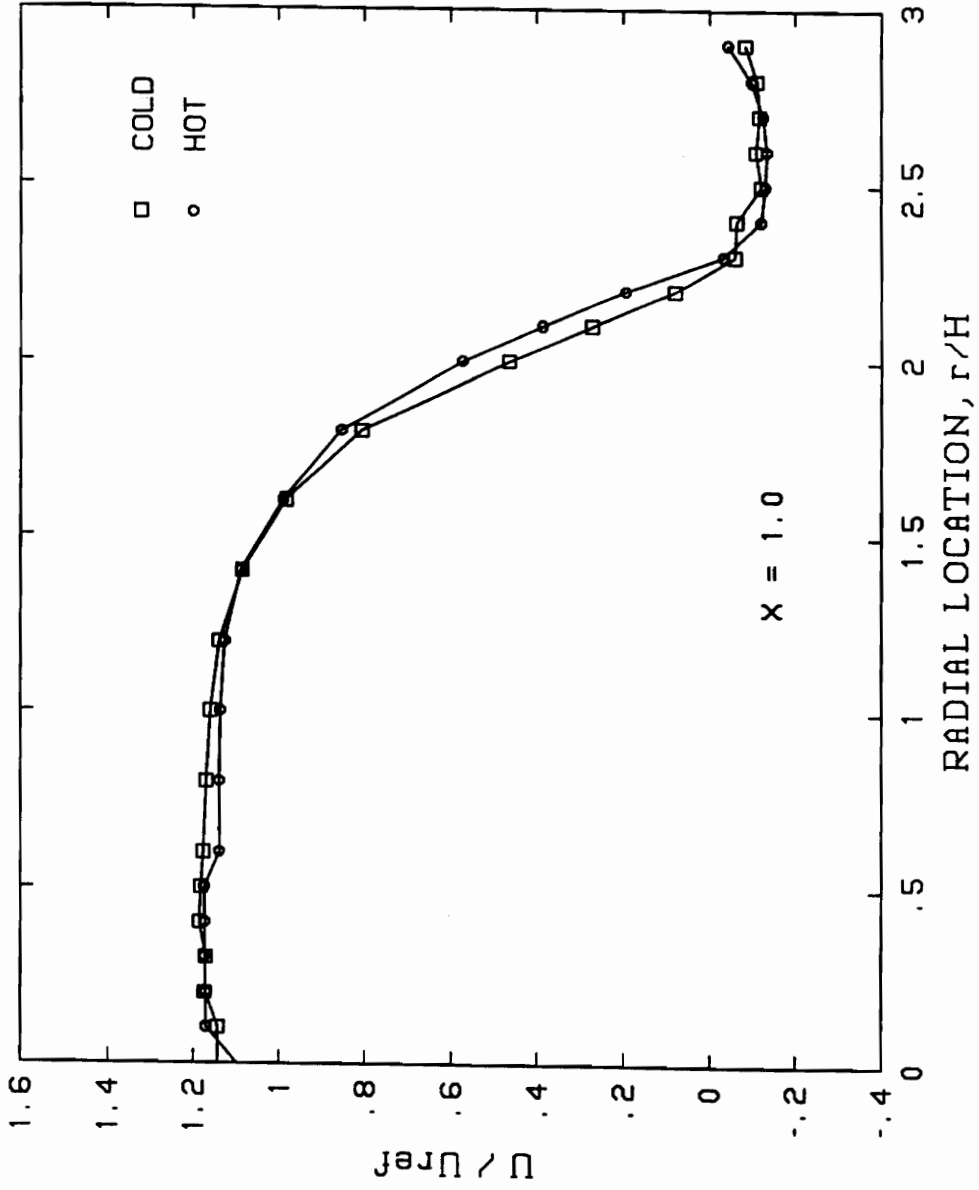


APPENDIX B
VELOCITY PROFILES

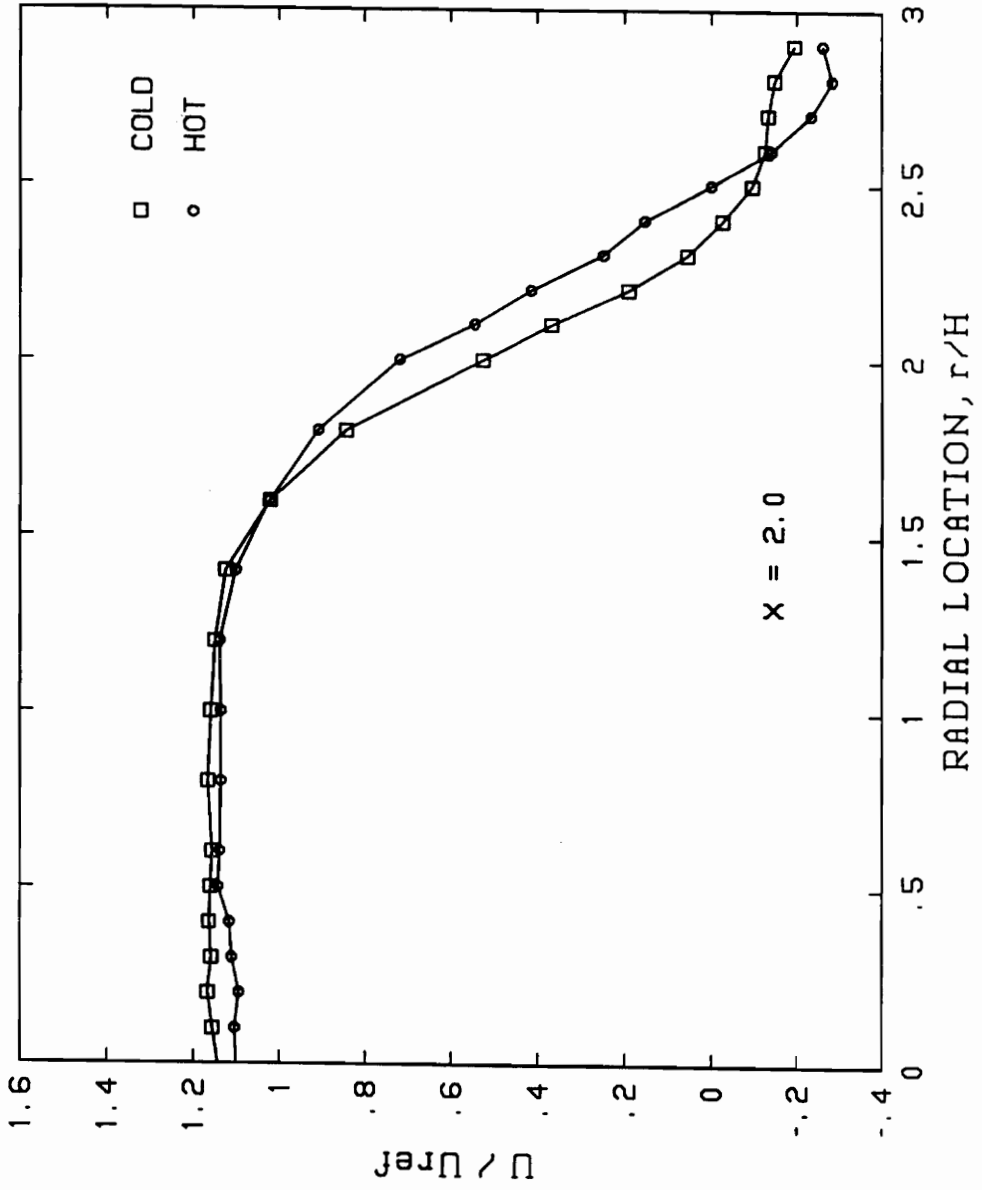
COMPARISON BETWEEN COLD AND HOT DATA



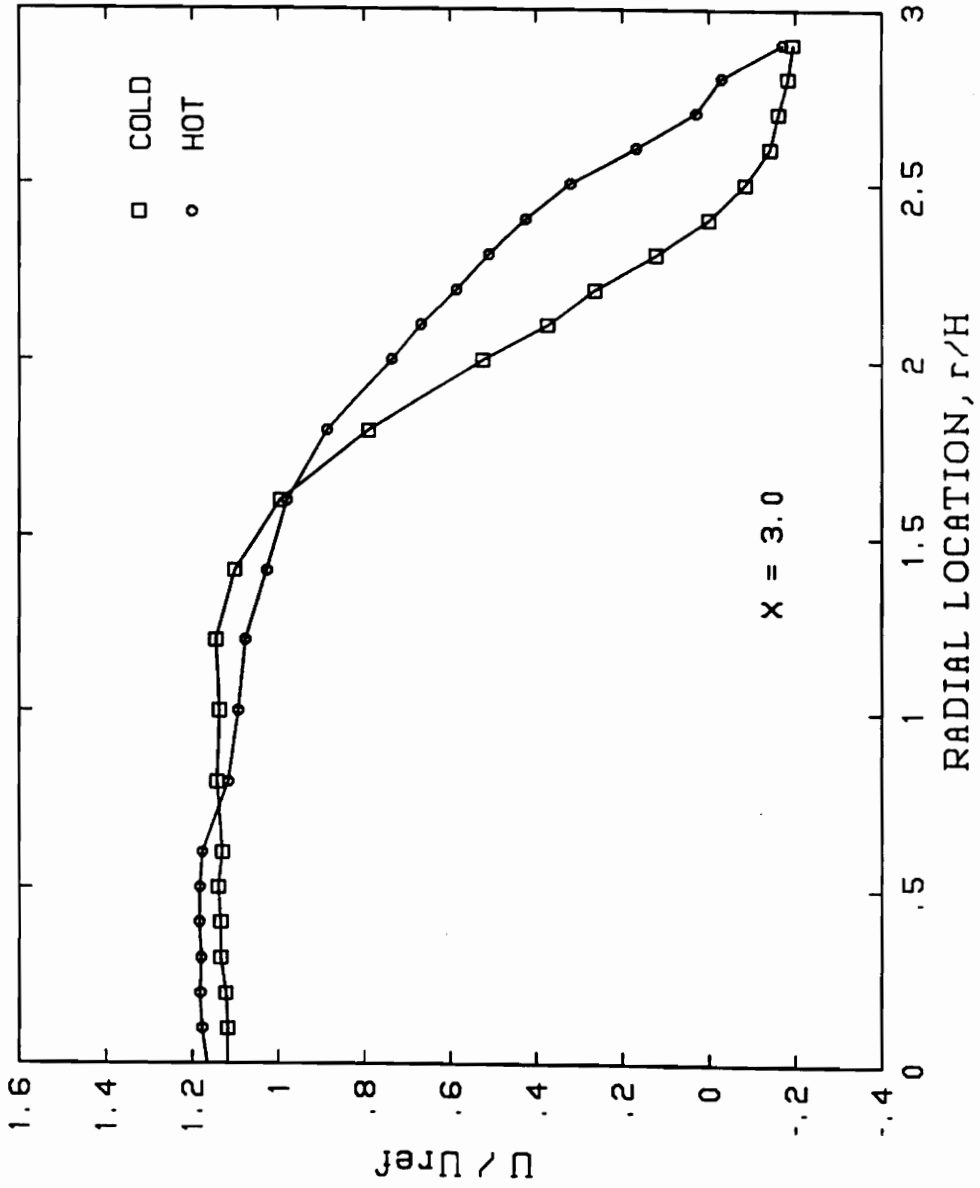
COMPARISON BETWEEN COLD AND HOT DATA



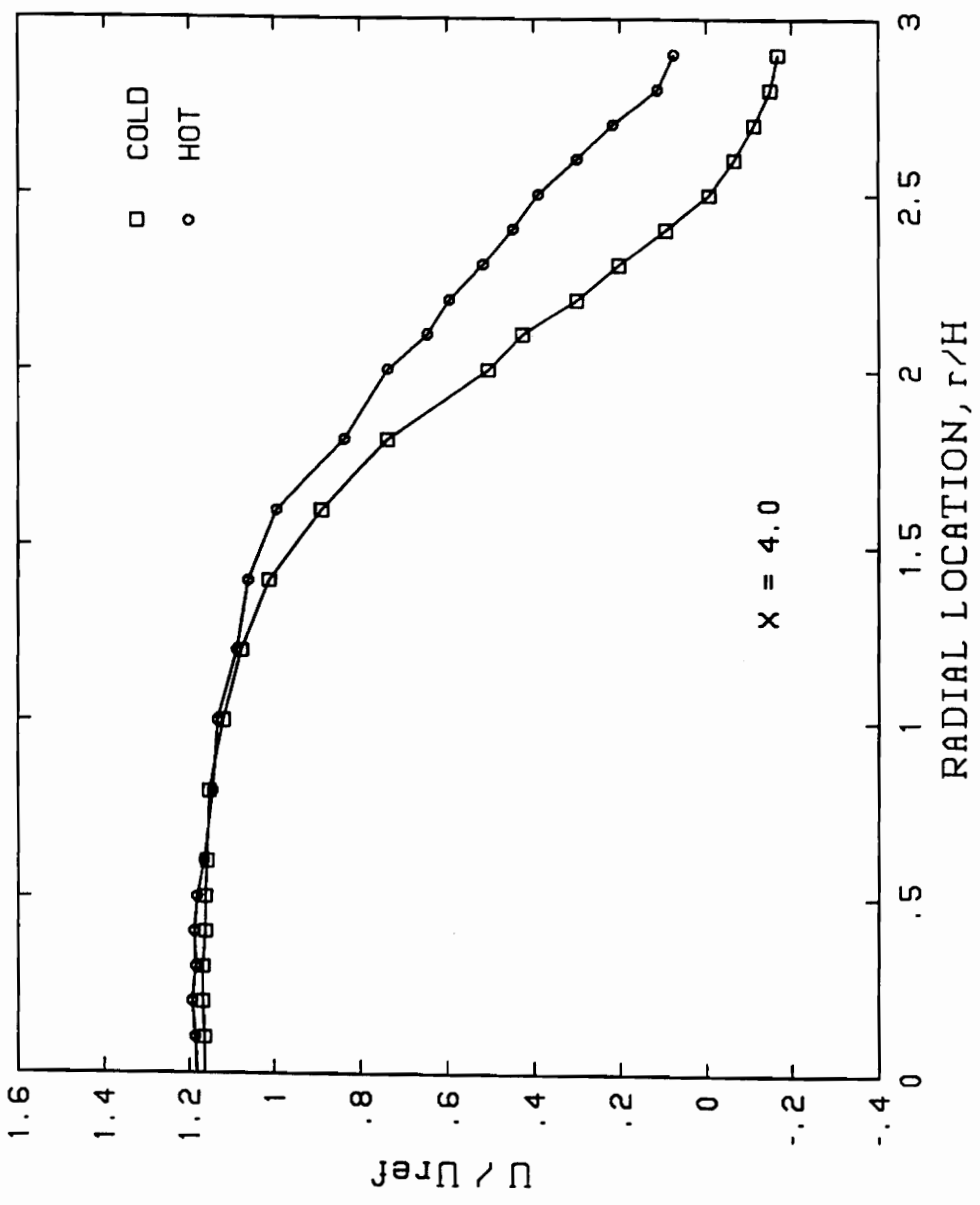
COMPARISON BETWEEN COLD AND HOT DATA



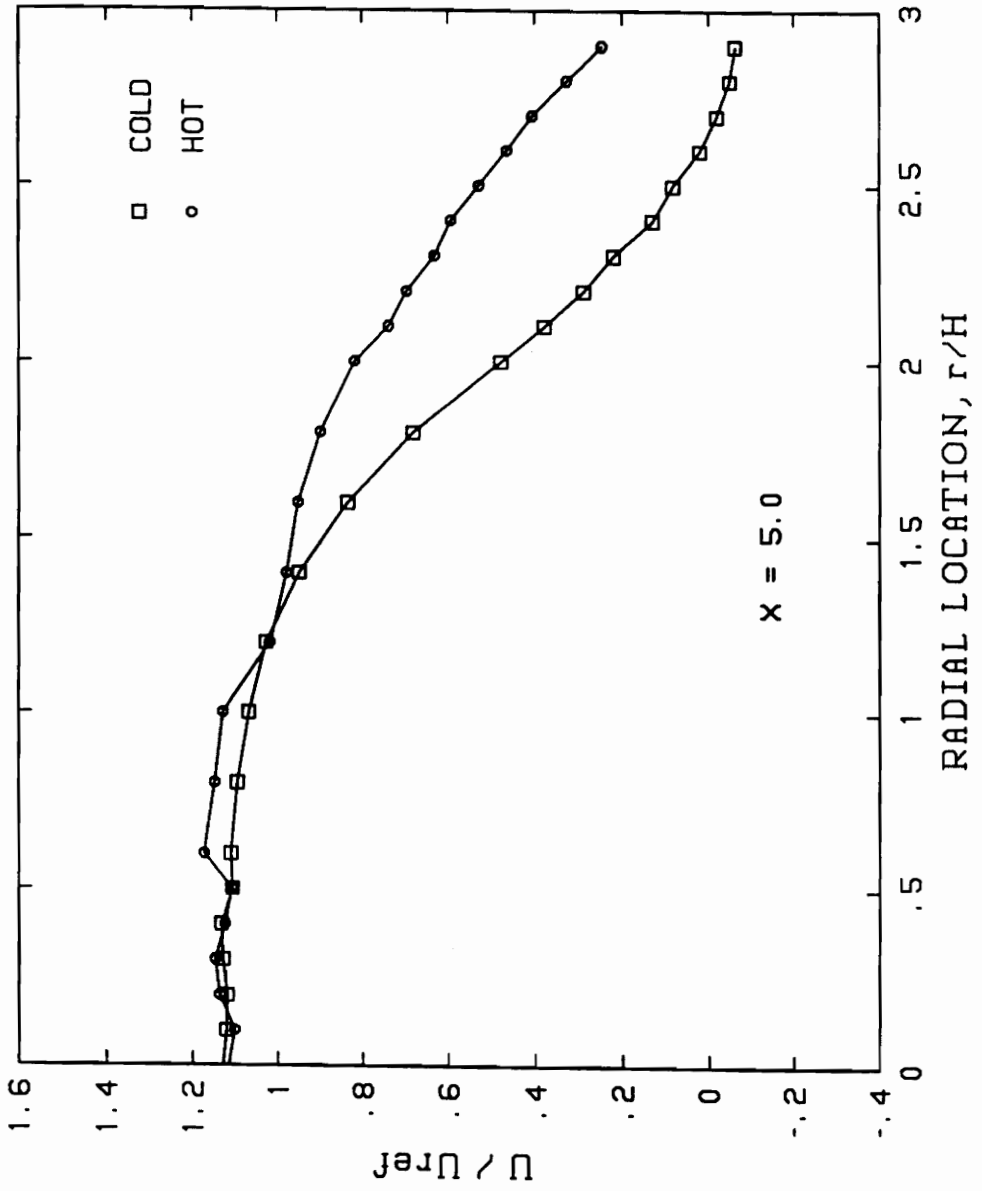
COMPARISON BETWEEN COLD AND HOT DATA



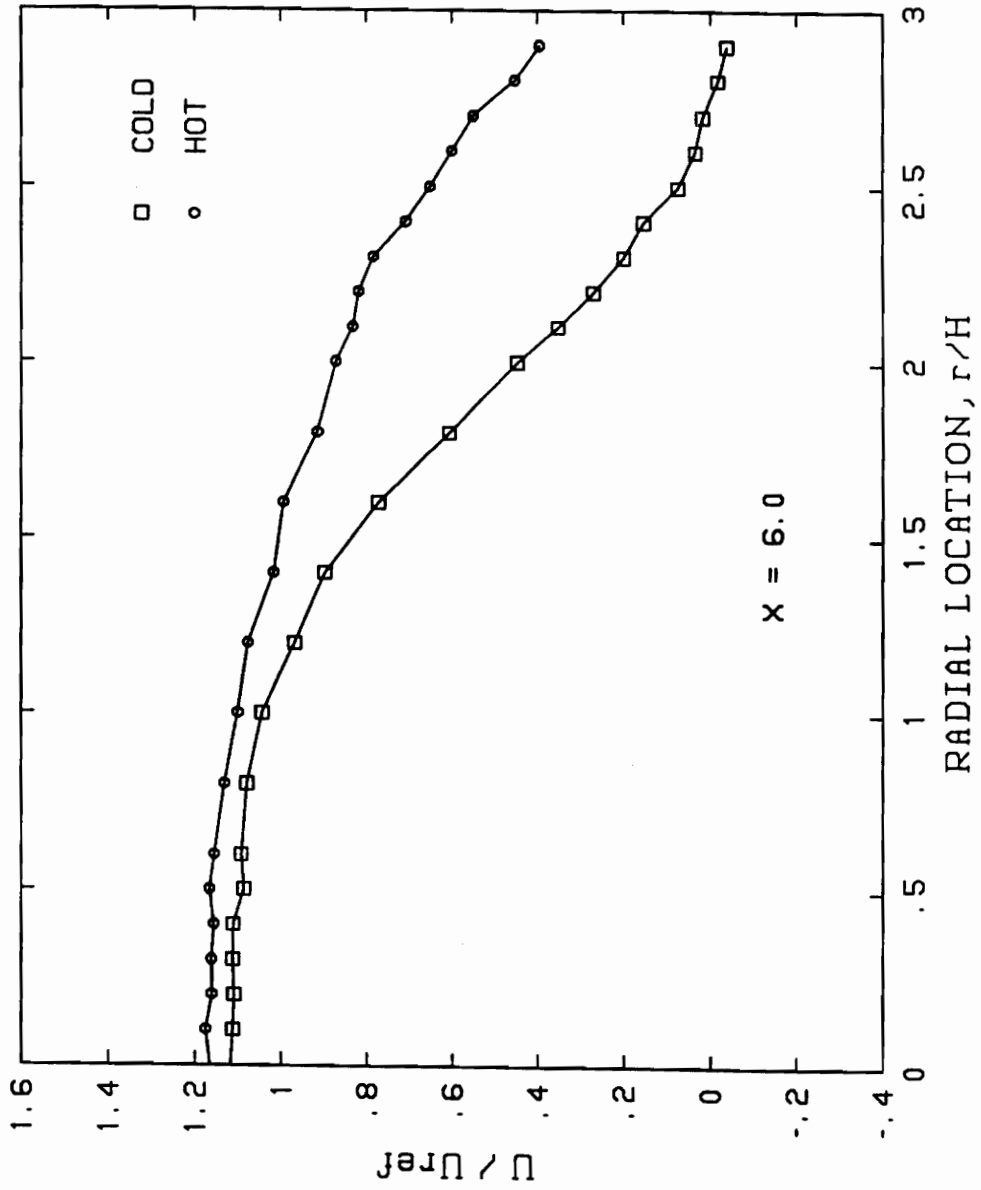
COMPARISON BETWEEN COLD AND HOT DATA



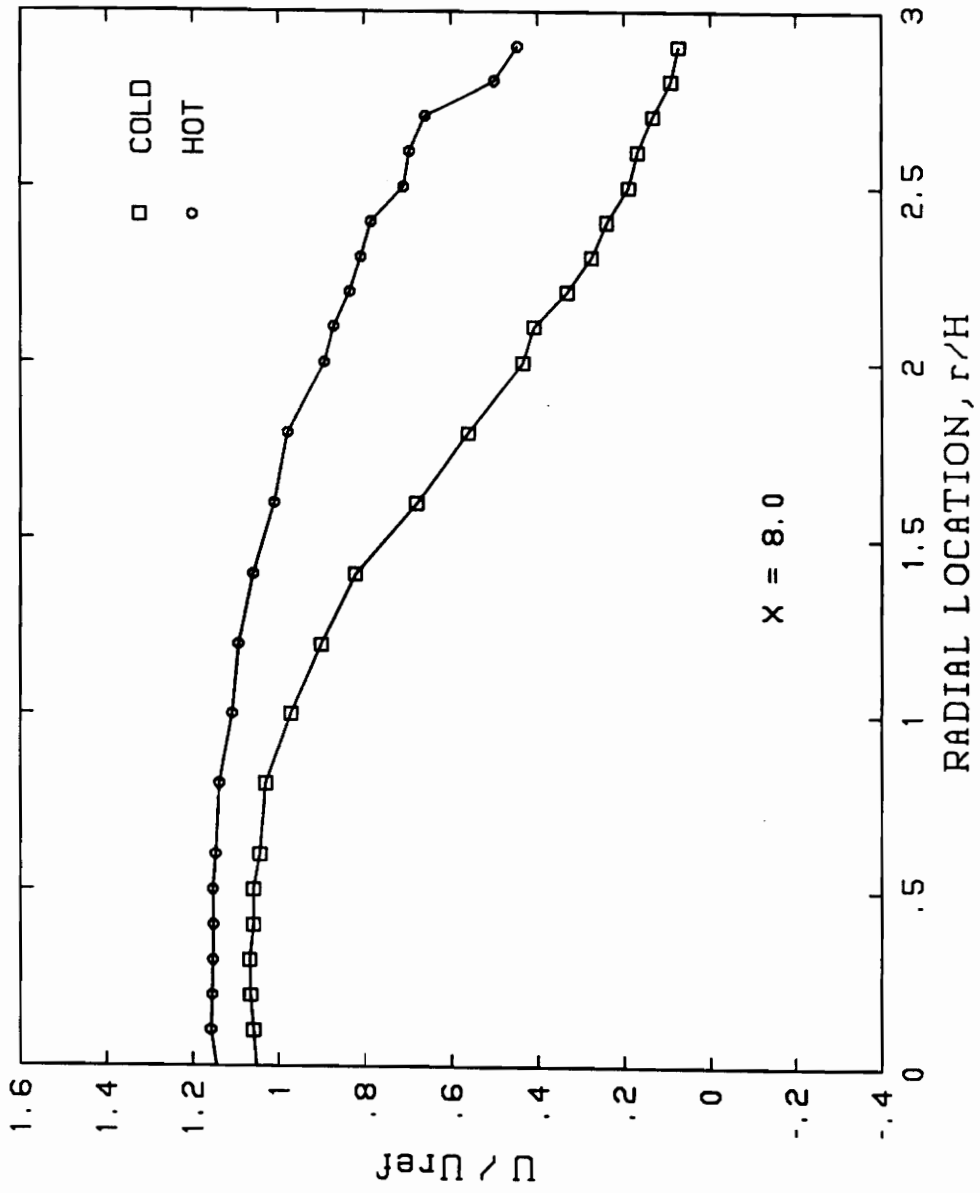
COMPARISON BETWEEN COLD AND HOT DATA



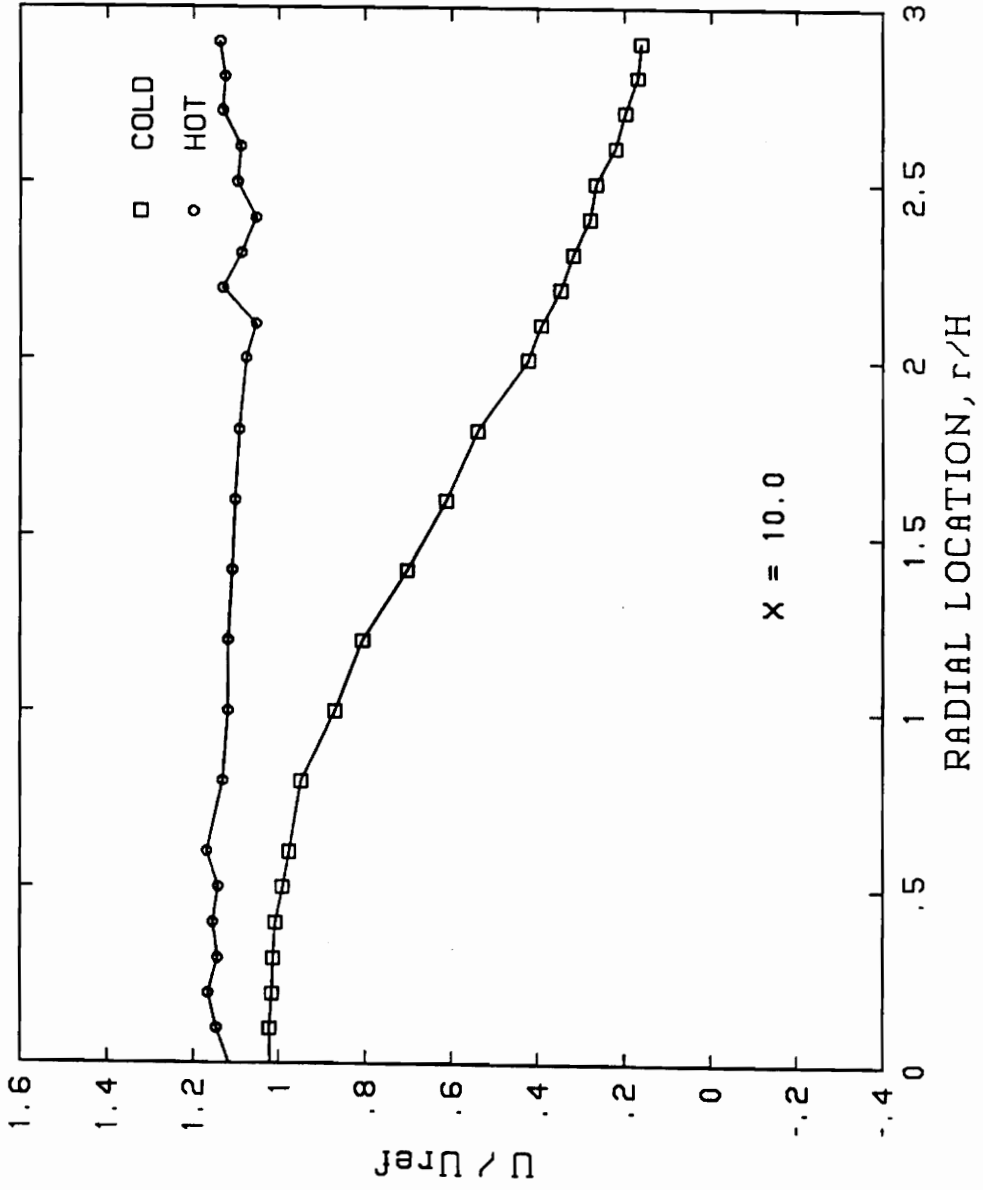
COMPARISON BETWEEN COLD AND HOT DATA



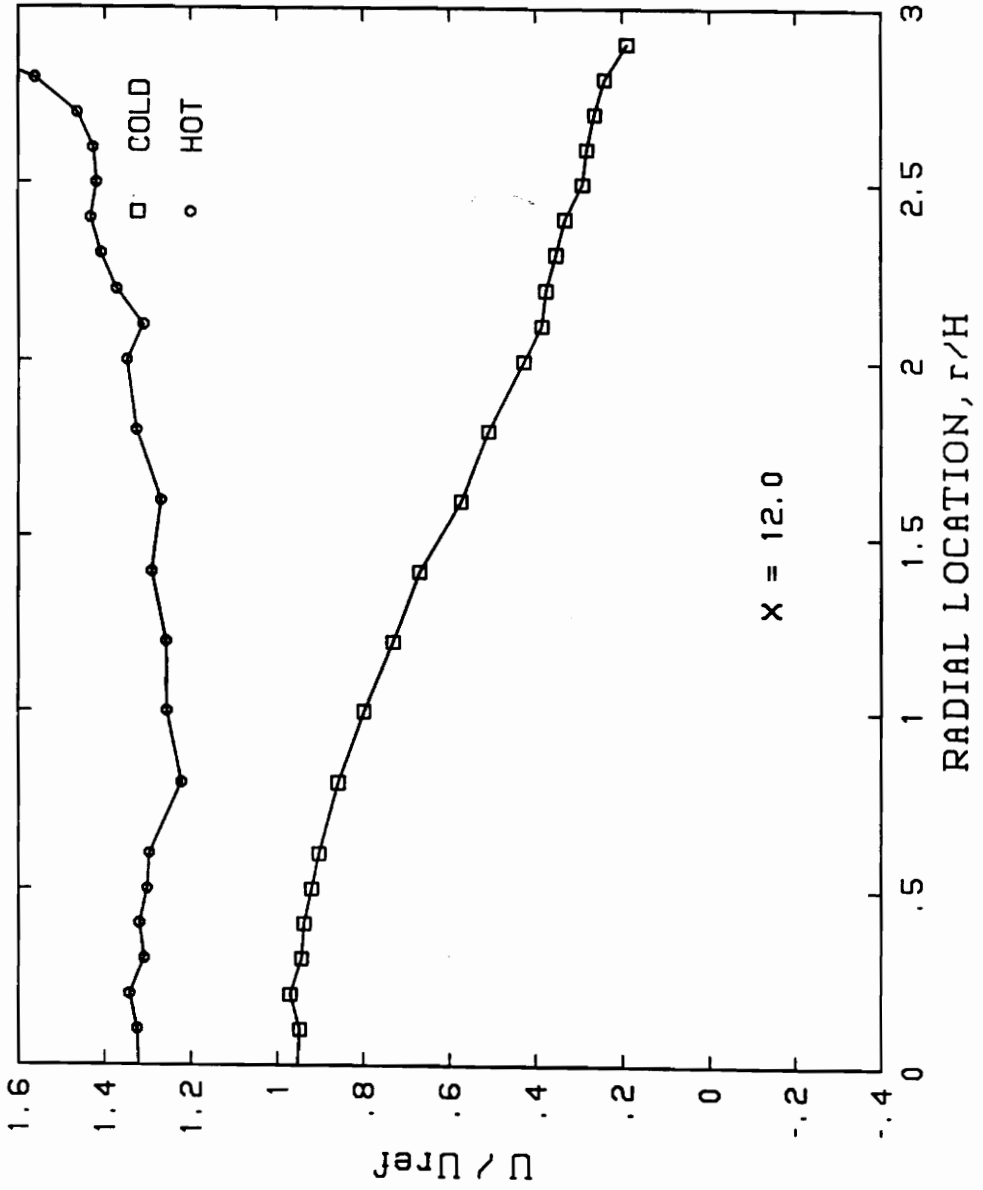
COMPARISON BETWEEN COLD AND HOT DATA



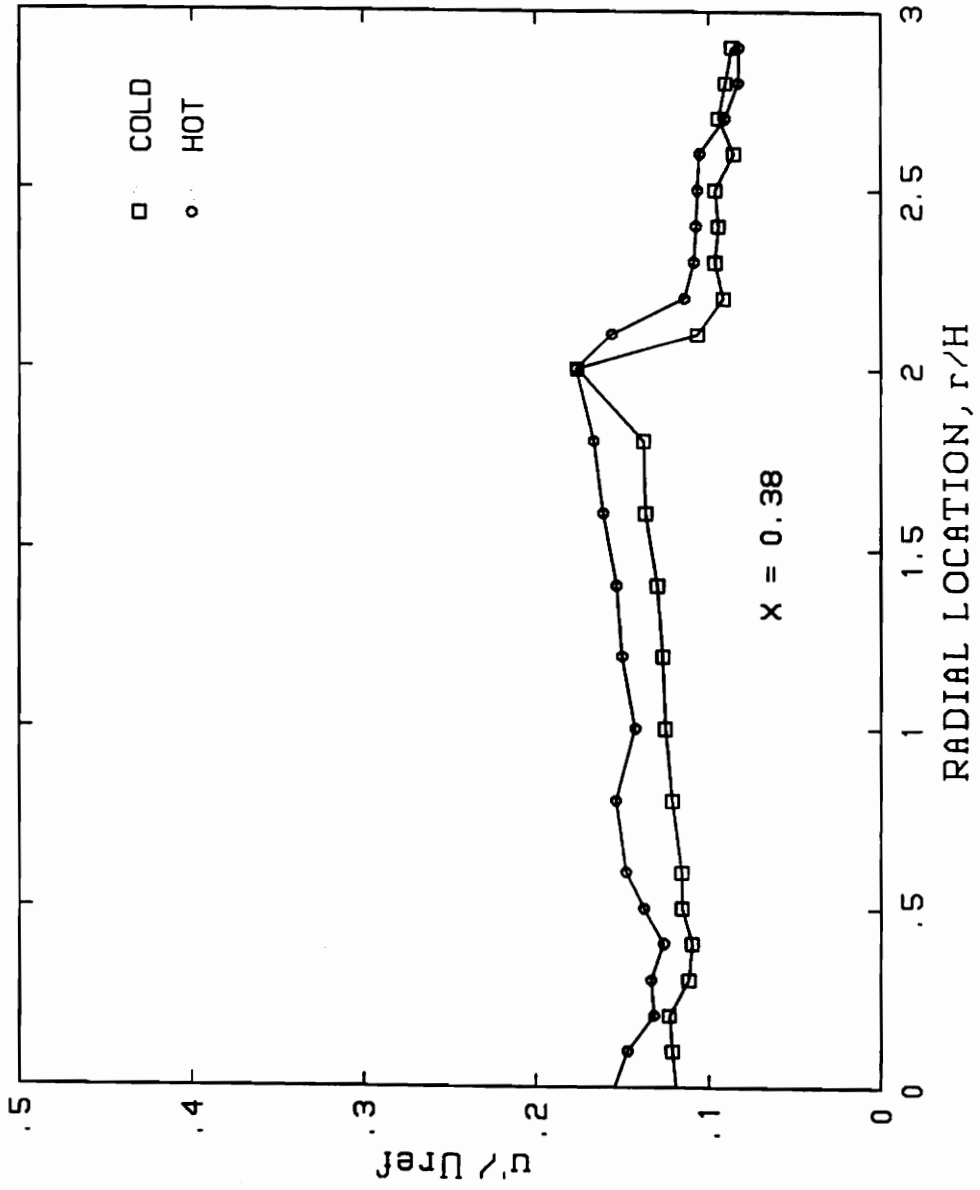
COMPARISON BETWEEN COLD AND HOT DATA

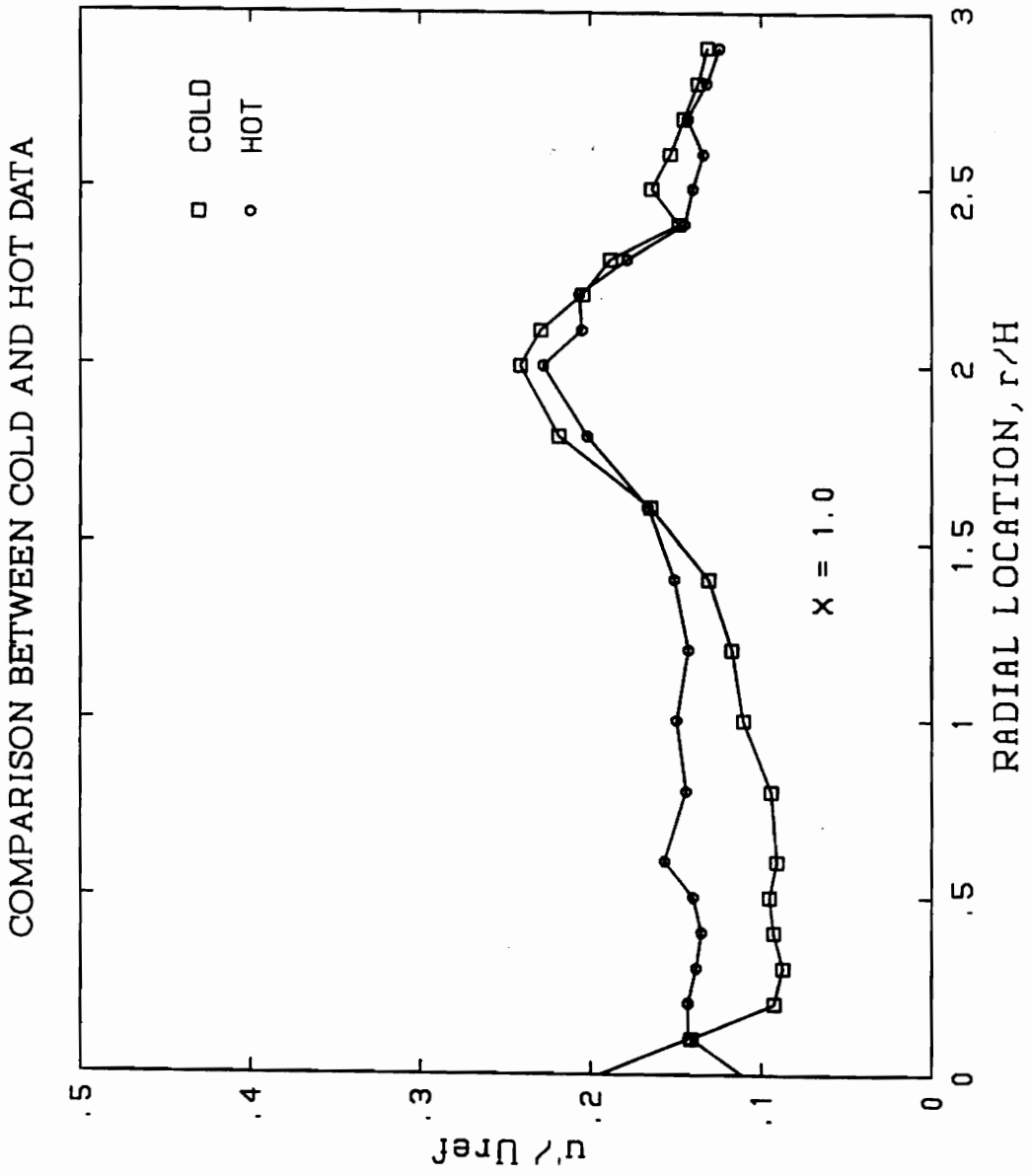


COMPARISON BETWEEN COLD AND HOT DATA

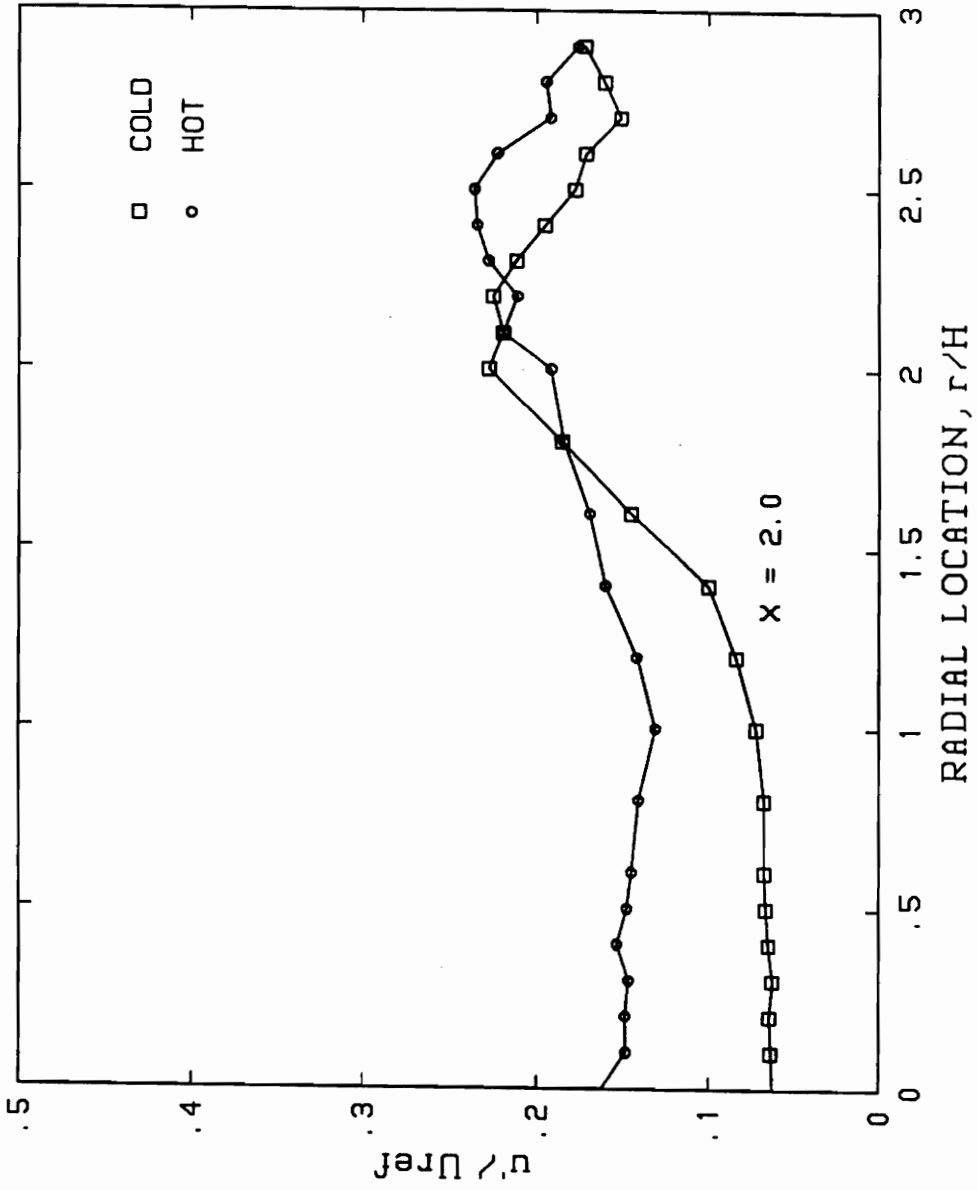


COMPARISON BETWEEN COLD AND HOT DATA

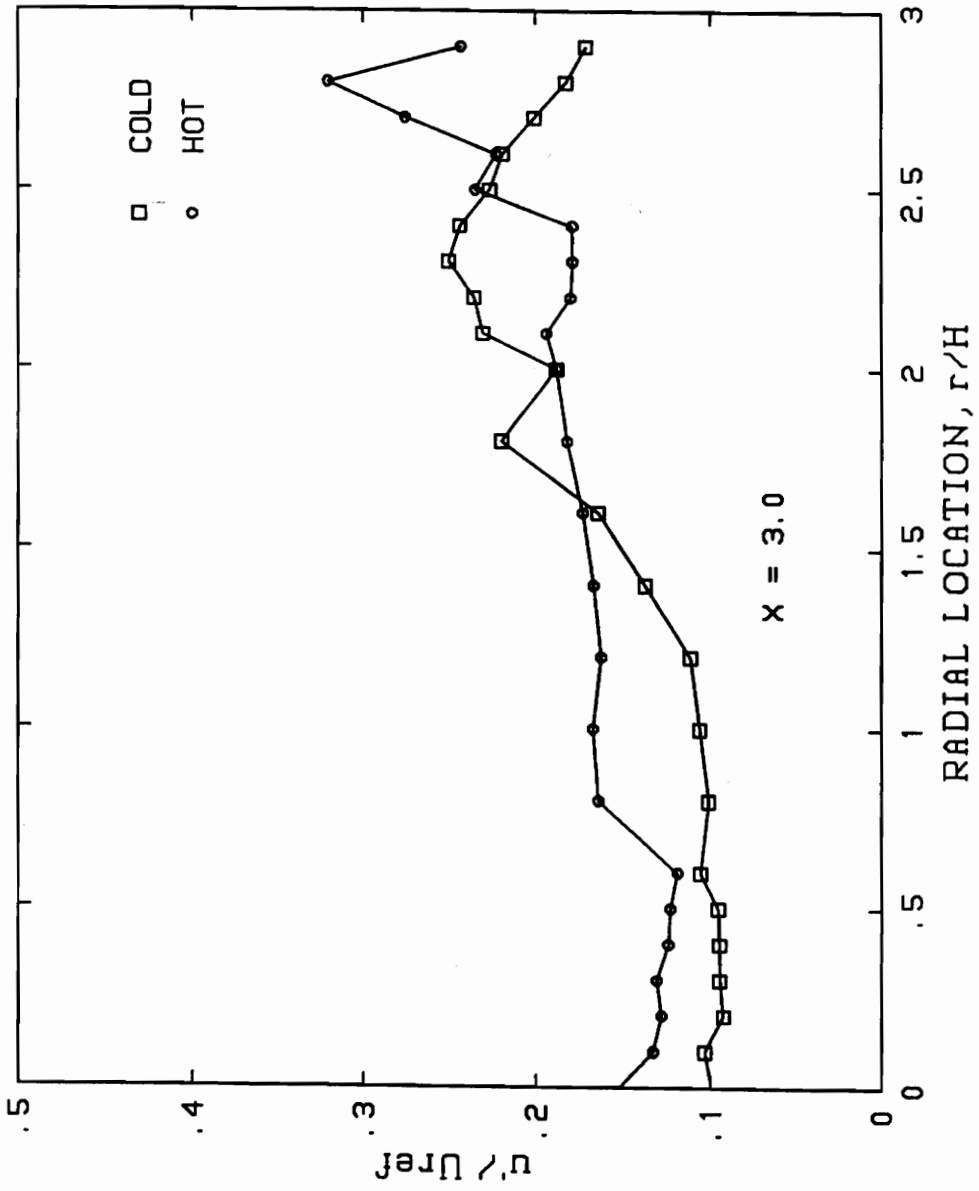




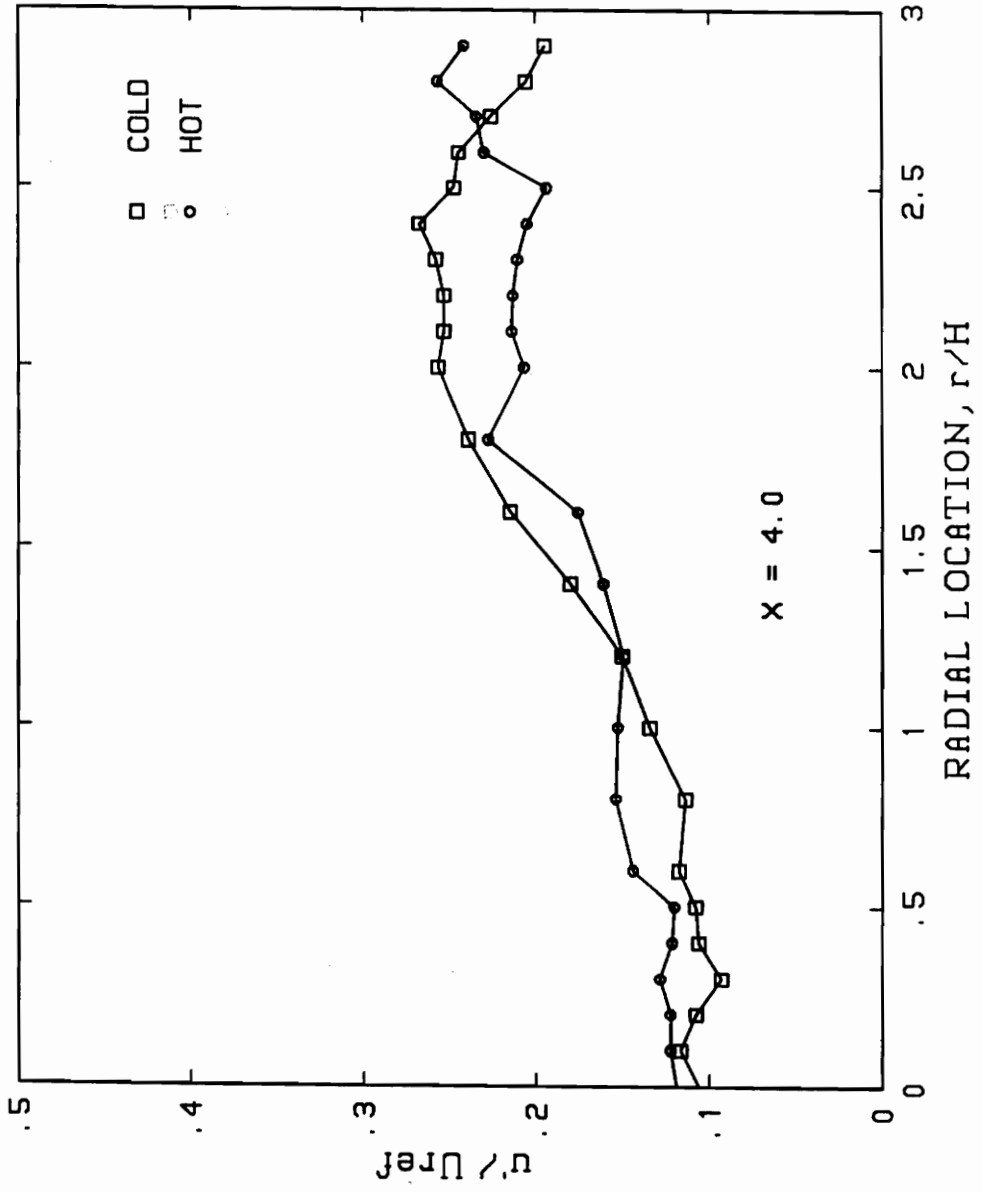
COMPARISON BETWEEN COLD AND HOT DATA



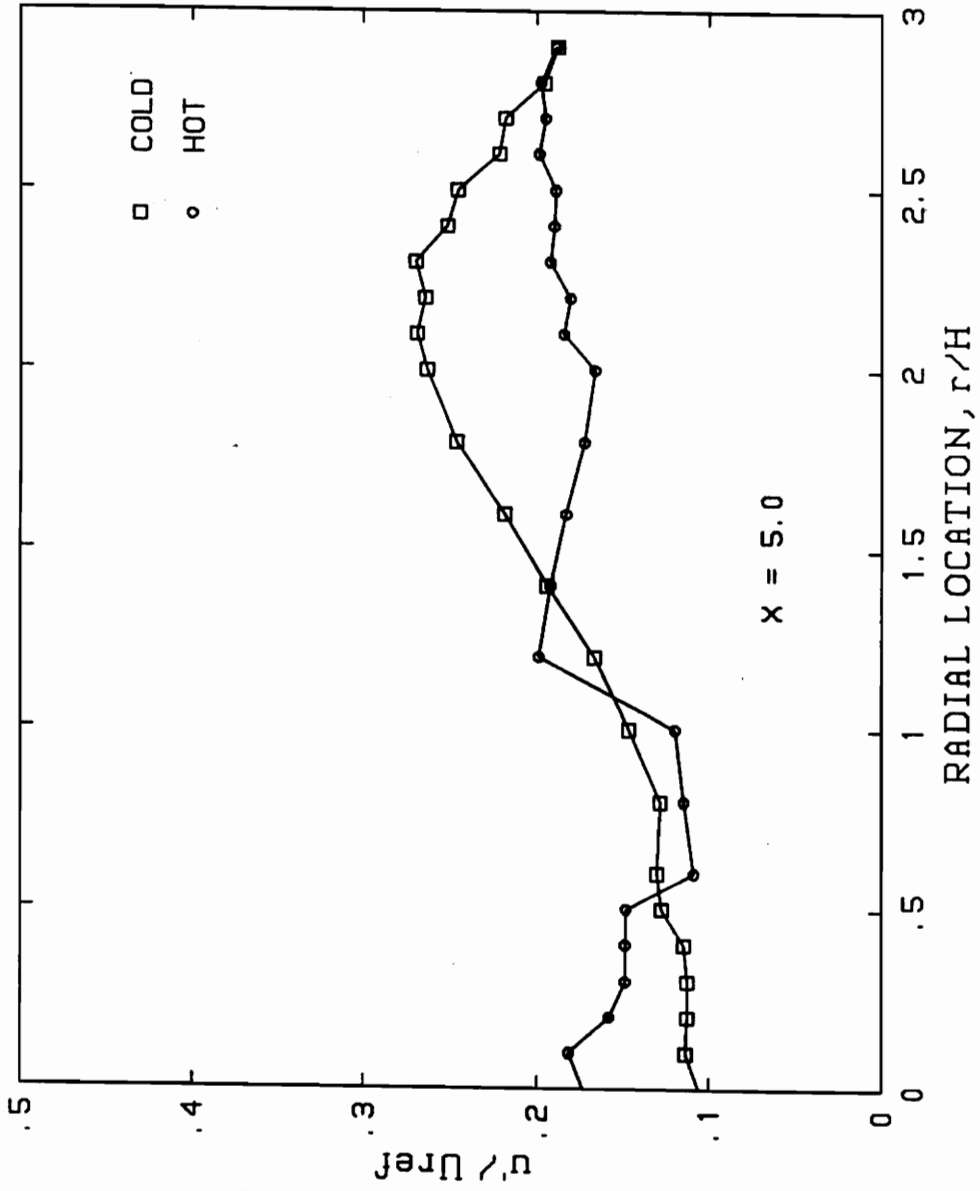
COMPARISON BETWEEN COLD AND HOT DATA



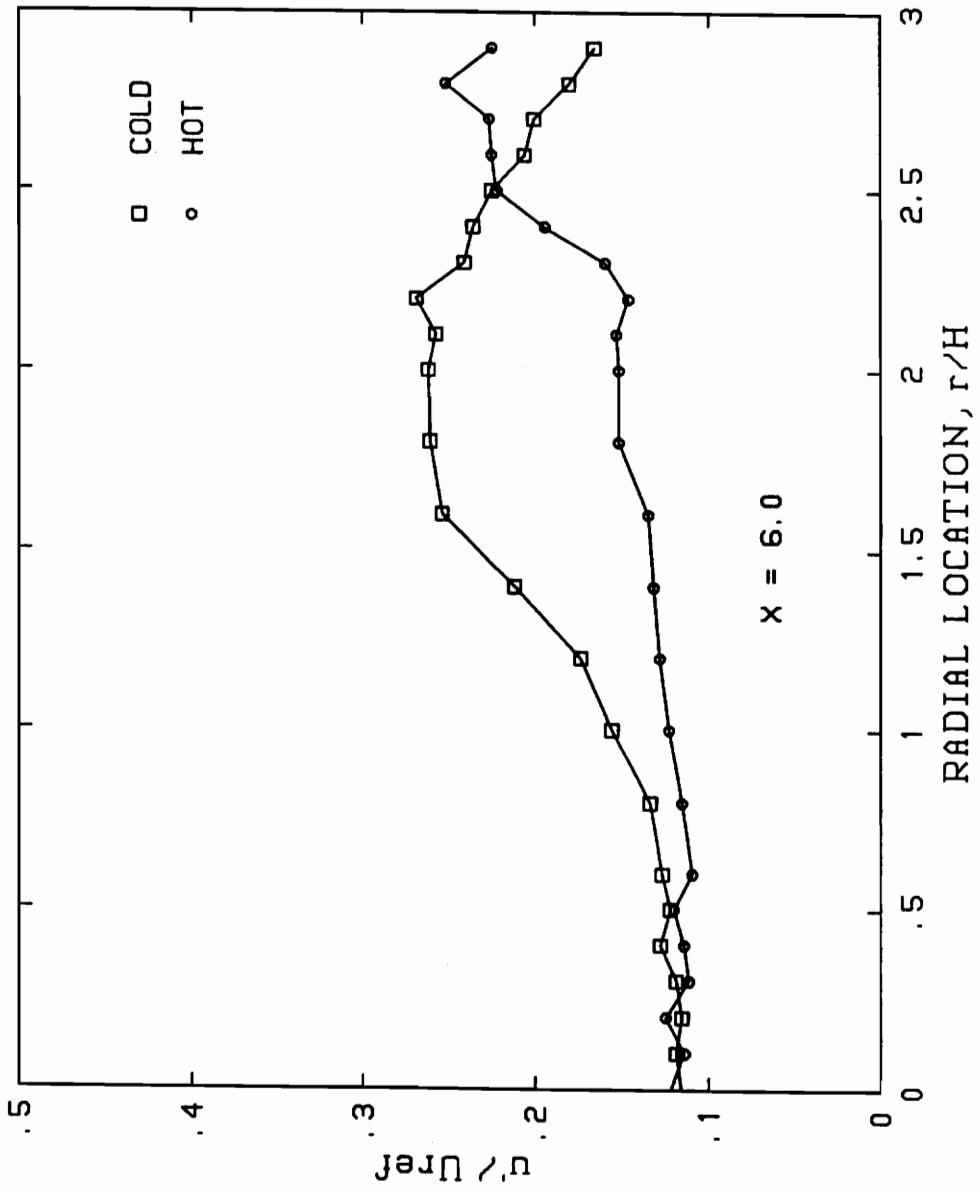
COMPARISON BETWEEN COLD AND HOT DATA



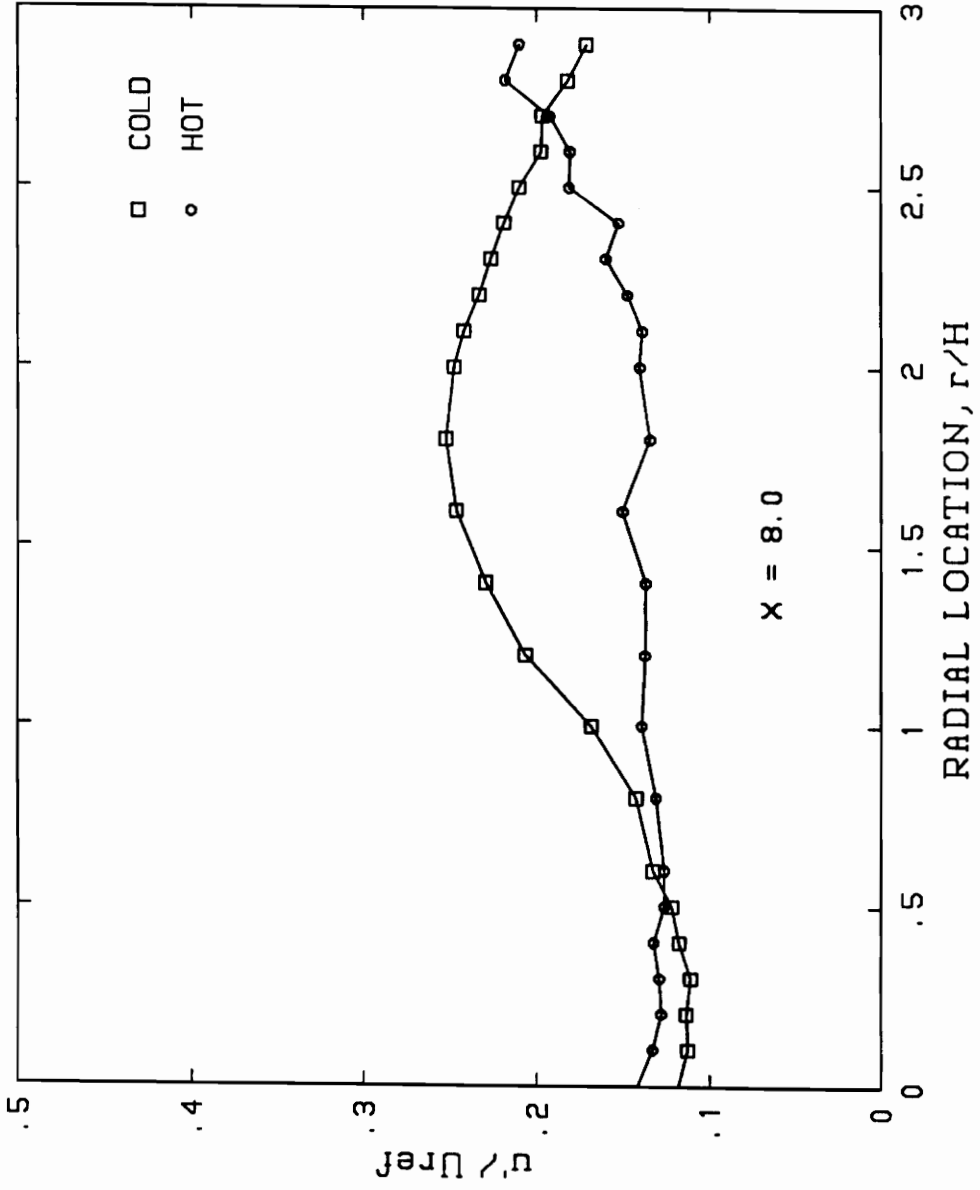
COMPARISON BETWEEN COLD AND HOT DATA



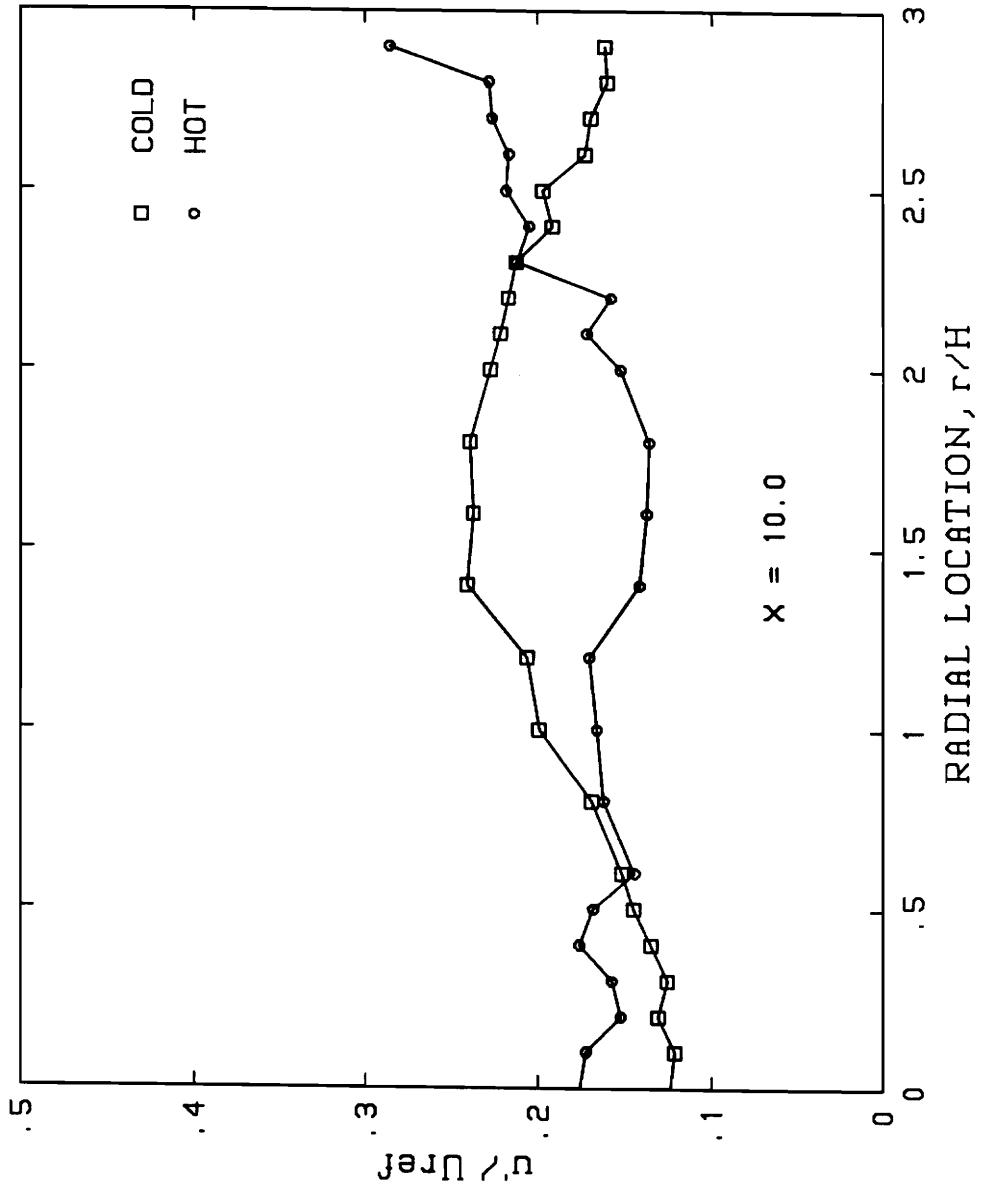
COMPARISON BETWEEN COLD AND HOT DATA



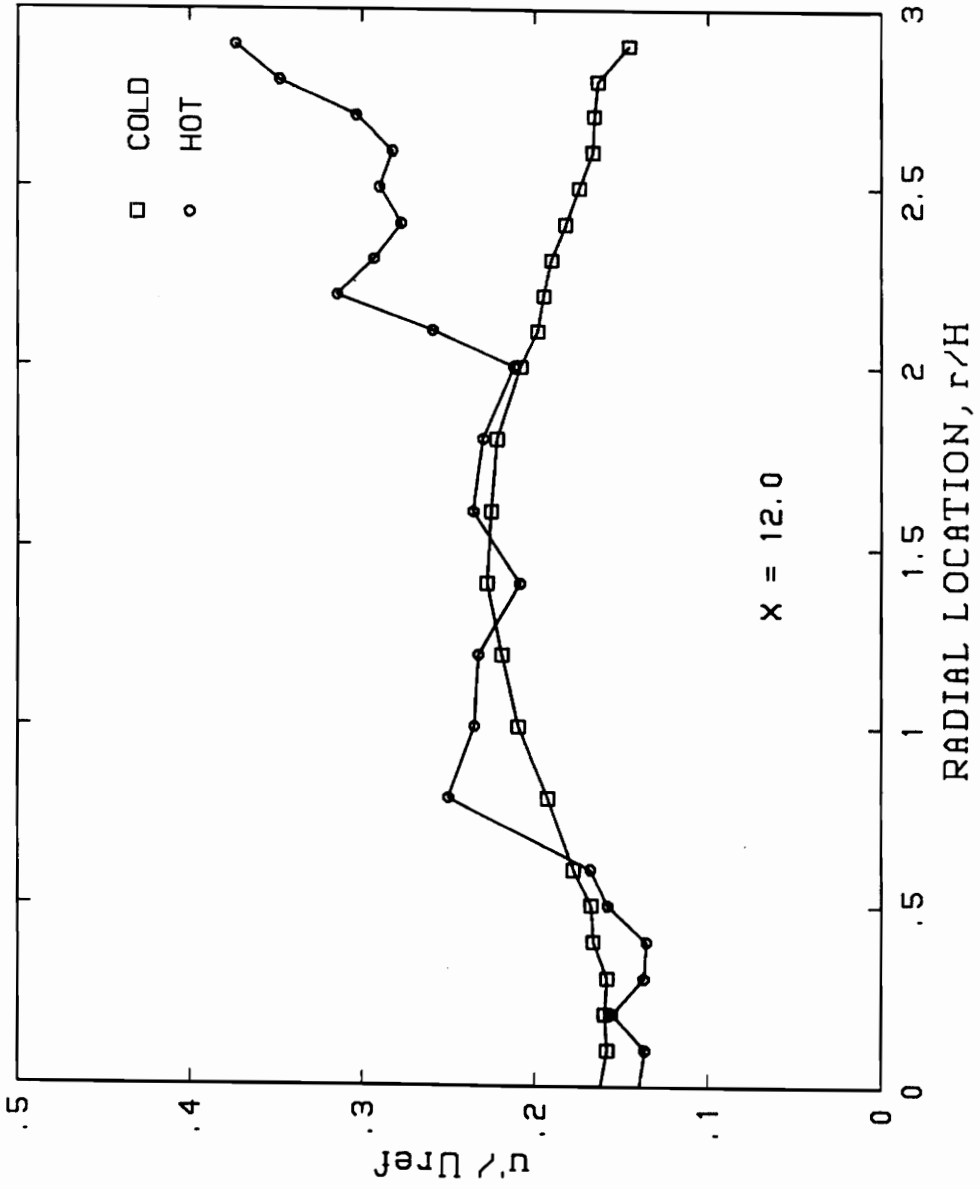
COMPARISON BETWEEN COLD AND HOT DATA



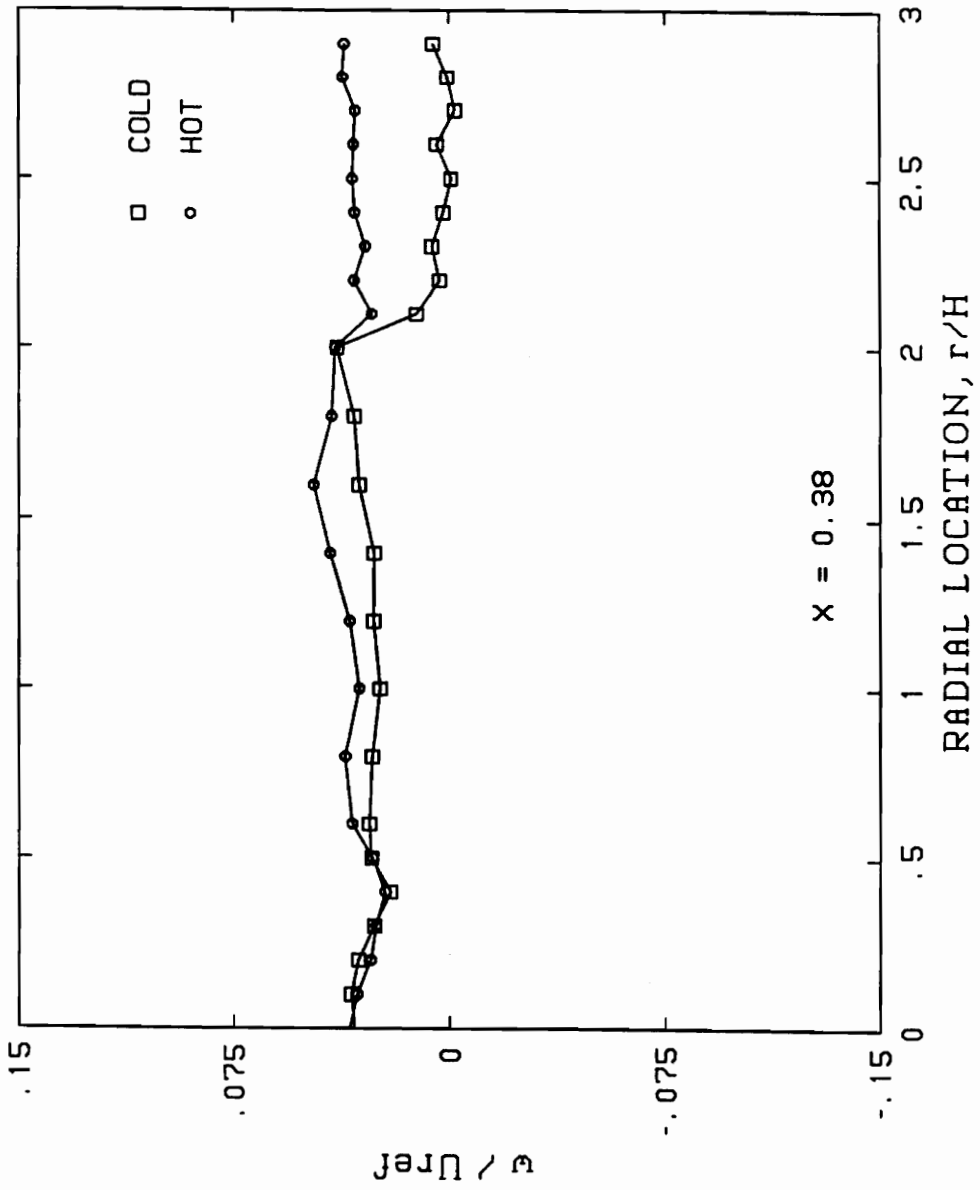
COMPARISON BETWEEN COLD AND HOT DATA



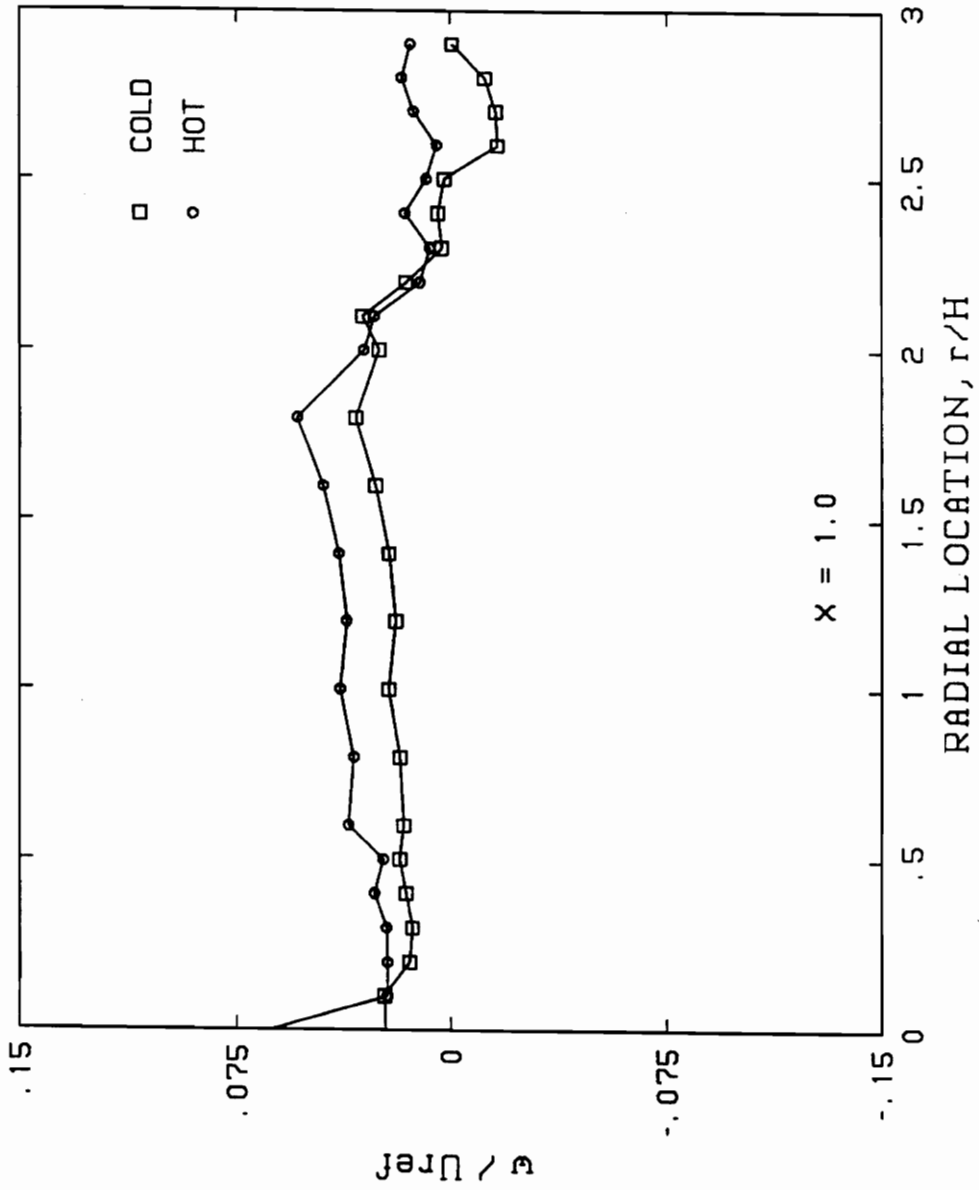
COMPARISON BETWEEN COLD AND HOT DATA



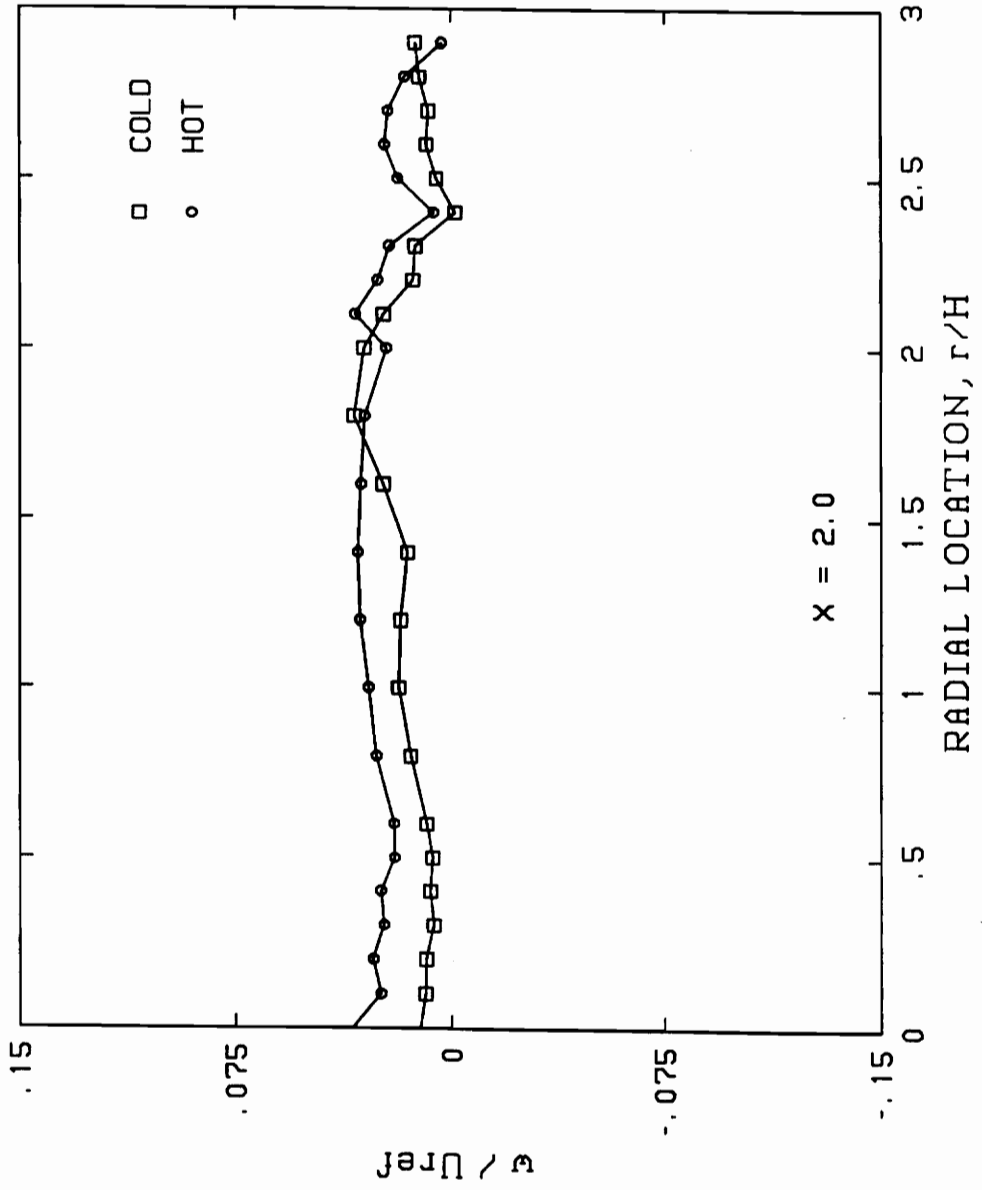
COMPARISON BETWEEN COLD AND HOT DATA



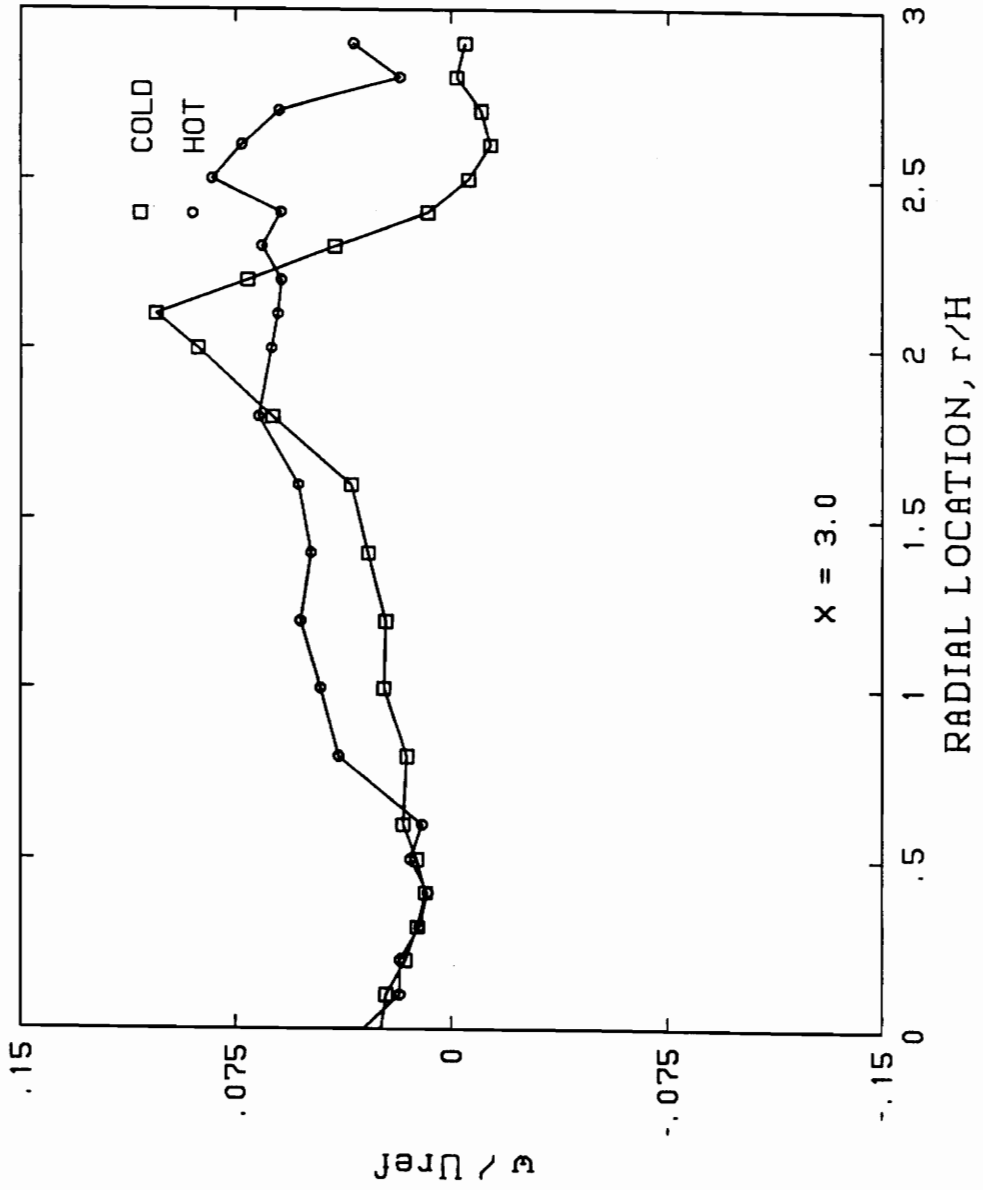
COMPARISON BETWEEN COLD AND HOT DATA



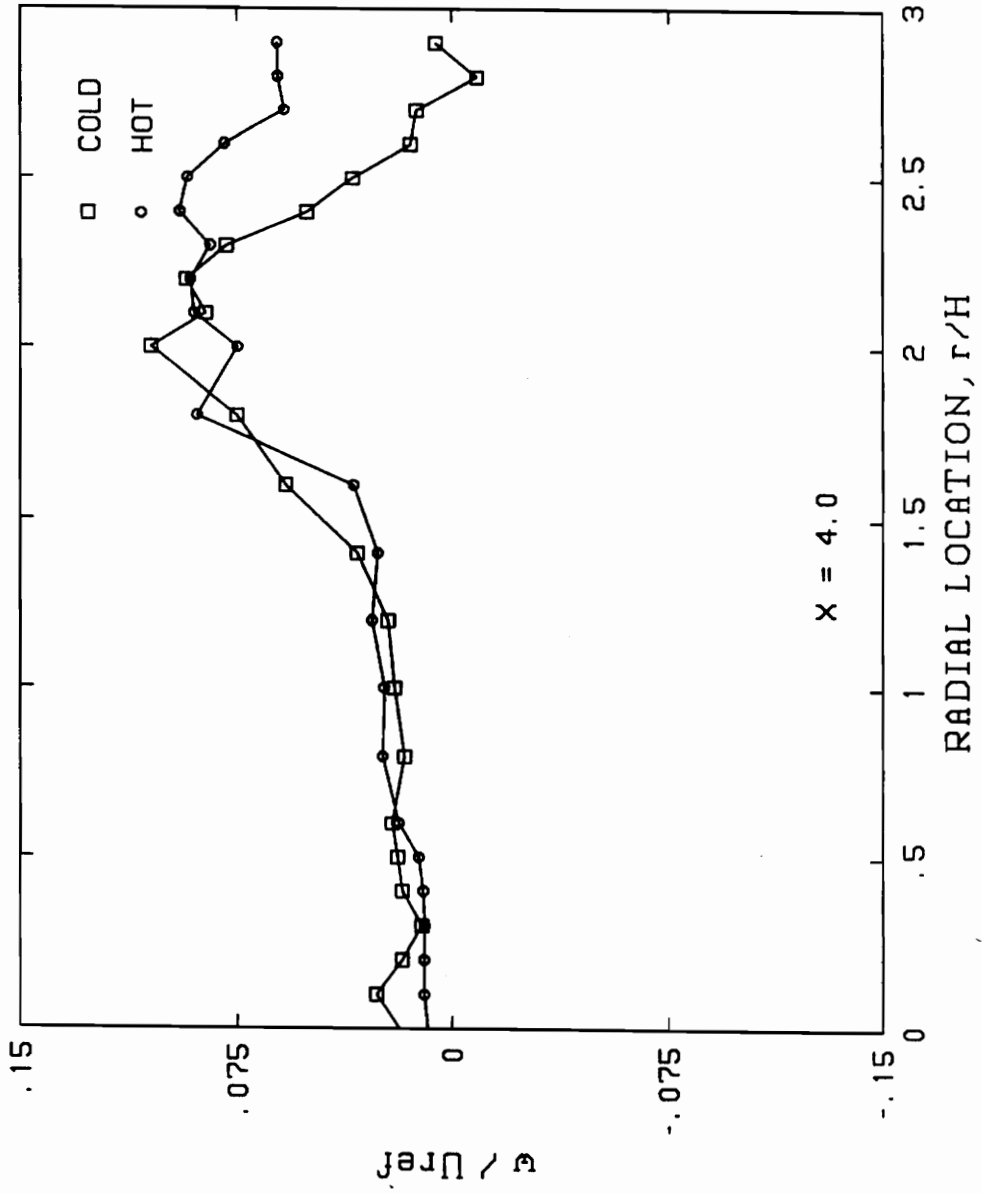
COMPARISON BETWEEN COLD AND HOT DATA



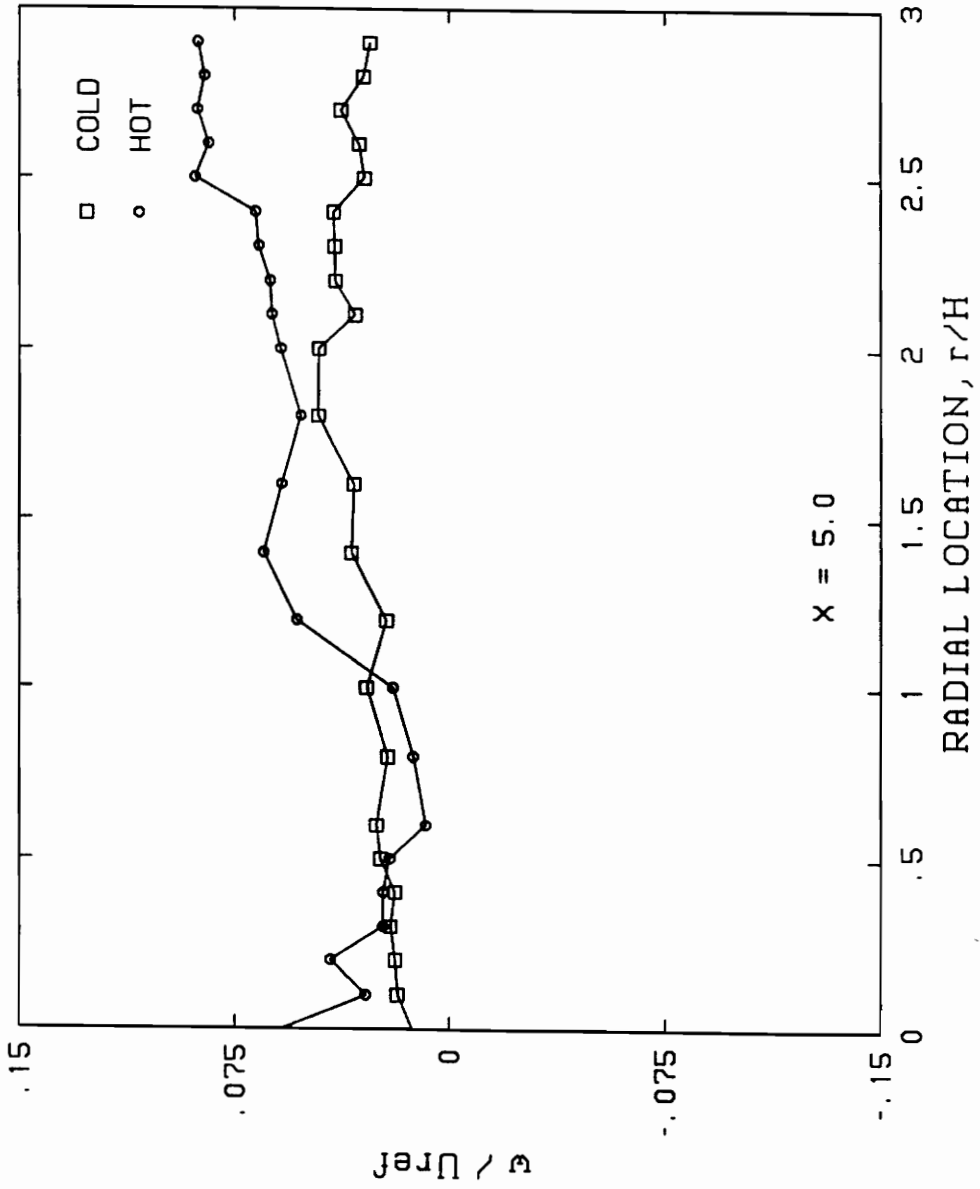
COMPARISON BETWEEN COLD AND HOT DATA



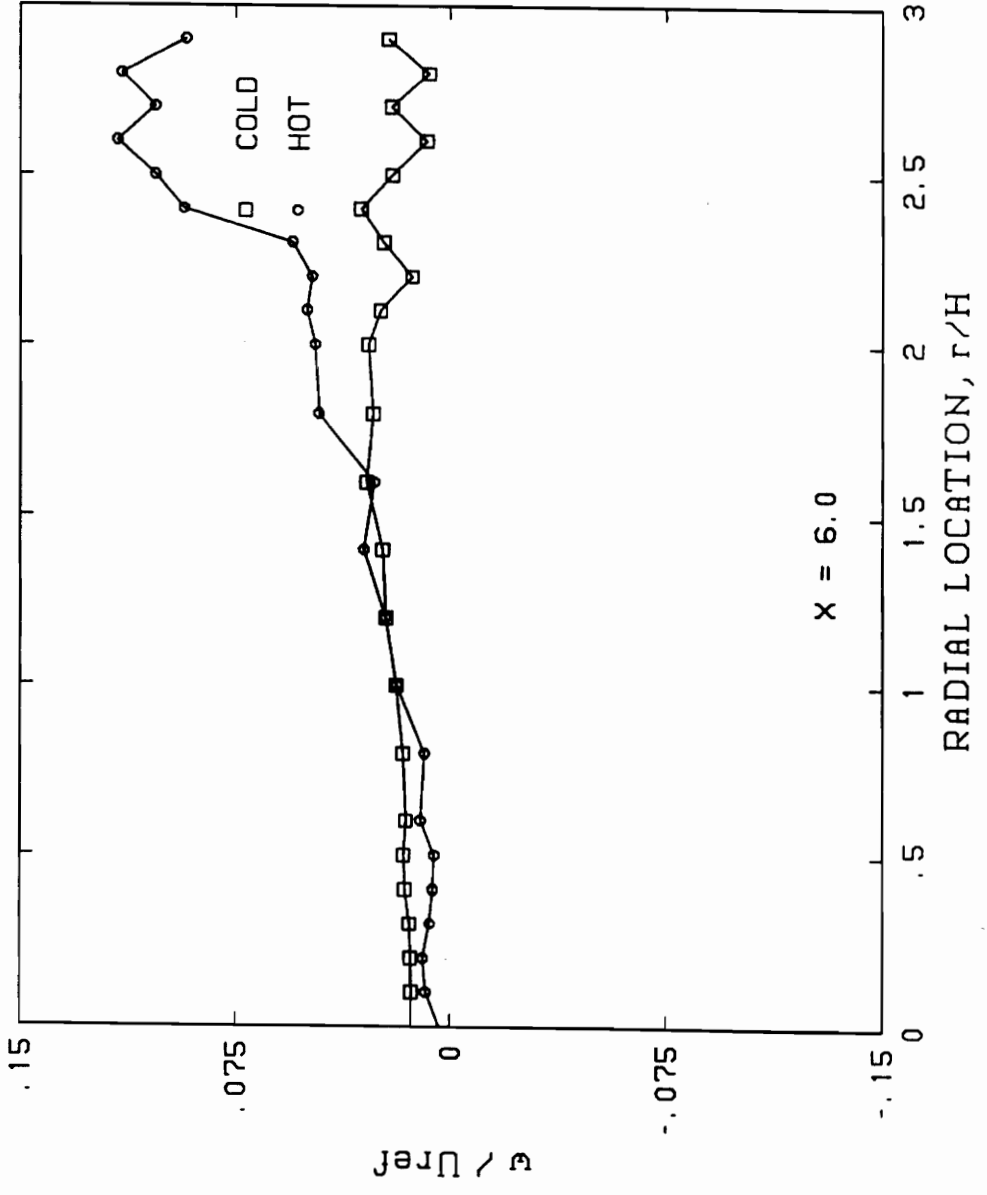
COMPARISON BETWEEN COLD AND HOT DATA



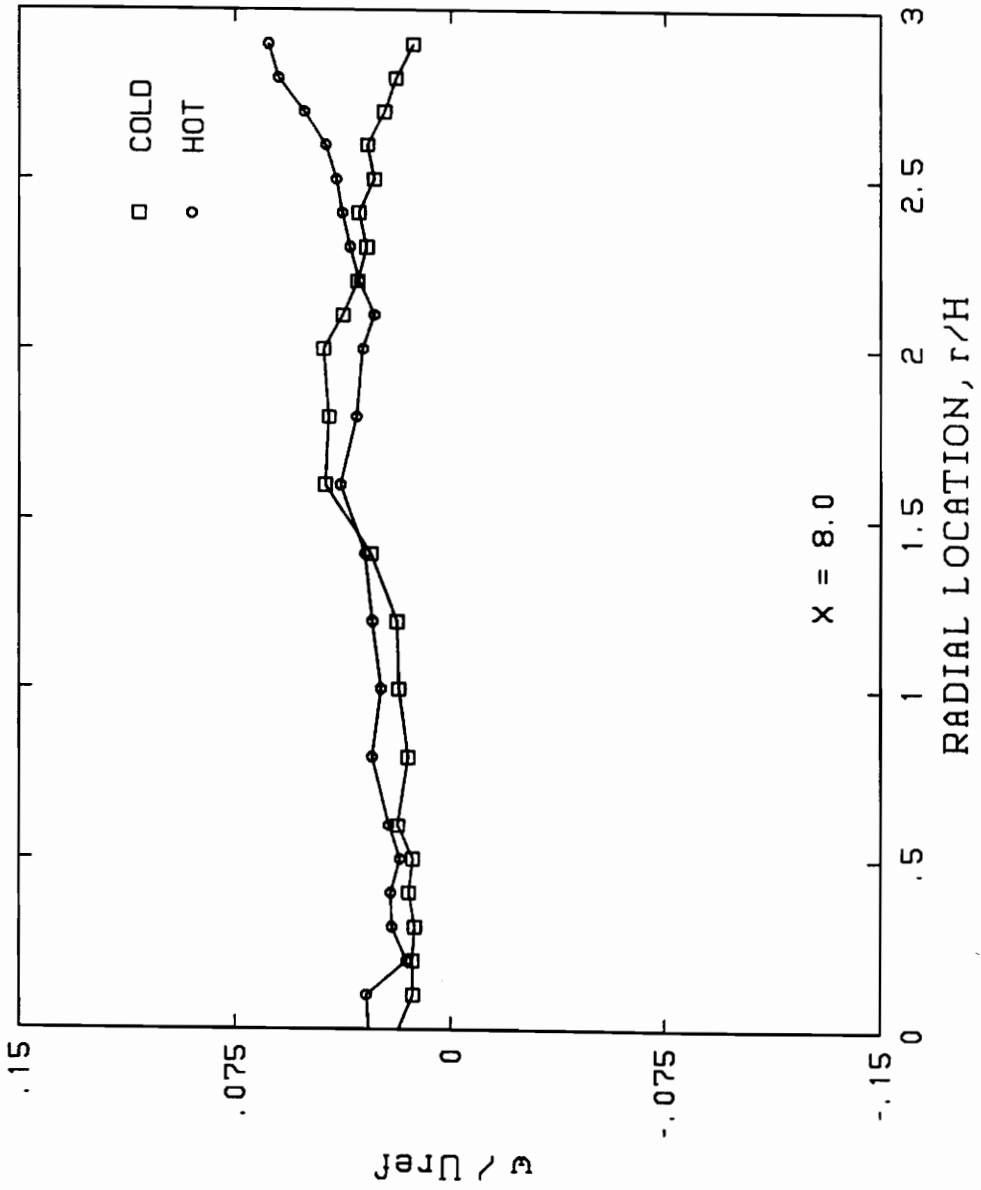
COMPARISON BETWEEN COLD AND HOT DATA

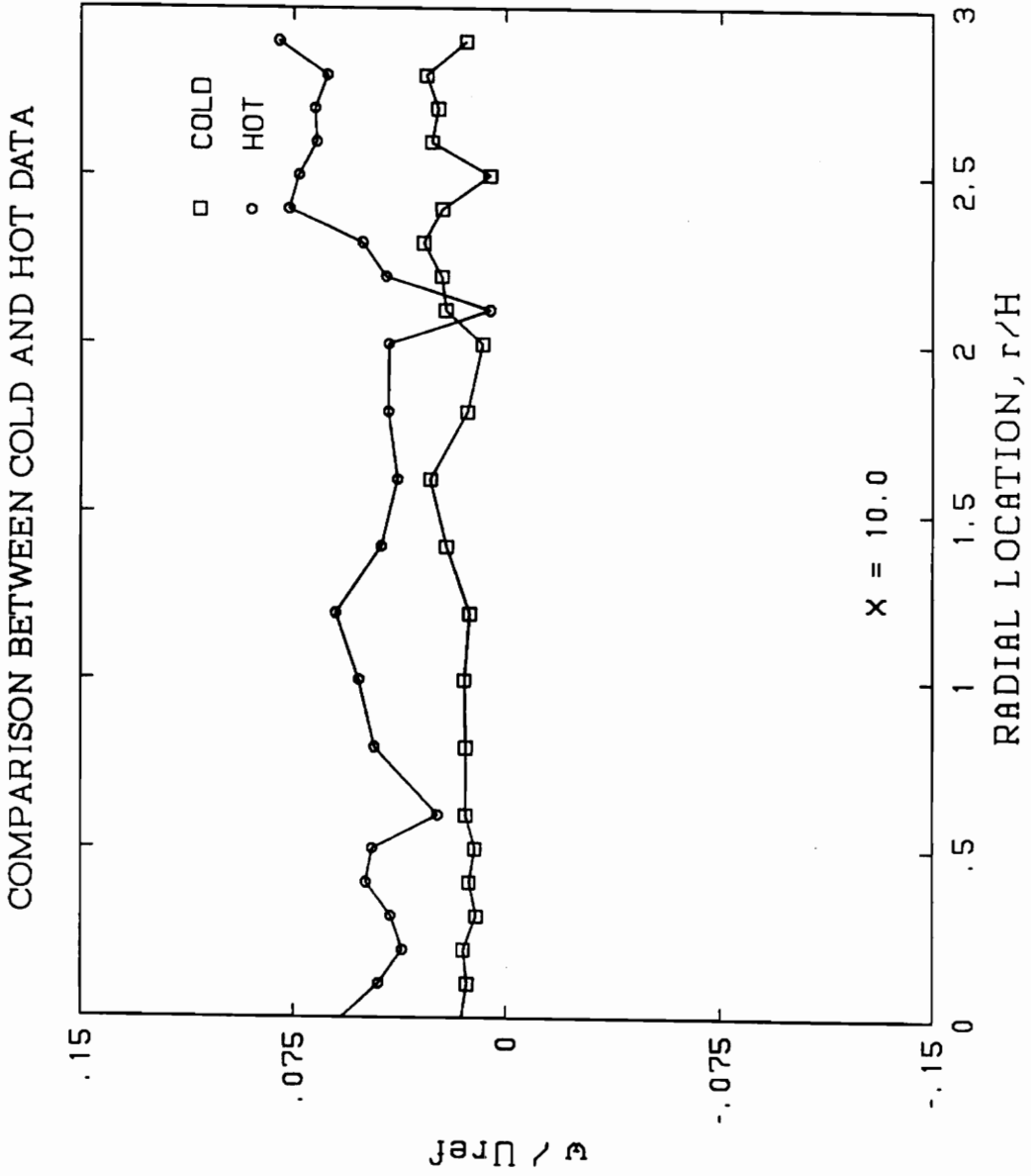


COMPARISON BETWEEN COLD AND HOT DATA

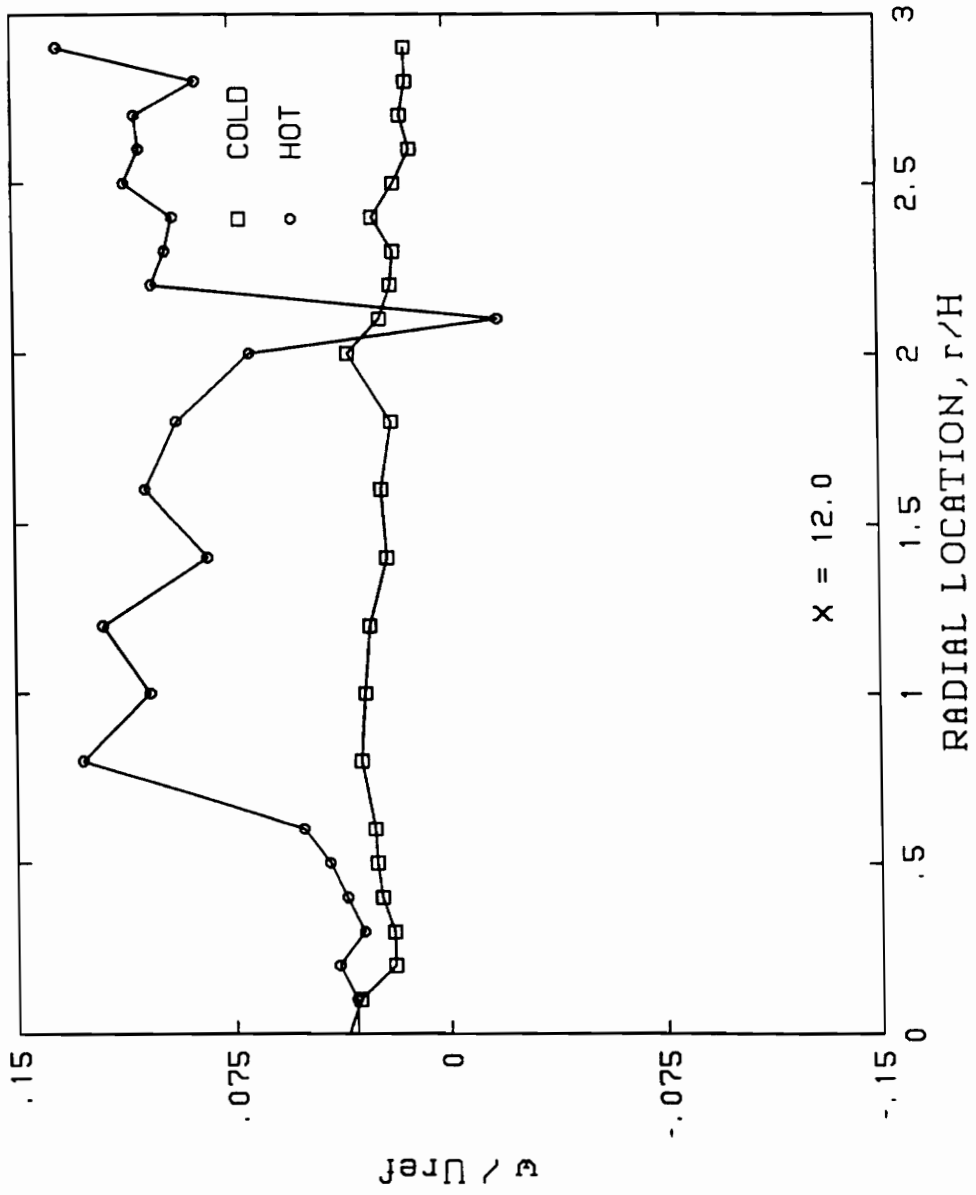


COMPARISON BETWEEN COLD AND HOT DATA

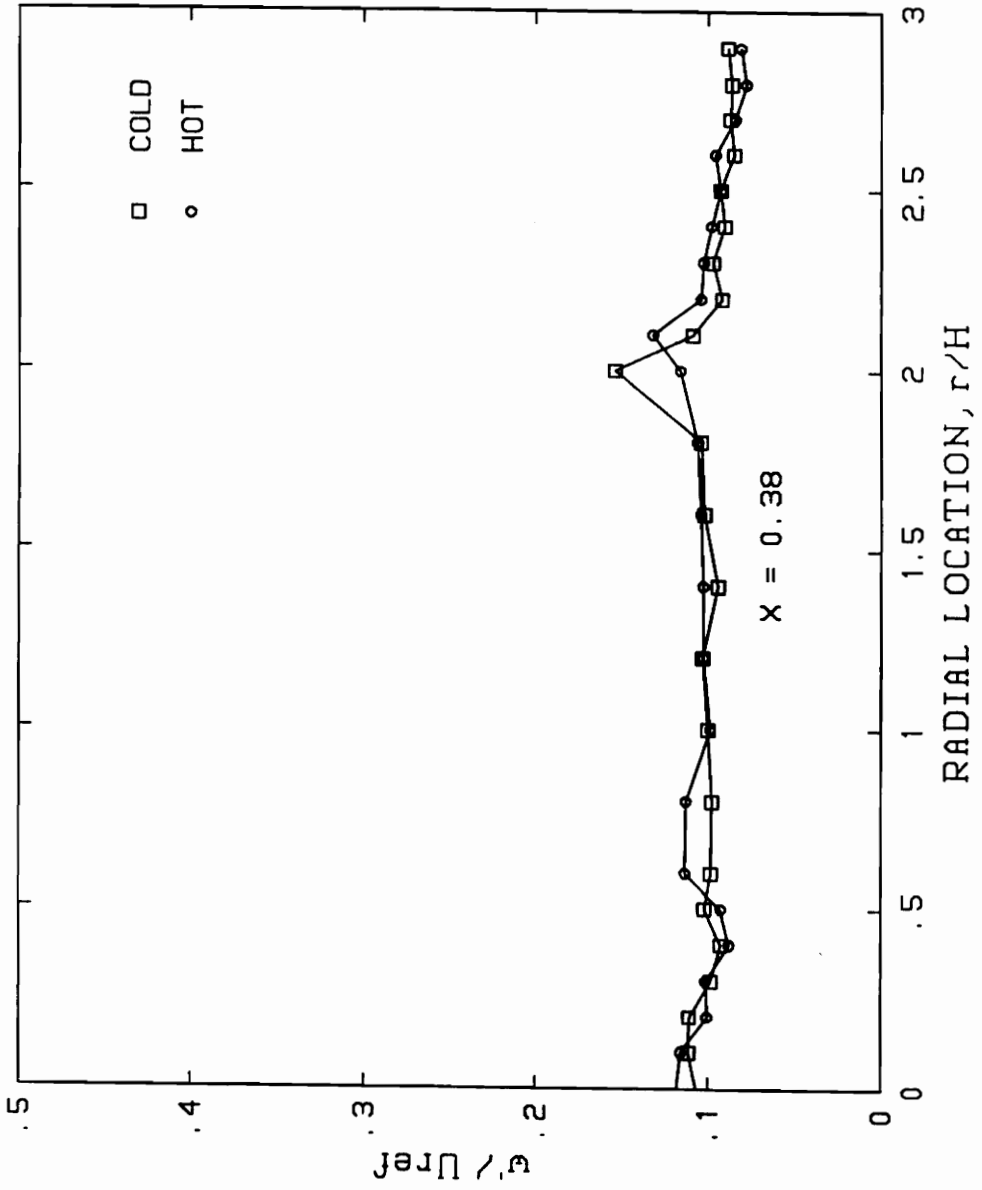




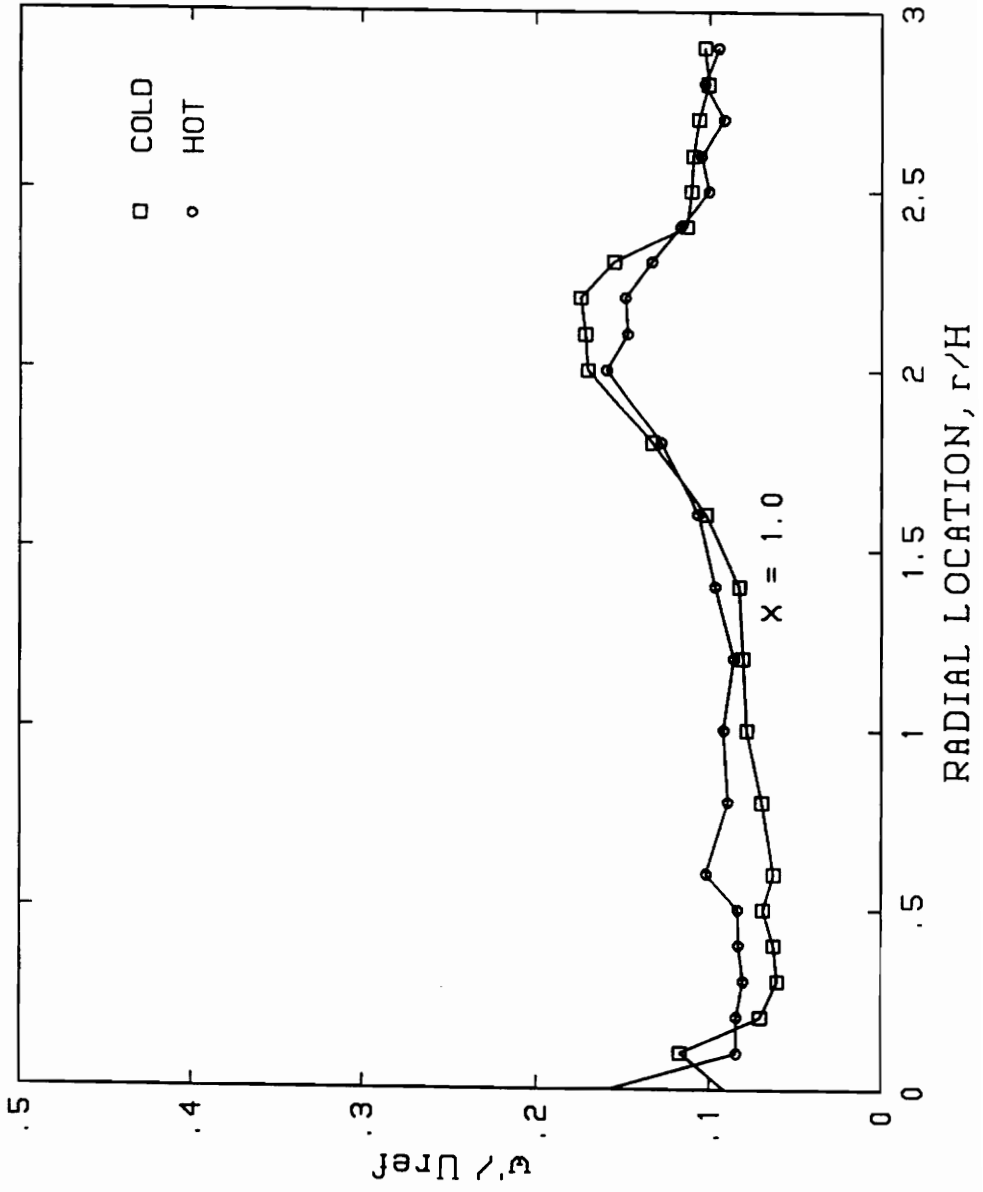
COMPARISON BETWEEN COLD AND HOT DATA



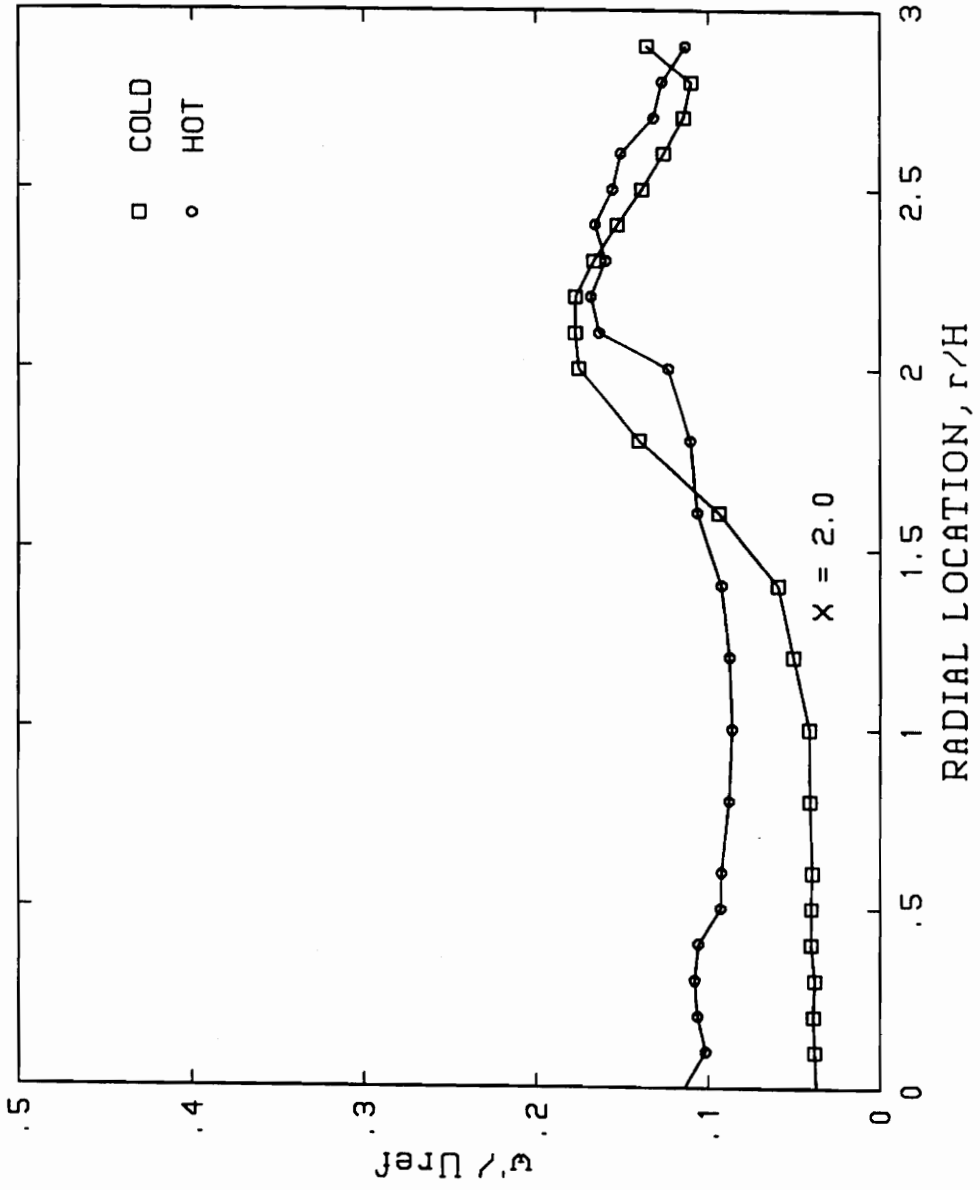
COMPARISON BETWEEN COLD AND HOT DATA



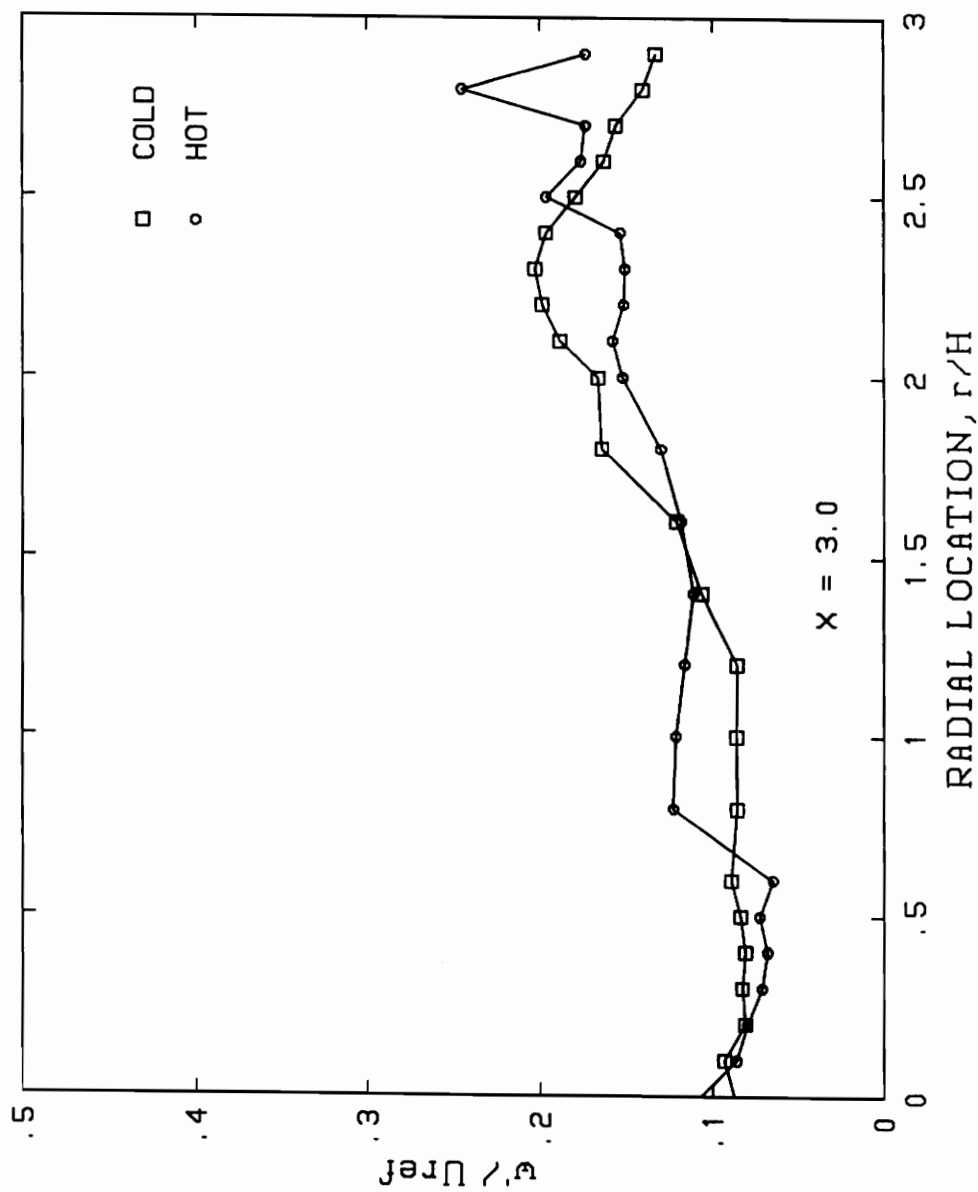
COMPARISON BETWEEN COLD AND HOT DATA

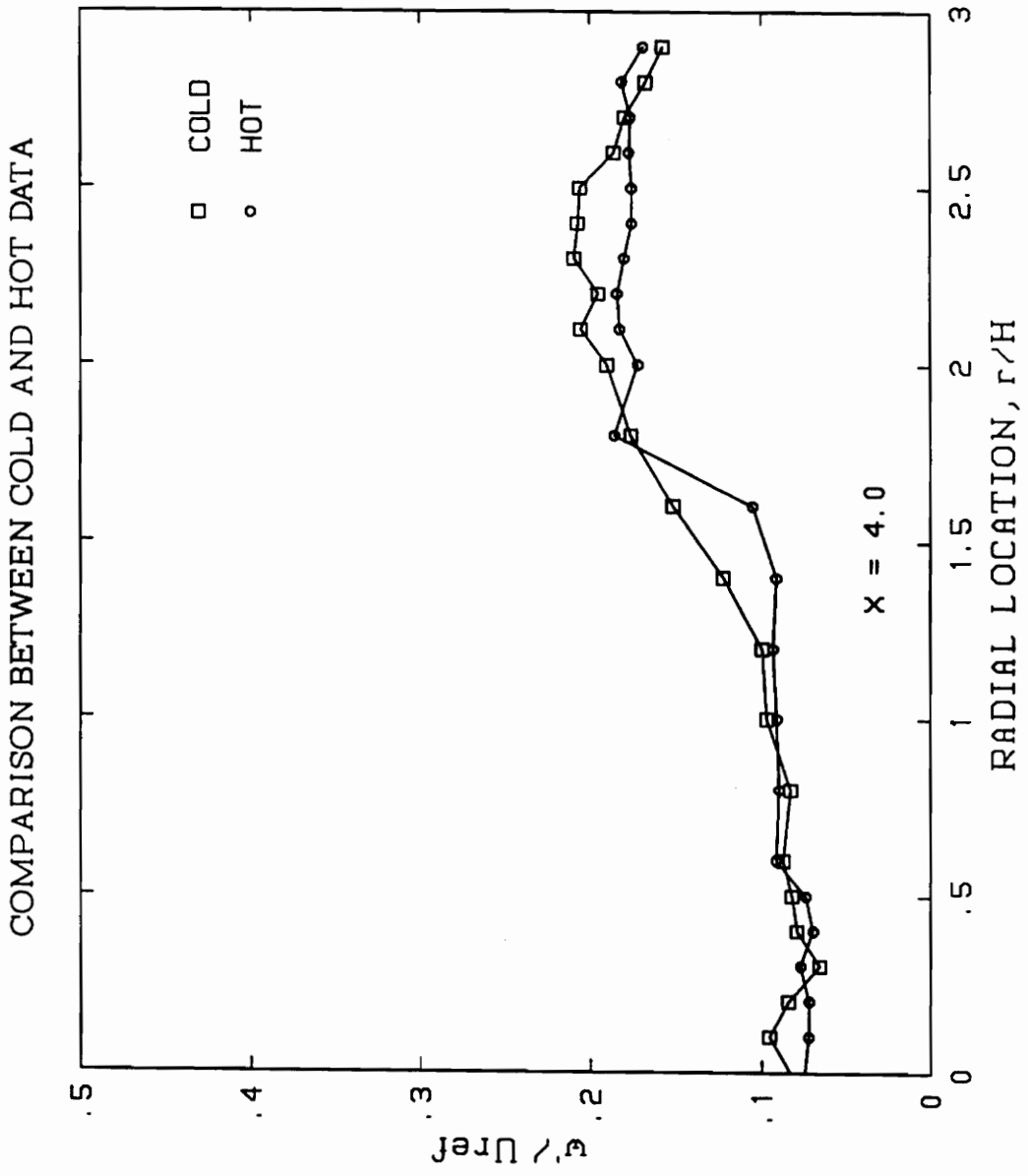


COMPARISON BETWEEN COLD AND HOT DATA

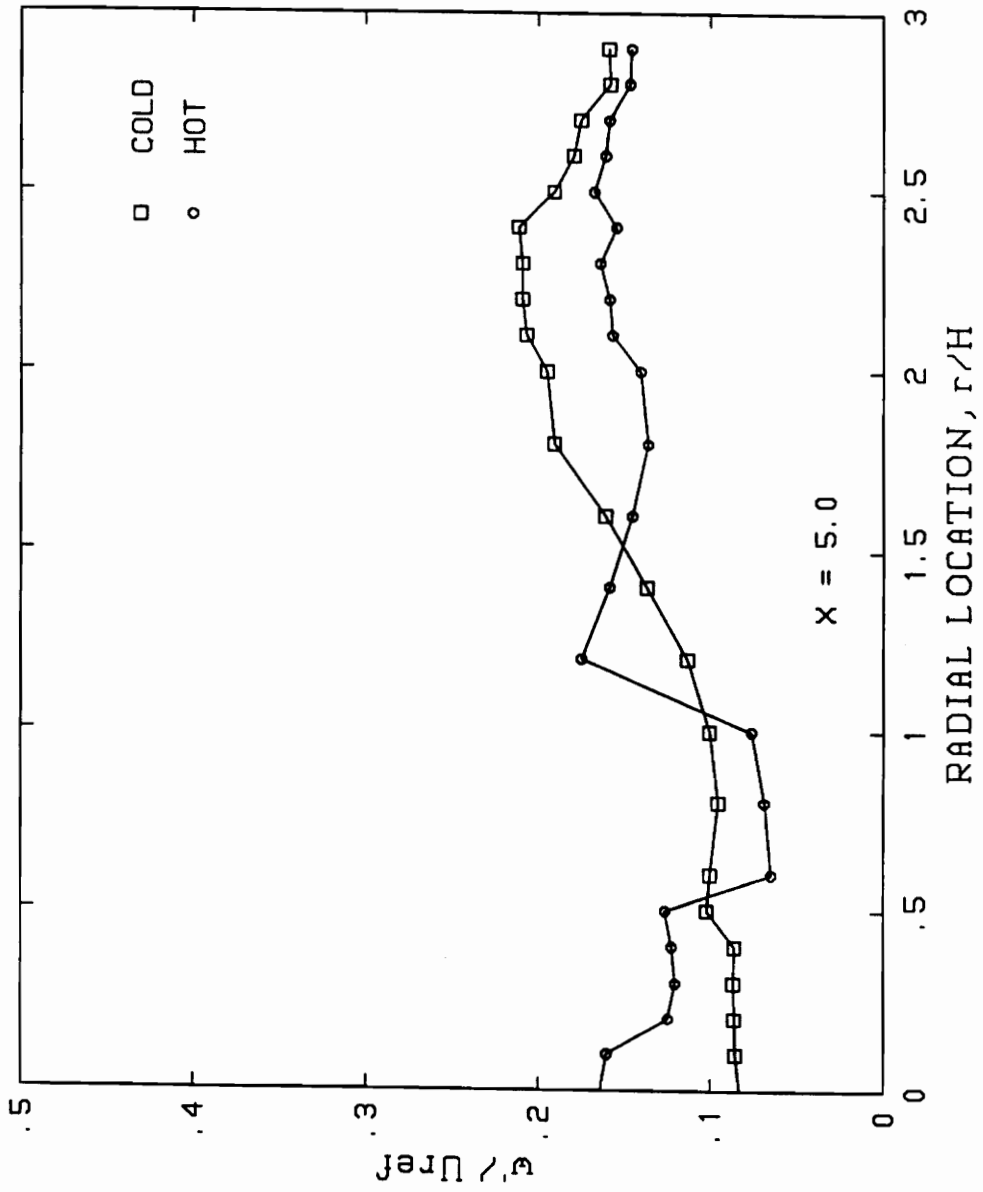


COMPARISON BETWEEN COLD AND HOT DATA

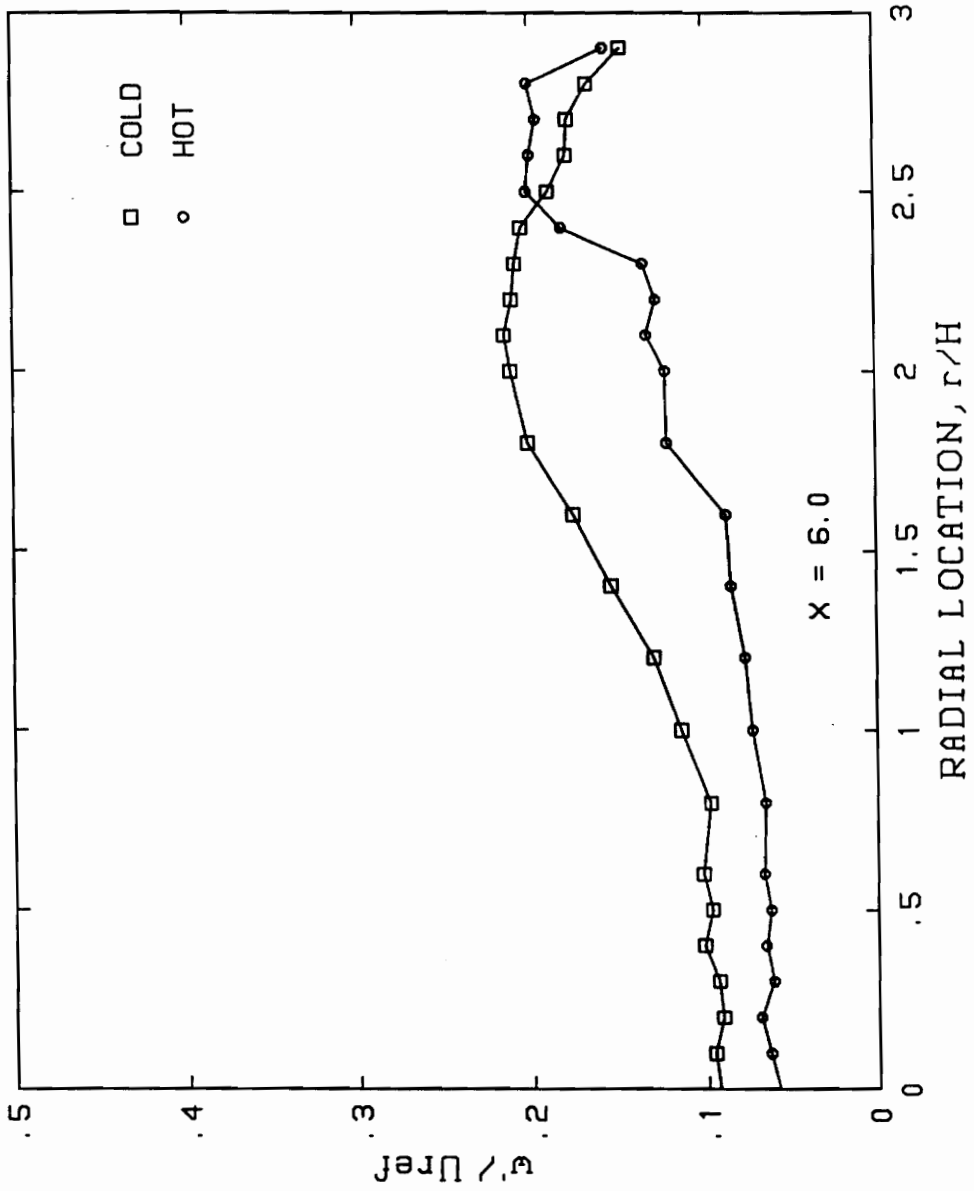


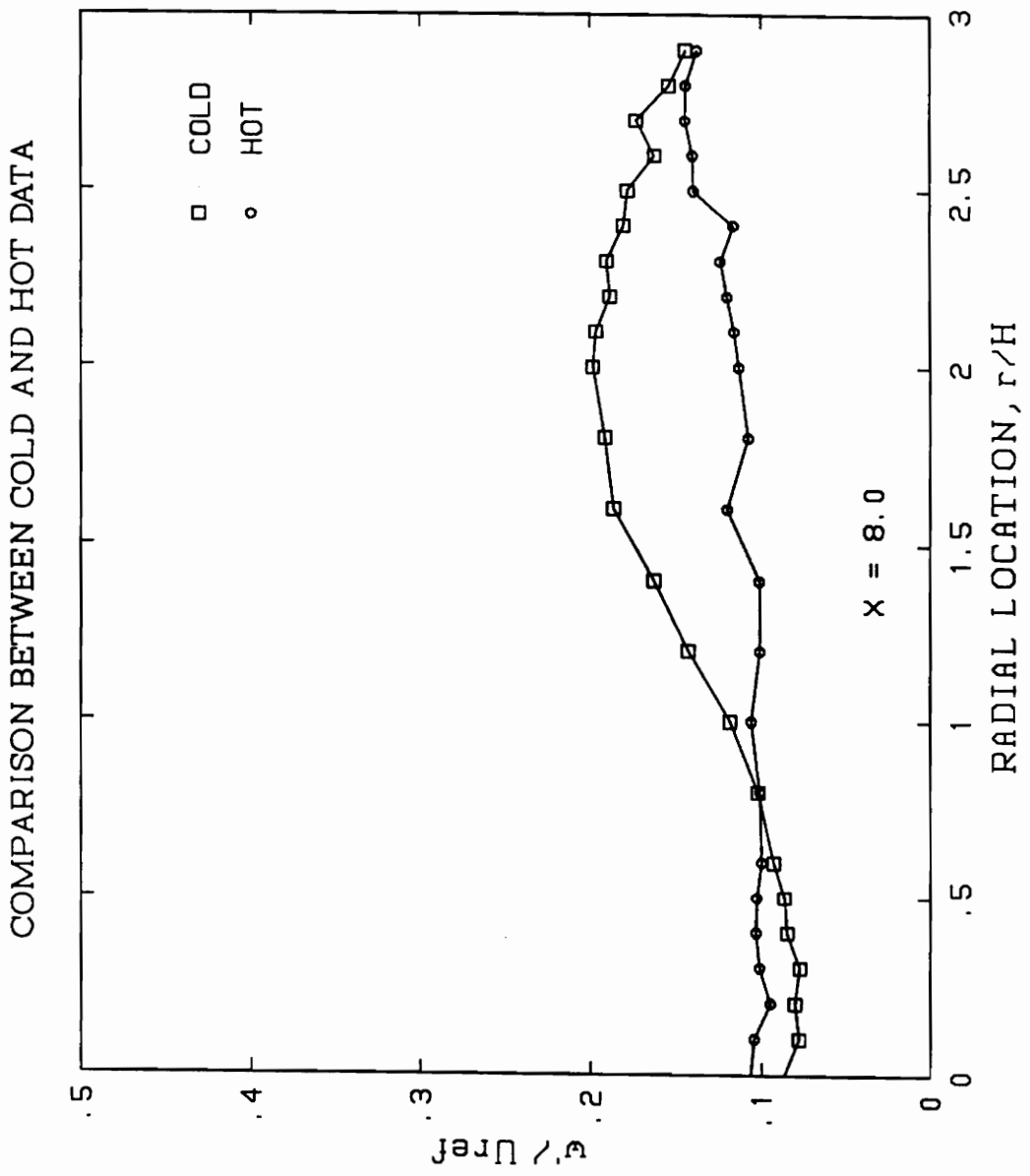


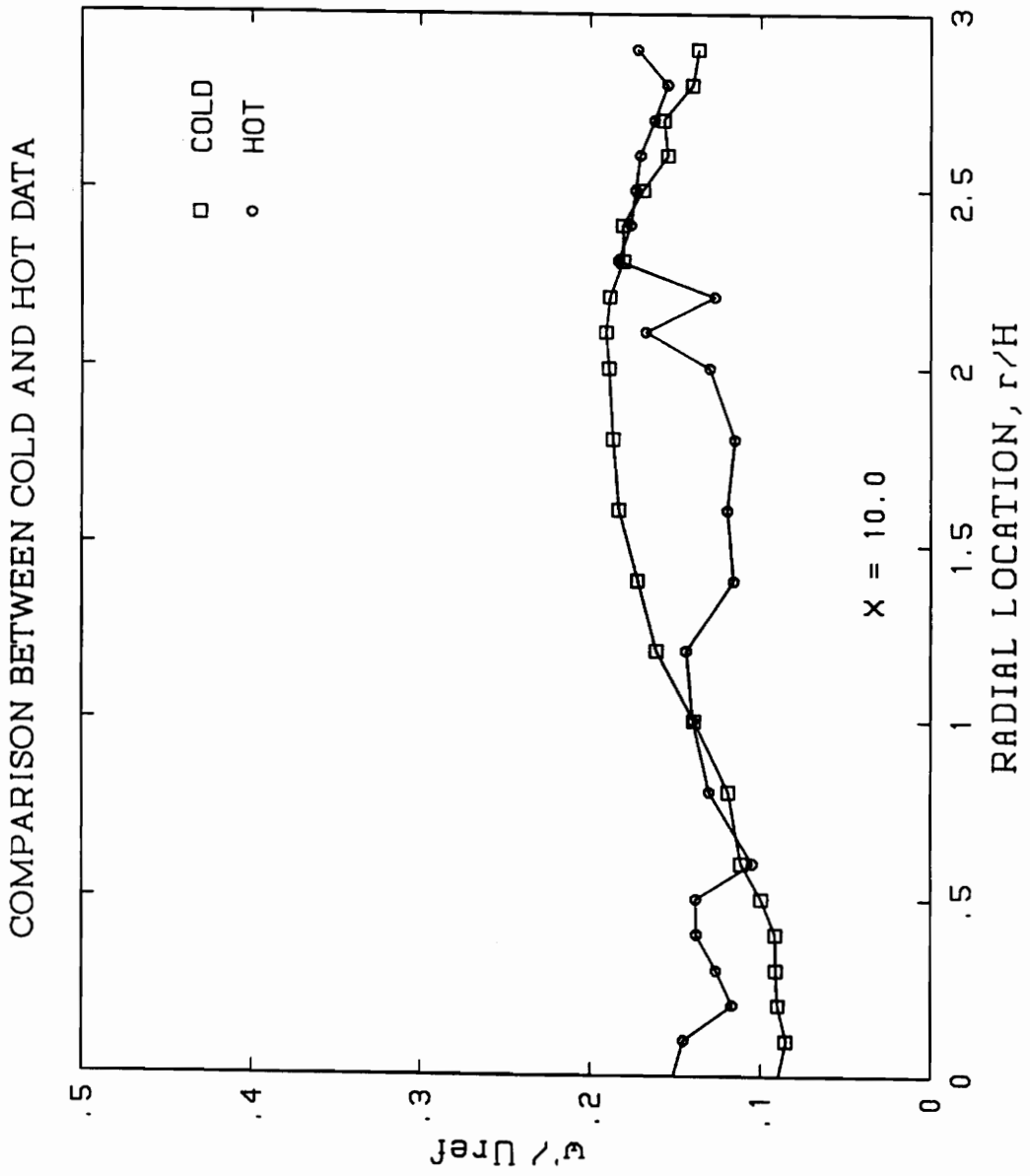
COMPARISON BETWEEN COLD AND HOT DATA



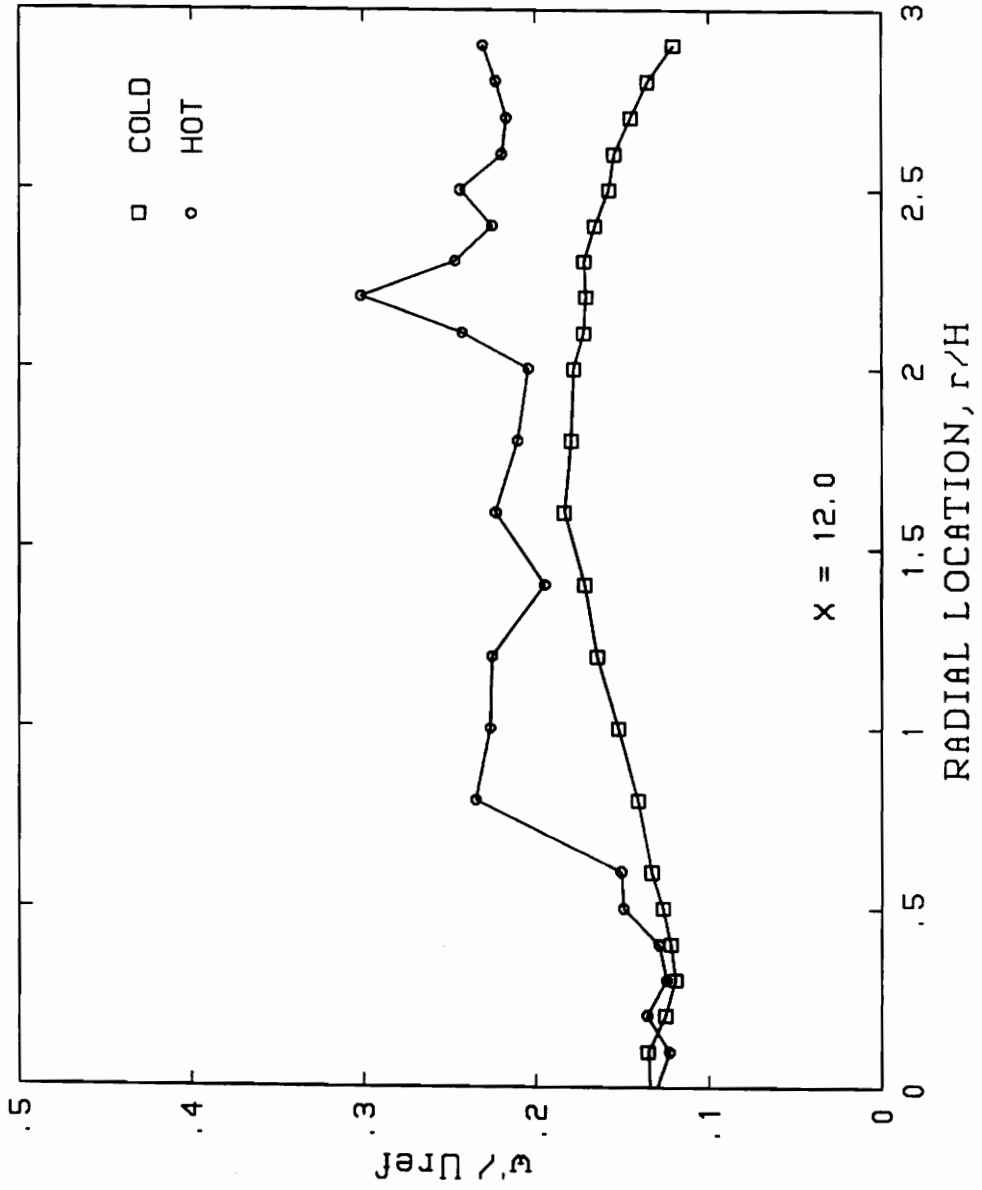
COMPARISON BETWEEN COLD AND HOT DATA

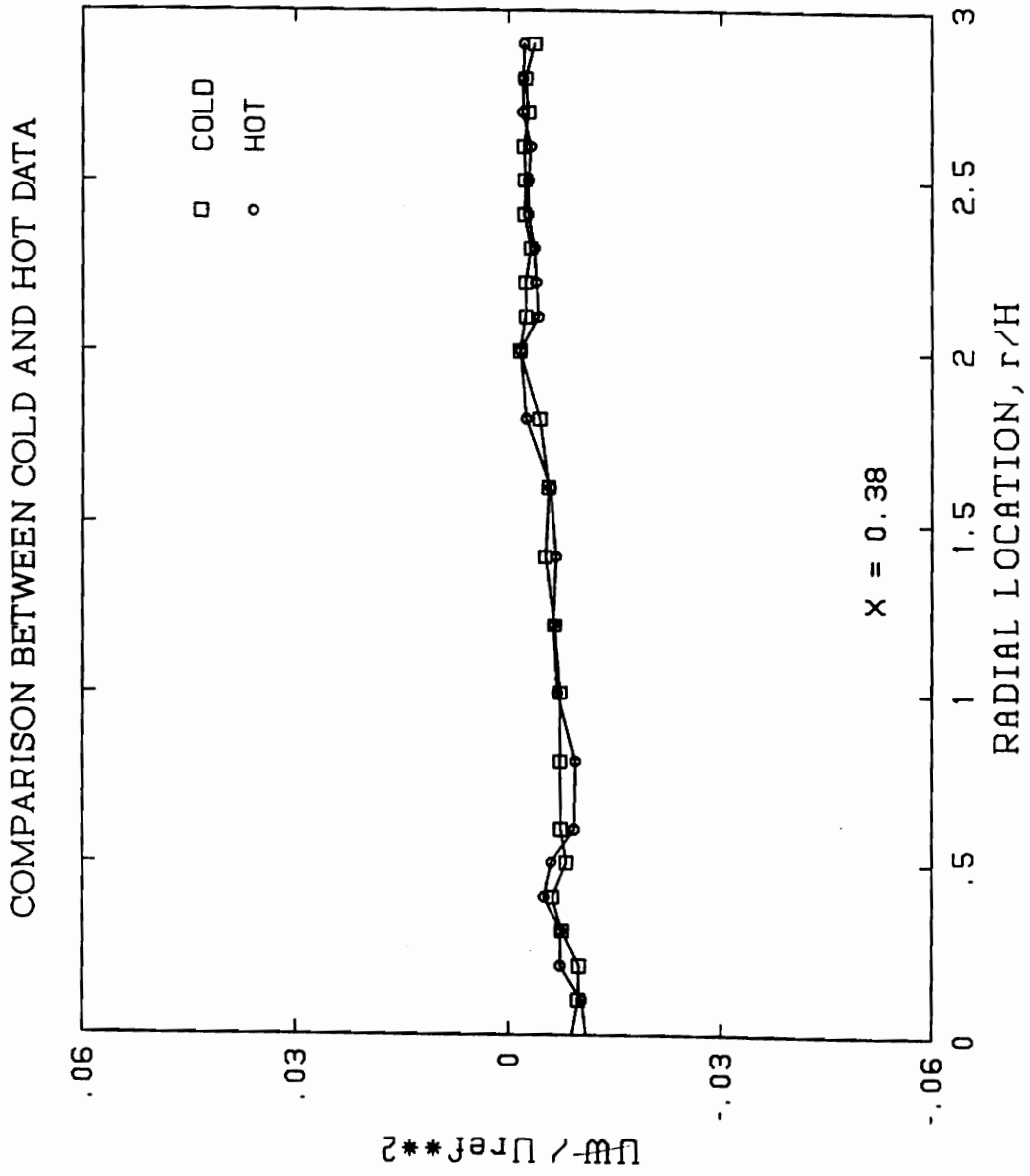




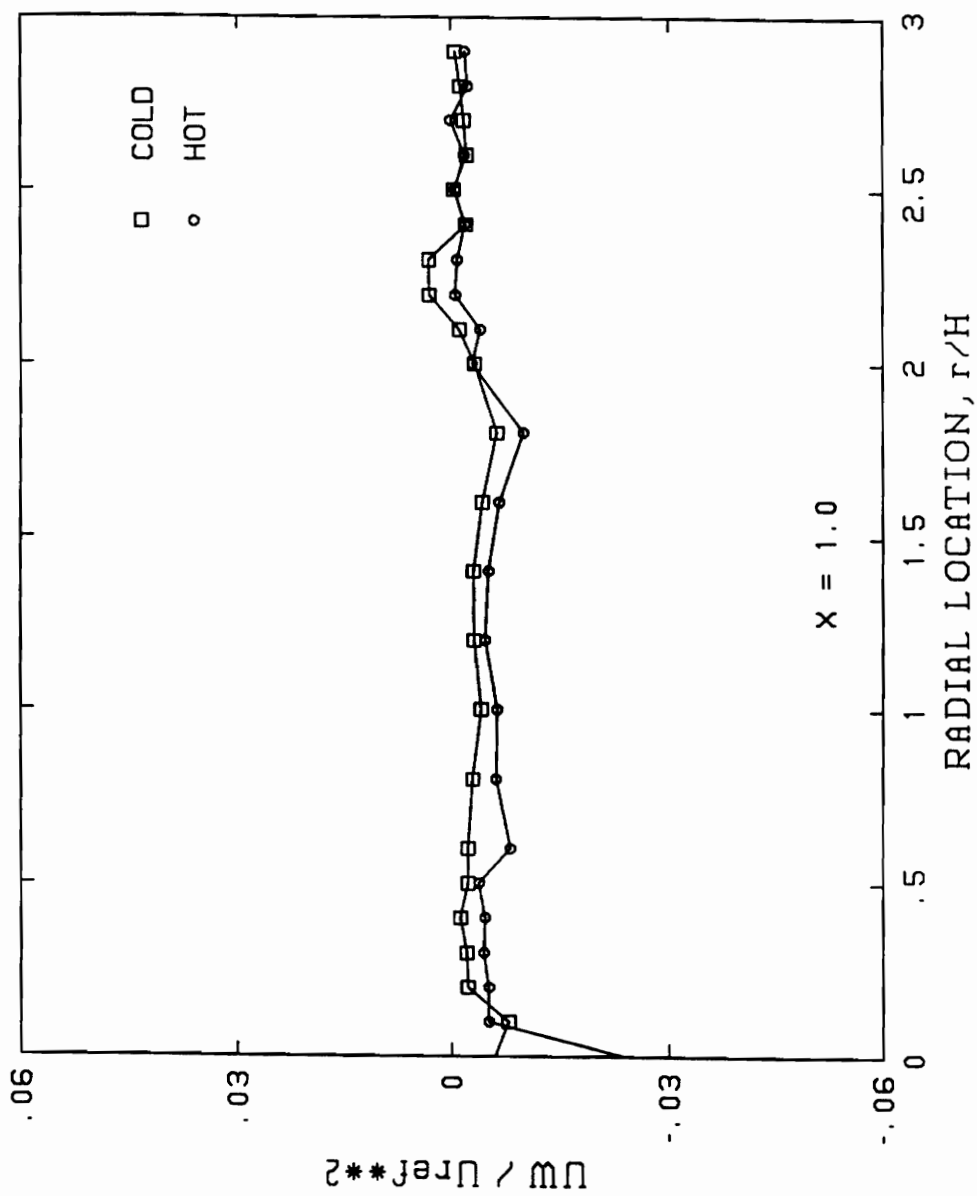


COMPARISON BETWEEN COLD AND HOT DATA

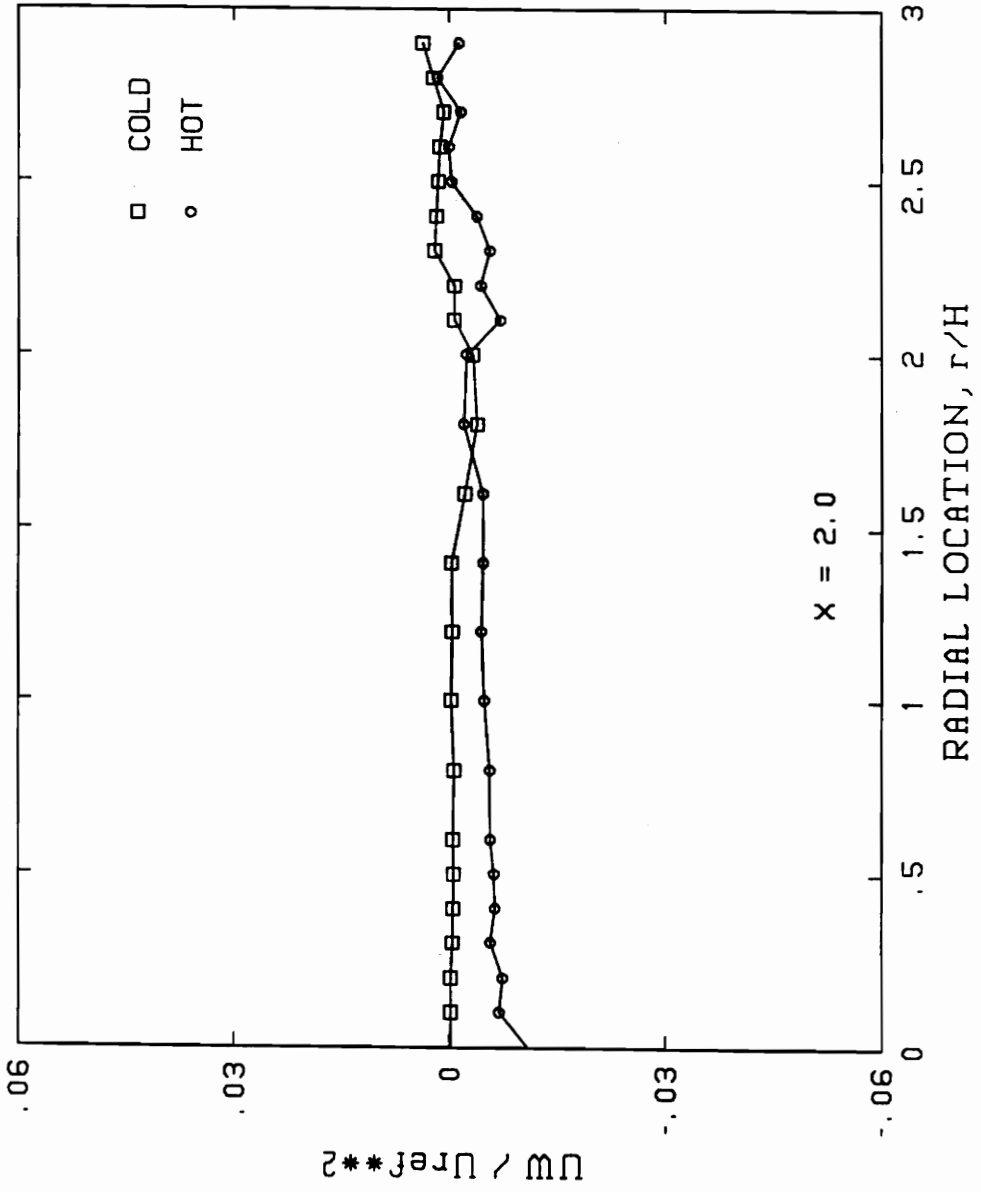




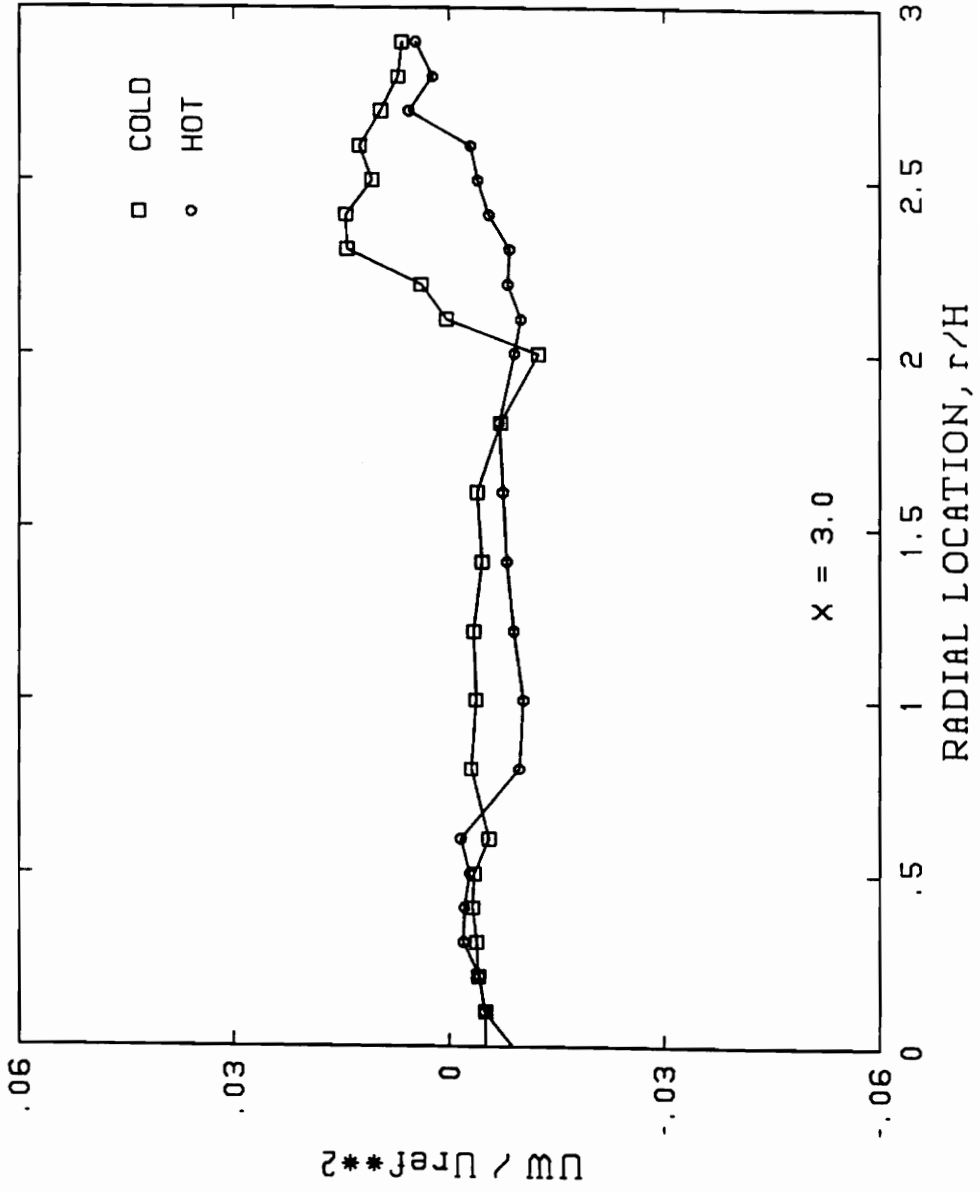
COMPARISON BETWEEN COLD AND HOT DATA



COMPARISON BETWEEN COLD AND HOT DATA



COMPARISON BETWEEN COLD AND HOT DATA

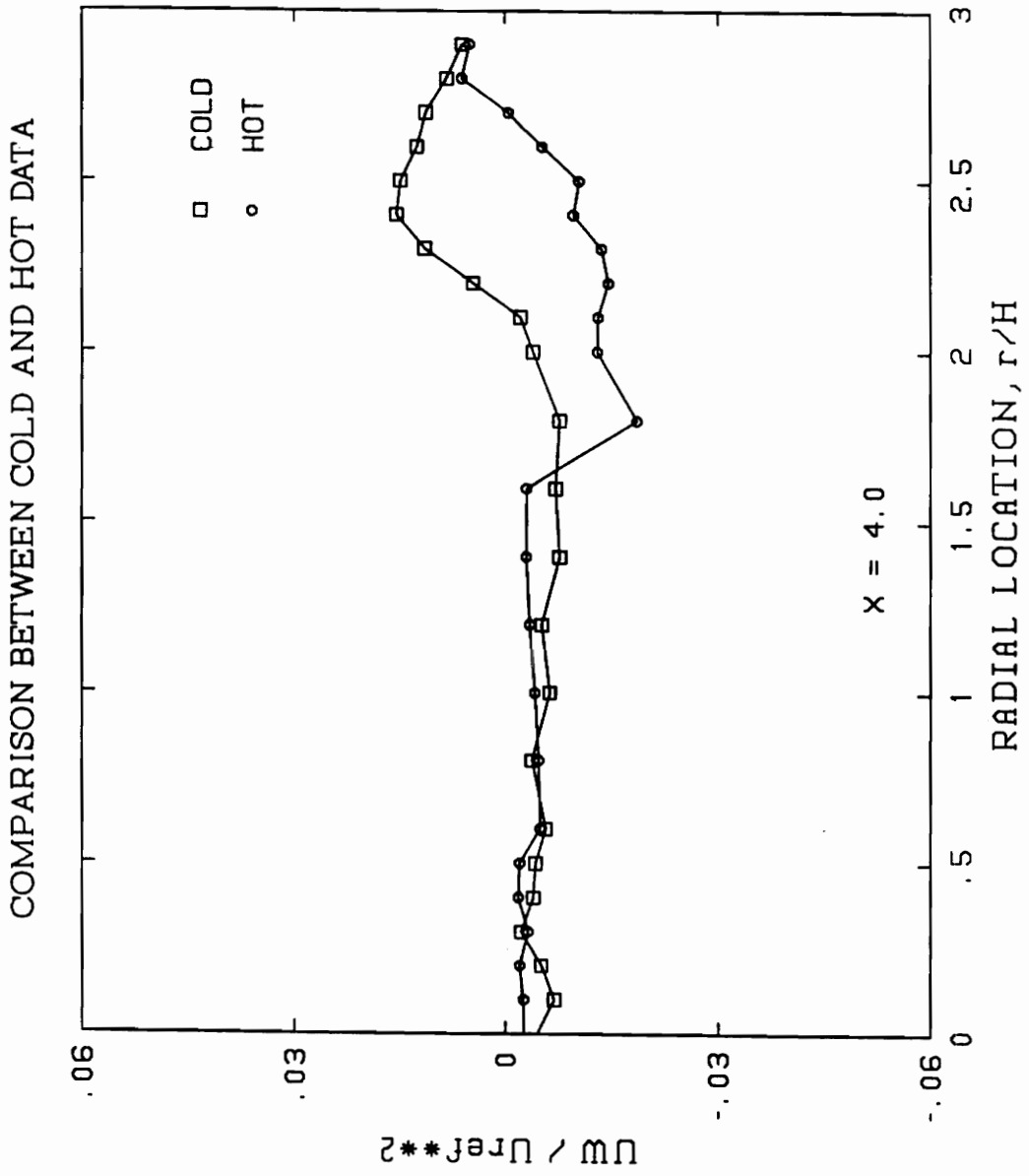


X = 3.0

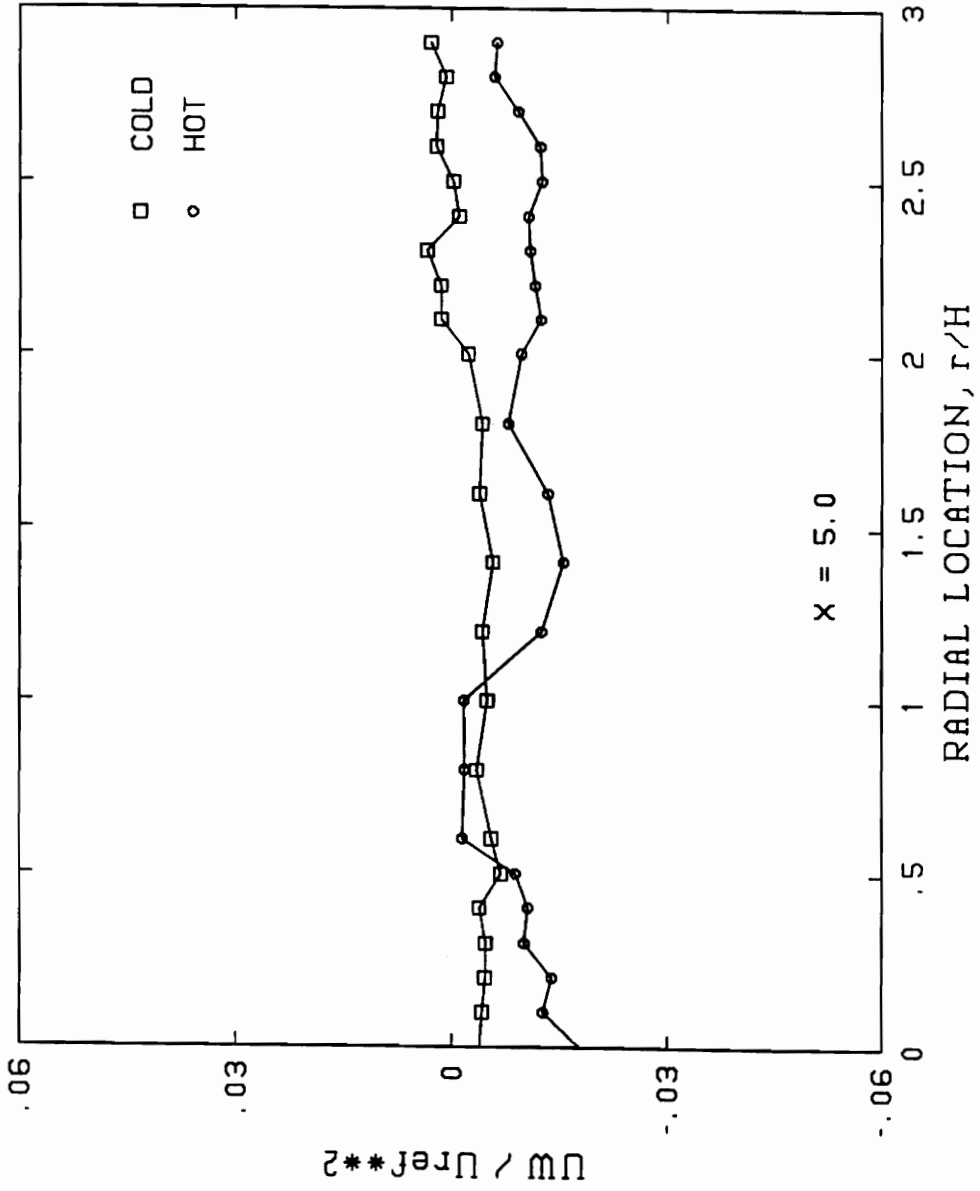
□ COLD
○ HOT

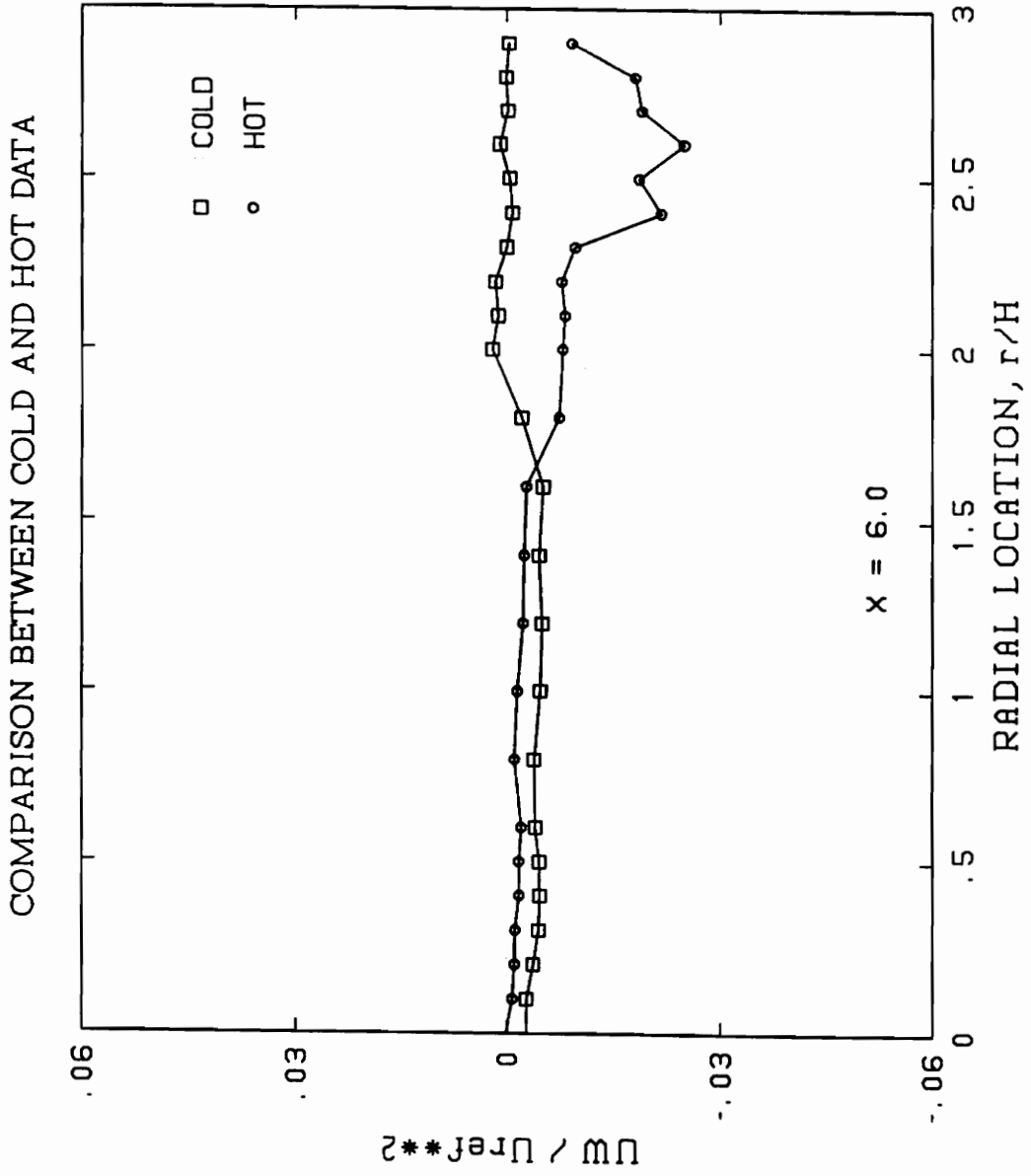
U_w / U_{ref}^2

RADIAL LOCATION, r/H

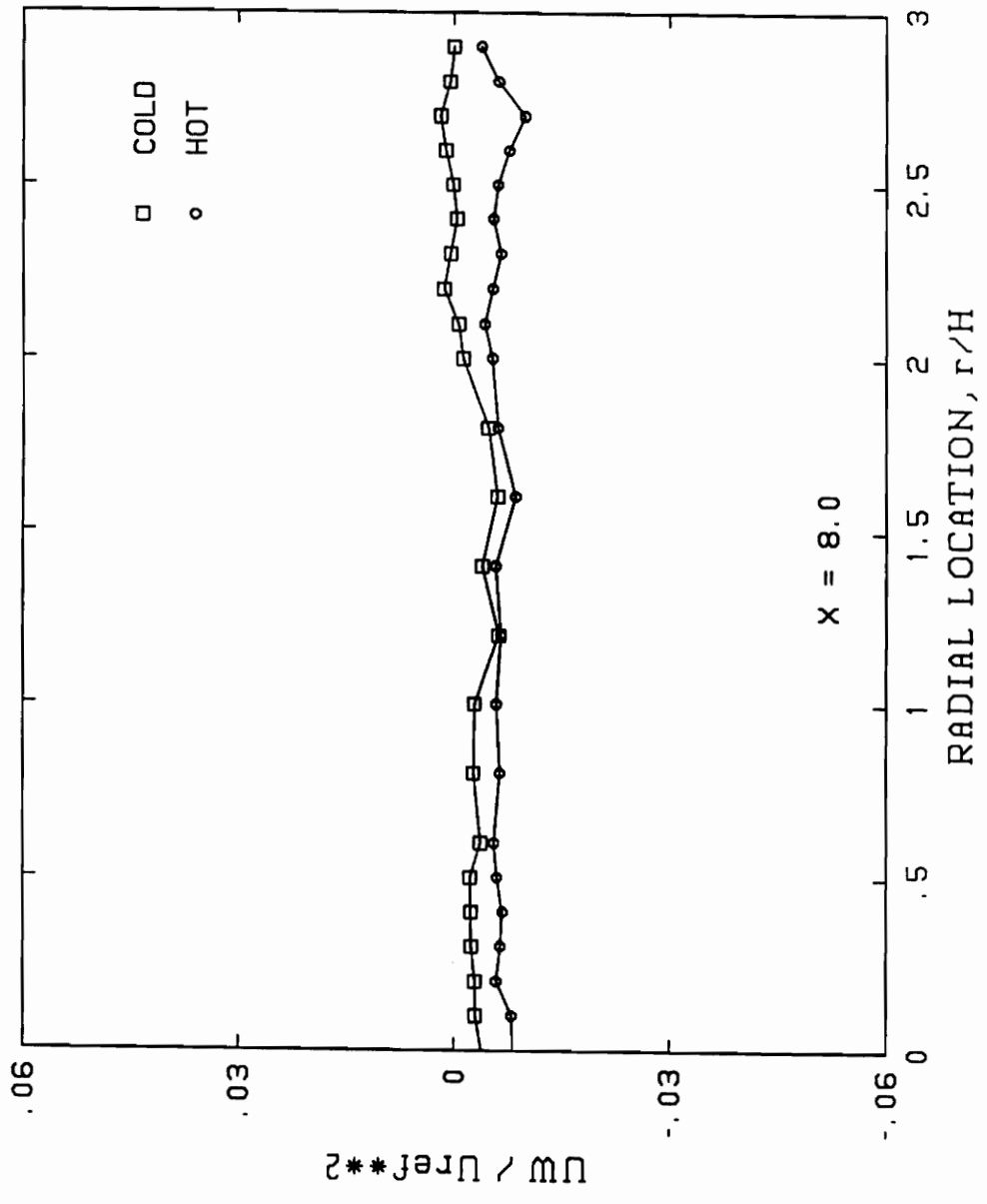


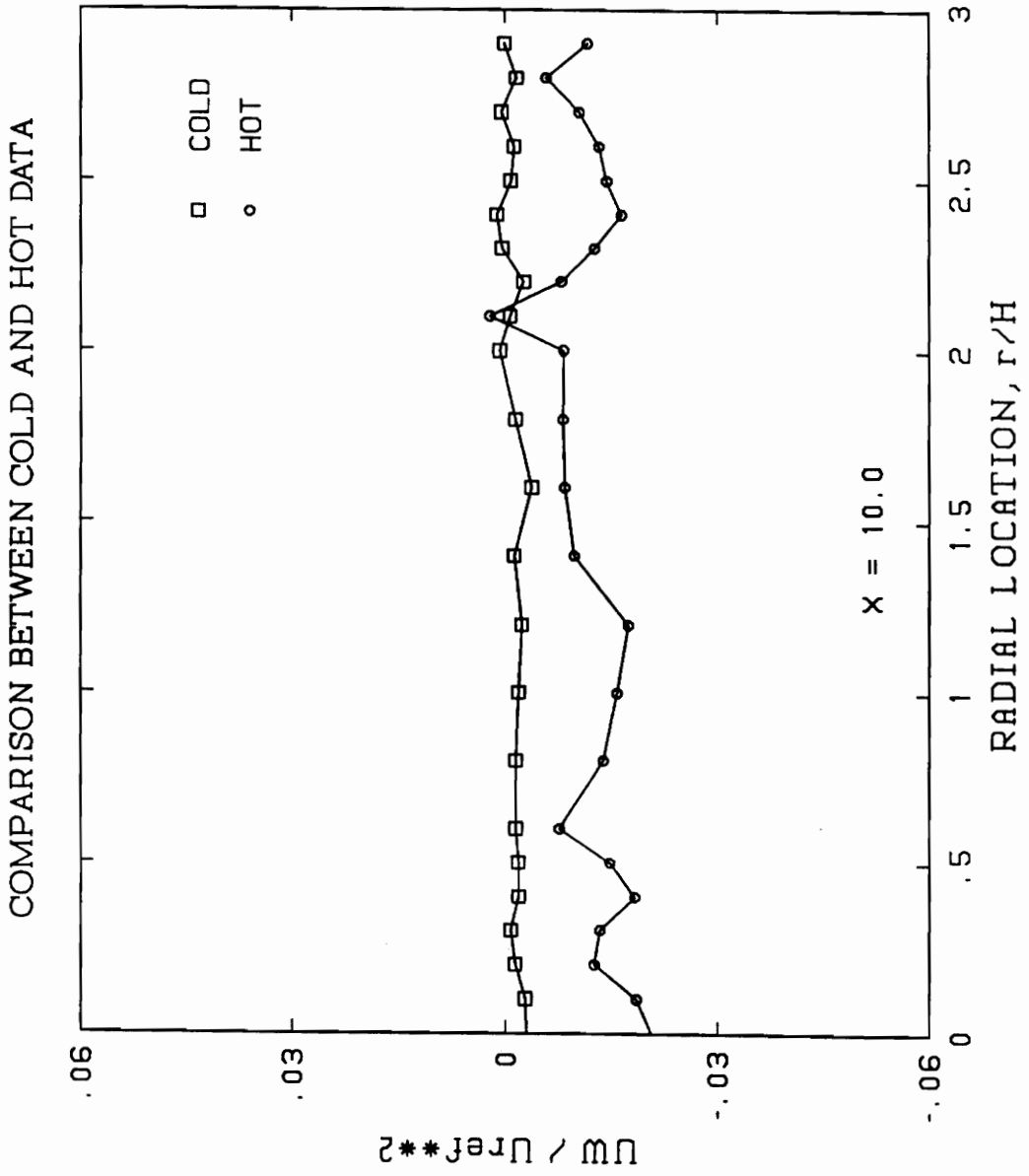
COMPARISON BETWEEN COLD AND HOT DATA



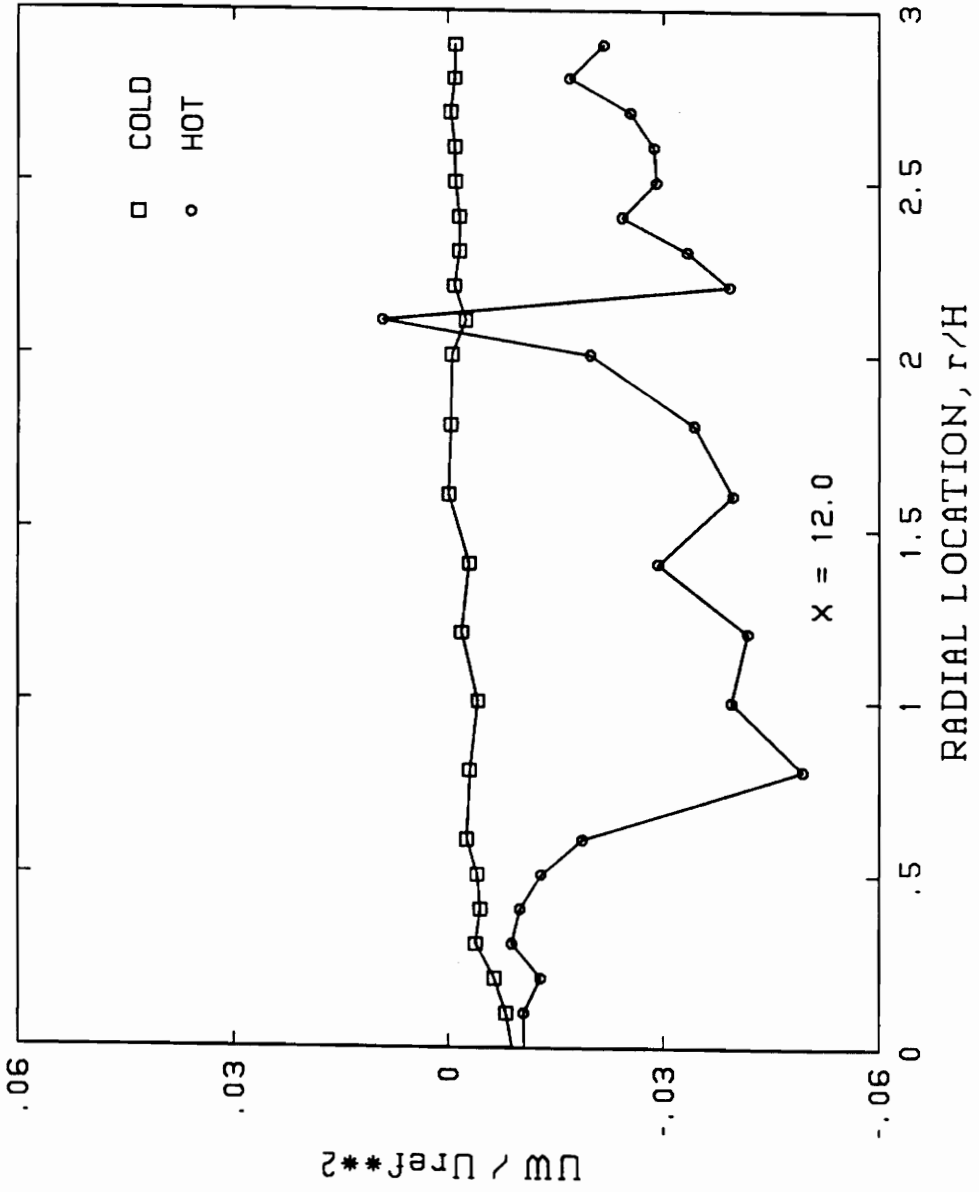


COMPARISON BETWEEN COLD AND HOT DATA





COMPARISON BETWEEN COLD AND HOT DATA



VITA

Robert Gabruk was born on September 30, 1966 in Plainfield, New Jersey to Lena and Zigmund Gabruk. He graduated as salutatorian from North Hunterdon Regional High School in Annandale, New Jersey in June of 1984. Following high school graduation, Mr. Gabruk attended Virginia Polytechnic Institute and State University (VPI & SU) and received the degree of Bachelor of Science in Mechanical Engineering in May of 1988. The following academic year, Robert continued his studies at VPI & SU while working towards the degree of Master of Science in Mechanical Engineering. During his graduate studies, Mr. Gabruk participated in a graduate student research program at Wright-Patterson Air Force Base in Dayton, Ohio. The experimental research project that he worked on at Wright-Patterson provided the base for his Master of Science thesis.